# Optimising Reproductive Induction in yellowbelly flounder (*Rhombosolea leporina*): Evaluating GnRHa Dosage and Non-Invasive Gonadal Assessment.

A thesis

submitted in partial fulfillment

of the requirements for the degree

of

**Master of Science in Environmental Sciences**

at

**The University of Waikato**

by

**Adam Colthorpe**


THE UNIVERSITY OF
WAIKATO
*Te Whare Wānanga o Waikato*

2025

# Table of Contents

# List of Figures

# List of Tables

# Abstract

This study investigates two complementary tools to address reproductive dysfunction in wild-caught yellowbelly flounder (*Rhombosolea leporina*), a key bottleneck in the species' aquaculture development. First, the effects of varying doses of gonadotropin-releasing hormone analogue (GnRHa) on ovarian development and expression of gonadal *cyp19a1a*, a gene encoding aromatase, critical for 17β-estradiol synthesis were quantified at short-term timepoints. A single injection of 50 or 100 µg/kg induced transient upregulation of *cyp19a1a* by Day 1 post-treatment ($\log_2$ fold-changes of +2.38 and +2.65, respectively), while the 25 µg/kg and control groups showed downregulation (−0.53 and −0.07) relative to Day 0 baselines. However, expression declined significantly in all groups by Day 5, including a drop in the 100 µg/kg group to −0.68 ($p = 0.03$), indicating a brief stimulatory window likely insufficient to sustain steroidogenic activity or promote meaningful oocyte development. These findings support the need for sustained-release hormone systems or improved broodstock staging to enhance treatment efficacy.

Second, a novel, non-invasive Visual Gonadosomatic Index (VGSI) was evaluated to minimise handling stress while classifying reproductive condition and suitability for hormone treatment. Two metrics were developed using backlit imaging of the ventral gonads: gonad area relative to body area (Size GSI) and gonad length relative to body length (Length GSI). While neither metric correlated strongly with oocyte diameter or histological stage, Length GSI showed a modest but significant association with oocyte development ($R^2 = 0.1937$, $p = 0.009$), and both indices were positively associated with *cyp19a1a* expression (Size GSI: $R^2 = 0.5045$, $p = 0.021$; Length GSI: $R^2 = 0.3408$, $p = 0.076$). These results suggest VGSI may provide a coarse proxy for reproductive development, though further refinement and validation are required.

Together, these findings represent the first report of ovarian *cyp19a1a* expression in *R. leporina* and lay the groundwork for integrated hormonal and imaging-based strategies to improve reproductive control in this culturally and economically significant flatfish.

# Acknowledgments

I would like to thank my supervisor Dr Simon Muncaster for his assistance in designing and carrying out this research as well as Steve Bird for his help in making and ordering the primer sets in this study and providing very useful advice.

I would also like to thank all those who assisted in my lab work, in particular Tessa Hamer and Elizabeth Copeland who both provided invaluable information for carrying out my qPCR methods.

I want to thank Kevin Green from the Toi Ohomai Aquaculture lab for graciously letting us use his equipment for housing our fish, as well as his time and effort in keeping them alive when I wasn't there. Your assistance and expertise in Aquaculture were much appreciated.

Lastly, I want to thank my family and in particular my mum and dad who have supported me through this whole journey.

*Dedicated to Minkey.*

*Who always loved fish.*

# Chapter 1 – Introduction

## 1.1: Background in Aquaculture

Aquaculture is the cultivation of aquatic organisms such as fish or mollusks under optimized environmental conditions, typically using cages, tanks, or ponds. It involves managing the full life cycle of one or more species, with mature individuals maintained as broodstock to produce a consistent supply of larval offspring. Selective breeding is employed to enhance desirable traits while preserving genetic diversity (Ackefors et al., 2017). Juveniles are reared in controlled hatcheries before being transferred to grow-out systems for harvest and processing. At the same time, food security has become an escalating global concern, driven by climate change, environmental degradation, and a rapidly growing population that now exceeds eight billion people (Ritchie & Roser, 2023).Historically, wild-caught fisheries have dominated seafood supply, but overfishing, habitat loss, and environmental stress have reduced their productivity (Memarzadeh et al., 2019). In response, aquaculture has expanded rapidly as a sustainable alternative, attracting significant investment to meet rising demand (Garlock et al., 2020).

Finfish aquaculture offers key advantages for food security and economic growth. Fish have high feed conversion ratios (Mungkung et al., 2013), and aquaculture systems generally require less land and water than terrestrial farming (Edwards, 2015). This makes aquaculture particularly suitable for regions with limited arable land or freshwater. Moreover, aquaculture is typically less carbon-intensive than livestock production (MacLeod et al., 2020), and algae cultivation through integrated multi-trophic aquaculture (IMTA) can mitigate waste and emissions (Ahmed et al., 2017).

Tightly managed production systems allow for year-round output and provide tools to minimise environmental impact (Helfrich & Libey, 1991). These efficiencies, combined with scalability and strong market potential, have made aquaculture the fastest-growing food sector globally (Subasinghe et al., 2009).

## 1.2: Yellowbelly flounder (*Rhombosolea leporina*)

The yellowbelly flounder (*Rhombosolea leporina*) is a flatfish species found in tidal estuaries and shallow coastal waters throughout New Zealand (Ayling & Cox, 1982). Flatfish are collectively known in *te reo Māori* as *Pātiki* and are recognised as taonga, or cultural treasures. Their historical role as a reliable food source has contributed to their cultural significance. The diamond shape of *Pātiki* is reflected in traditional art, symbolising how women once supplemented iwi food supplies by harvesting flounder at night while the men

slept (Wallace et al, 2003).

In addition to its cultural importance, *R. leporina* is a highly desirable species for both commercial and recreational harvest. It is considered a delicacy with high-quality flesh, commanding strong market prices. Despite sustained commercial and recreational harvest, flatfish stocks that include *R. leporina* are subject to high exploitation pressure, with limited species-specific biomass data and increasing vulnerability to habitat degradation and climate change (Morrison et al., 2009).

*R. leporina* displays several traits that make it a strong candidate for aquaculture development. It is short-lived and reaches sexual maturity within two years, enabling accelerated selective breeding under culture. Although the species grows to a modest maximum size of less than 50 cm, growth is rapid, with individuals typically reaching the minimum legal size of approximately 25 cm and common marketable sizes of around 30–40 cm within two to three years (Colman, 1974). The species is naturally sedentary, occupying the benthic zone, which reduces metabolic demand for oxygen and allows farming in lower-flow systems. This reduces capital requirements for infrastructure and could support aquaculture development in smaller coastal communities.

Flatfish are already established in aquaculture globally. In particular, the olive flounder (*Paralichthys olivaceus*) is farmed at scale in Japan and South Korea, with production exceeding 43,000 tonnes in 2017 (Hamidoghli et al., 2020).

Compared with other flatfish such as *P. olivaceus*, there is limited research on the reproductive biology, diet, and environmental tolerances of *R. leporina*. As a species endemic to New Zealand, domestication from wild stock is a prerequisite for industry development. Establishing reliable broodstock is a key bottleneck, as wild-caught *R. leporina* frequently exhibits reproductive failure under captive conditions due to acute and chronic stress (Ellis-Smith, 2022). This impairs gamete quality and consistency. Developing protocols to overcome this reproductive failure would accelerate the production of an F1 generation, better adapted to captivity and less prone to failure in future breeding efforts.

### 1.3: The Brain–Pituitary–Gonad Axis

The reproductive capability of finfish develops through puberty, a process that transforms a sexually immature juvenile into a sexually mature adult by activating the hormonal and gametogenic functions of the brain–pituitary–gonad (BPG) axis (Schulz & Miura, 2002; Taranger et al., 2010). The timing of puberty is influenced by genetic factors (Gjerde, 1984) and ecological conditions such as food availability and population density (Schulz & Henk,

1999). In teleosts, sexual maturation is also regulated by endogenous biological clocks that interact with environmental cues like photoperiod and water temperature, triggering seasonal physiological changes (Bromage et al., 2001).

The BPG axis consists of three interconnected components (Weltzien et al., 2004; Figure 1.1). Neuroendocrine neurons link the central nervous system (CNS) with the endocrine system by producing gonadotropin-releasing hormones (GnRHs), which stimulate gonadotrope cells in the pituitary. These cells produce and release the gonadotropins follicle-stimulating hormone (FSH) and luteinizing hormone (LH). These hormones circulate through the bloodstream and bind to membrane-bound receptors on steroidogenic cells within the gonads. In the ovary, the thecal and granulosa cells form a follicular bilayer around each oocyte. Stimulation of these cells by FSH and LH initiates sex steroid production, driving oogenesis (Nagahama, 1997).

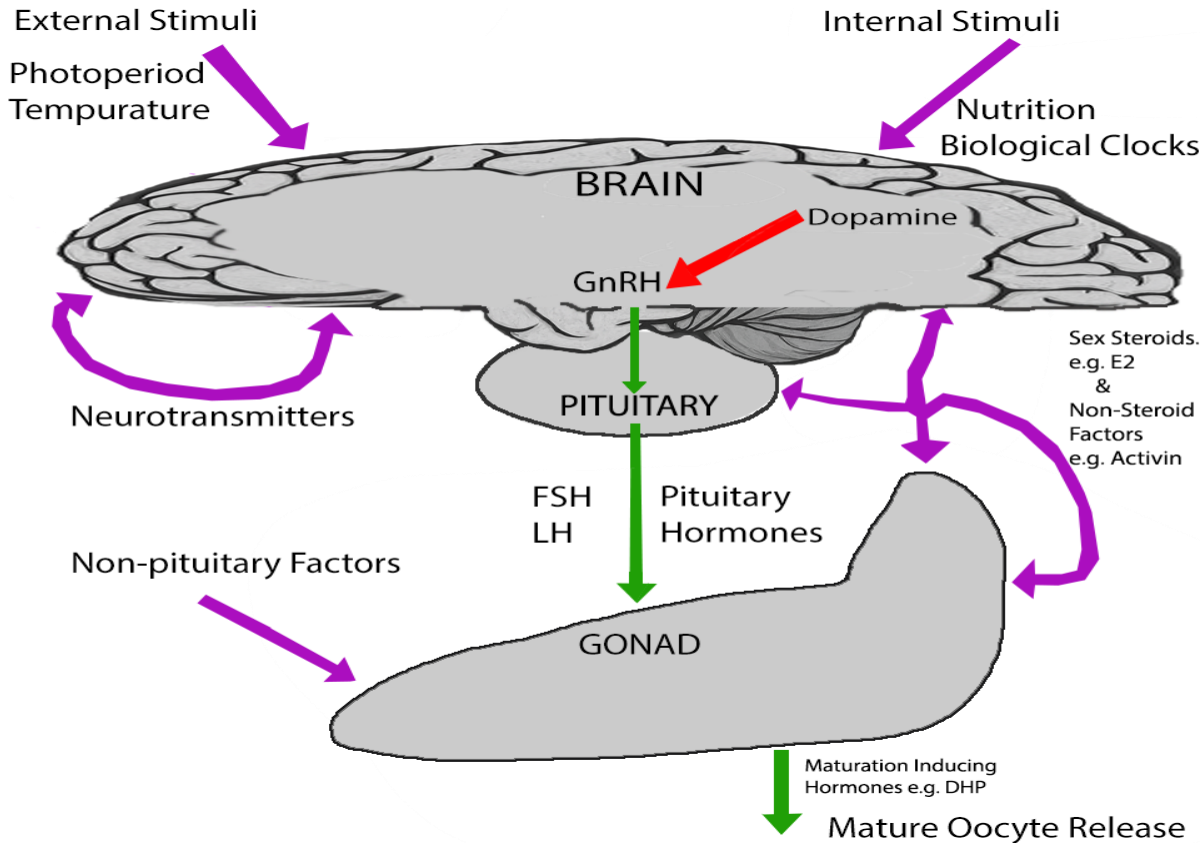


*Figure 1.1. Schematic of the female teleost brain–pituitary–gonadal (BPG) axis, adapted from Weltzien et al. (2004). External and internal stimuli regulate GnRH release, which stimulates pituitary gonadotropins (FSH/LH) to promote gonadal steroidogenesis*

FSH and LH mediate two key events in oogenesis. First, FSH drives a rapid oocyte growth phase marked by vitellogenesis, during which thecal cells produce testosterone (T), which is converted into 17β-estradiol (E2) by the aromatase enzyme (*cyp19a1a*) in granulosa cells. E2 then stimulates hepatic synthesis of vitellogenins, which are transported via circulation and

incorporated into the oocyte (Nagahama & Yamashita, 2008).

Second, LH promotes final oocyte maturation, involving meiotic resumption and ovulation. Under LH stimulation, thecal cells produce 17α-hydroxyprogesterone, which is converted in granulosa cells into the maturation-inducing hormone (MIH). While the specific MIH varies between species, the most common is 17α,20β-dihydroxy-4-pregnen-3-one (17α,20β-DP) (Nagahama & Yamashita, 2008), catalysed by the enzyme 20β-hydroxysteroid dehydrogenase (20β-hsd). Together, these sex steroids drive oogenesis, with some (e.g. T) also participating in negative feedback loops that coordinate the FSH-to-LH transition across the BPG axis.

### 1.4: Reproductive Failure in Teleosts

In the wild, *R. leporina* flounder exhibit a strongly seasonal reproductive cycle, with gonadal development occurring through winter and peak spawning typically taking place in spring and early summer, often as synchronised mass-spawning events triggered by increasing temperature and photoperiod. In captivity, however, wild-caught fish frequently fail to complete the normal gametogenic cycle, particularly during their first season and often throughout their lifespan. This dysfunction is partly due to the absence of natural environmental cues such as seasonal temperature fluctuations and photoperiod. Other contributing factors may include unsuitable substrate, tank depth, or salinity (Mylonas et al., 2011). These issues can be mitigated by mimicking natural conditions and minimising stress through optimal water quality and limited handling.

Female teleosts are especially prone to three primary types of reproductive failure, each corresponding to a different stage of oogenesis (Mylonas & Zohar, 2009). The first is failure to initiate or complete vitellogenesis, the oocyte growth phase driven by estrogen production under FSH stimulation (Nagahama, 2008; Selvaraj et al., 2021). The second, and most common, is failure to undergo final oocyte maturation and ovulation despite successful vitellogenesis. This is often linked to insufficient pituitary LH release and resulting deficits in maturation-inducing steroid production (Mylonas & Zohar, 2009). For example, several marine scombrid species exhibit low pituitary GnRH and LH levels in captivity, preventing maturation (Senarat et al., 2019). The third type occurs when ovulated oocytes are retained and not released. Identifying the specific point of failure within the gametogenic process is essential for managing reproductive dysfunction in captive broodstock.

### 1.5: Hormone Treatments in Aquaculture

Early attempts to stimulate the BPG axis and overcome reproductive dysfunction in fish used pituitary homogenates, their extracts, or alternative gonadotropins such as human chorionic gonadotropin (hCG). However, these approaches carry notable drawbacks (Zohar & Mylonas, 2001). As a result, most modern hormonal interventions use synthetic gonadotropin-releasing hormone analogues (GnRHa) (Mylonas et al., 2010). GnRHa, a small peptide hormone, does not trigger immune responses in fish and is easier to administer than exogenous gonadotropins. It directly stimulates pituitary gonadotrope cells, inducing endogenous gonadotropin release and promoting sex steroid production in the gonads. Unlike hCG or crude pituitary extracts, which act directly at the gonadal level and can vary in purity and potency, GnRHa offers a cleaner, more physiological approach by engaging the fish's own endocrine cascade. This makes it particularly valuable for species with reproductive dysfunctions rooted in upstream hormonal suppression, as it initiates a coordinated endocrine response while minimising risks of over-stimulation, immune rejection, or inconsistent ovulation outcomes.

The effectiveness of hormonal treatment depends on delivery method, timing, and dose. Dose is particularly critical: insufficient amounts may fail to elicit a response, while excessive doses can reduce efficacy or compromise gamete quality (Kjørsvik, 2003). Because optimal doses vary by species, treatment protocols should be refined through experimental trials that track oocyte development, ovulation, and spawning success.

A prior study on wild-caught *R. leporina* found that ovulation could be induced with a 50 µg/kg dose of GnRHa, while a higher dose of 100 µg/kg caused significant delays in ovulation (Ellis-Smith, 2022). Control fish failed to either initiate or progress through final oocyte maturation or ovulation. The present study expands on this work by examining the effects of four GnRHa doses (0, 25, 50, and 100 µg/kg) in wild-caught *R. leporina*. Reproductive indicators, including ovarian gene expression and oocyte development, were assessed to help refine hormonal induction strategies for this species.

### 1.6: Research Objectives and Hypotheses

This study investigates two complementary strategies for overcoming reproductive dysfunction in *R. leporina* broodstock. The first objective is to quantify how varying doses of exogenous GnRHa influence ovarian expression of the aromatase gene *cyp19a1a*, a key marker of steroidogenic activation during vitellogenesis. The second objective is to evaluate the feasibility of a non-lethal Visual Gonadosomatic Index (VGSI), based on backlit imaging of the ovary, as a practical tool for staging reproductive maturity. The study tests the hypothesis that higher GnRHa doses will induce stronger *cyp19a1a* expression at early timepoints, particularly in broodstock with advanced oocyte development. It also evaluates whether VGSI metrics correlate with oocyte diameter, histological maturation stage or responsiveness to GnRHa.

Together, these approaches aim to identify molecular and morphological indicators of reproductive readiness that can improve the timing and reliability of induced spawning protocols in this culturally and economically significant species.

# Chapter 2 – *cyp19a1a* Expression

## 2.1: Introduction

Reproductive dysfunction in *R. leporina* (yellowbelly flounder) presents a significant barrier to developing reliable captive breeding protocols for aquaculture. Wild- caught broodstock often struggle to adapt to captivity and frequently fail to complete final oocyte maturation (FOM) and ovulation, even when earlier stages of ovarian development proceed normally (Koverman, 2018; Ellis-Smith, 2022). These reproductive issues are a key limiting factor for the domestication and commercial-scale propagation of many flatfish species (Guzmán et al., 2009). Hormonal manipulation, particularly through the application of exogenous gonadotropin-releasing hormone analogues (GnRHa), remains one of the primary tools used to override these dysfunctions and help stimulate reproduction in captivity (Zohar & Mylonas, 2001; Weltzien et al., 2004).

GnRHa functions by stimulating the pituitary to release endogenous gonadotropins, specifically follicle-stimulating hormone (FSH) and luteinising hormone (LH), which promote steroidogenesis and oocyte development (Zohar et al., 2010; Weltzien et al., 2004; Guzmán et al., 2009). In several flatfish species, GnRHa treatment has successfully induced ovulation and improved spawning success under captive conditions (Berlinsky et al., 1996; Guzmán et al., 2009). However, both inter- and intra-specific variability in responsiveness to hormonal induction remains a significant challenge, and protocols often require species-specific optimisation (Watanabe, 2005; Guzmán et al., 2009). In *R. leporina*, very limited data exist on hormonal responsiveness, and optimal dosing strategies remain poorly defined (Ellis-Smith, 2022).

The present study was designed to investigate the effects of varying doses of GnRHa on reproductive activation in *R. leporina*. Specifically, the aim was to assess how different GnRHa doses influence the ovarian expression of key steroidogenic markers involved in oocyte development. This was approached by measuring the gene expression of the ovarian aromatase gene *cyp19a1a*, which encodes the aromatase enzyme responsible for converting testosterone into 17β-estradiol (E2) (Weltzien et al., 2004; Zohar et al., 2010). Estradiol plays a central role in promoting vitellogenesis by stimulating the hepatic production of vitellogenin proteins, which are subsequently incorporated into developing oocytes (Nagahama & Yamashita, 2008; Weltzien et al., 2004). As such, *cyp19a1a* expression is widely used as a molecular proxy for ovarian estrogen production during early and mid-stages of oocyte growth (Zohar & Mylonas, 2001; Guzmán et al., 2009).

Gene expression assays such as quantitative PCR (qPCR) offer a cost-effective and logistically practical alternative to direct steroid hormone assays, particularly in small-scale experimental designs. While direct plasma E2 measurement remains the gold standard for assessing circulating estrogen levels, the use of immunoassays (e.g. ELISA, RIA) introduces additional logistical and financial challenges that were not feasible for this study. Accordingly, a gene expression approach was adopted to evaluate steroidogenic activation following hormonal induction with GnRHa.

Although GnRHa reliably triggers pituitary gonadotropin release, the downstream ovarian aromatase response can vary depending on both the developmental stage of the oocytes and the physiological condition of individual broodstock (Berlinsky et al., 1996; Guzmán et al., 2009). Variability in aromatase activation following hormonal induction has been documented in other flatfish species and may contribute to inconsistent spawning outcomes under controlled conditions (Berlinsky et al., 1997). By evaluating *cyp19a1a* expression following GnRHa treatment across a range of doses, this study aims to characterise both the efficacy and variability of aromatase activation in *R. leporina*, contributing to the development of optimised hormonal induction protocols for this species.

## 2.2: Methods

### 2.2.1: Experimental Design

Sexually mature female yellowbelly flounder (*Rhombosolea leporina*) were sourced from wild populations for use in this trial. An initial group of 34 mature females (2–3 years old) was collected by commercial net fishers operating within Raglan Harbour (37.80° S, 174.88° E, New Zealand) during mid-August. Fish were transported live to the Toi Ohomai Institute of Technology aquaculture facility within 3 h of capture under oxygen-supplemented conditions, with dissolved oxygen maintained above 80% saturation and water temperature held at approximately 13–15 °C to minimise transport stress. Upon arrival, fish were subjected to a controlled acclimation period prior to experimental manipulation. During acclimation, water temperature and photoperiod were gradually adjusted to match experimental conditions in order to minimise thermal and handling stress. Additional individuals were subsequently sourced prior to the trial start date in September to account for any mortality during acclimation and to ensure sufficient final sample size (Table B6). Following acclimation, broodstock were transferred to the University of Waikato Coastal Marine Field Station for the experimental phase of the study. All fish were maintained under consistent environmental conditions throughout the trial. All procedures involving live animals were conducted in accordance with institutional animal ethics approval.

The experimental system consisted of three independent recirculating aquaculture systems (RAS), each with a working seawater volume of 1100 L at a salinity of 35‰. Water within each RAS system was renewed at a rate of one complete exchange per day. Water quality was monitored daily, including dissolved oxygen, ammonia, ammonium, and nitrite levels, using an API Saltwater Master Test Kit and OxyGuard Polaris oxymeter. Tanks were covered with light-blocking material to control ambient light exposure and fitted with white LED lighting programmed to replicate the ambient seasonal photoperiod. Fish did not eat for the duration of the trial to standardise metabolic conditions, and stocking density was maintained at approximately 6 kg/m², with 14 fish allocated per tank at the start of the experiment. Aeration and circulation were maintained via diffusers installed in each tank, and additional filtration was provided using UV sterilisation units (Pond One ClearTec 5W), mechanical filters (cleaned daily), sump filtration, and dedicated biofilters. Water temperature was not artificially controlled and remained at an ambient average of approximately 18.5°C across the experimental period (Figure 2.1). Dissolved oxygen concentrations remained stable throughout the trial (Figure 2.1). Tanks were visually inspected daily for mortalities and any signs of ovulation.

The experiment was arranged as a balanced randomized block design, with each of the three RAS tanks receiving equal distributions of fish from all four treatments (0, 25, 50, 100 µg/kg GnRHa to avoid tank-specific bias (Table B5). Sampling occurred on Days 0 (control), 1, and 5 following hormonal administration. During sampling, fish were lightly anaesthetised using 2-phenoxyethanol prior to handling, resulting in minimal observable stress and rapid recovery following the procedure, after which ovarian biopsies were collected using a non-lethal aspiration technique. A flexible catheter attached to a syringe was inserted through the uro-genital vent and advanced into the ovarian cavity, allowing gentle suction to extract a small sample of ovarian tissue. Biopsy samples were transferred into petri dishes containing Sera's clearing solution for microscopic evaluation. Oocyte staging was performed using an Olympus CX23 compound microscope, and images were captured with an Olympus EP50 digital microscope camera for subsequent analysis.

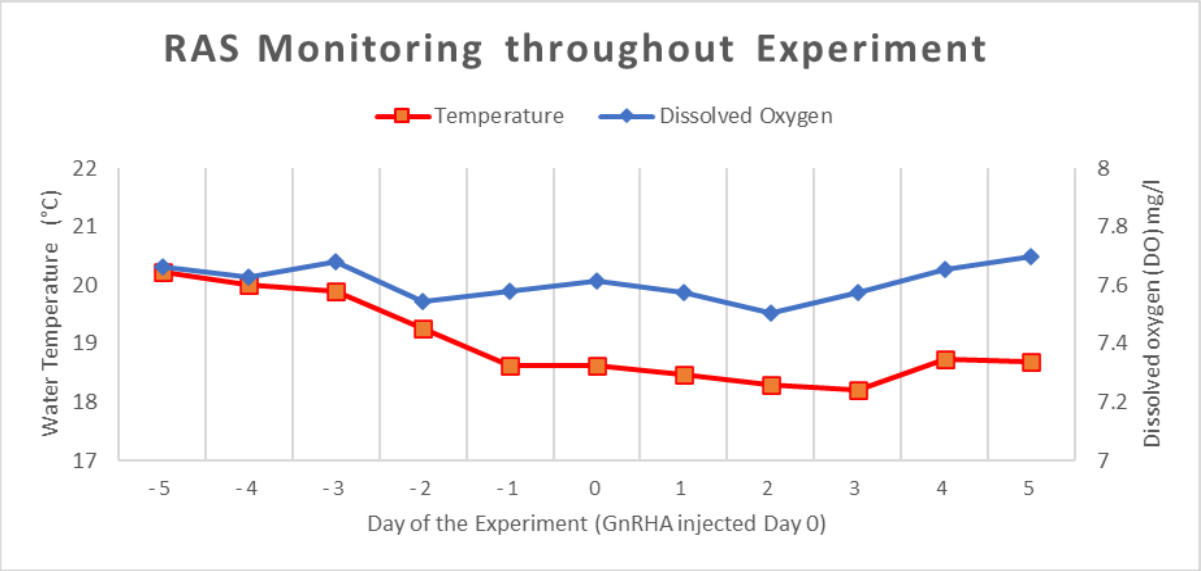


*Figure 2.1: Water temperature (°C) and dissolved oxygen concentrations (mg/L) recorded during the five days preceding and following GnRHa administration (Day 0)*

*Figure 2.2: The experimental RAS system, consisting of three separate recirculating tanks with dedicated biofiltration units.*

### 2.2.2 : GnRHa Administration

Each fish was tagged using a Mark III Fine Fabric (Hallprint.com) tagging gun, with individual number- and colour-coded tags inserted into the lateral dorsal musculature posterior to the head for subsequent identification, and individual body weight and length measurements were recorded at the time of tagging. After tagging, fish were transferred to recovery tanks before being returned to their respective RAS systems for the remainder of the trial (Figure 2.2).

At the start of the trial (Day 0), fish were randomly assigned to one of four treatment groups:

1. Saline sham control
2. GnRHa at 25 µg/kg body weight
3. GnRHa at 50 µg/kg body weight
4. GnRHa at 100 µg/kg body weight

The GnRHa stock solution was prepared at a concentration of 100 µg/mL by dissolving GnRHa powder into a laboratory-prepared marine teleost Ringer's solution formulated according to standard aquaculture physiological saline compositions (Wedemeyer, 1996). All injections were administered intramuscularly into the body wall adjacent to the gonad following anesthesia.

Prior to injection, fish were anesthetised using a 2-phenoxyethanol solution (5 mL/L). Once anesthetized, the total length and weight of each fish were recorded, and external photographs were taken for identification and later morphological analysis. Individual injection volumes were calculated based on body weight to deliver precise dosing for each fish. Sham control fish received weight-normalized saline injections matching the injection volume of the treatment groups.

### 2.2.3 : Sample Collection

Sampling was conducted on three separate days. On Day 0 (pre-injection), five untreated control fish were sampled to serve as a baseline reference group. Subsequent sampling was performed on Day 1 and Day 5 post-injection. On Day 1, a total of 16 fish were sampled across all treatment groups, while 20 fish were sampled on Day 5. Fish selected for sampling each day were chosen at random, with individuals evenly drawn from each treatment group and distributed proportionally across tanks to maintain consistent stocking densities throughout the trial.

Prior to sampling, fish were deeply anesthetised using 2-phenoxyethanol before being

humanely euthanized via decapitation. Sampling was conducted using a short-term experimental design, with four individuals from each treatment group sacrificed at day 0 and day 1 to capture the immediate transcriptional response, and all remaining fish sampled at the conclusion of the trial on day 5 to assess short-term treatment effects. Brain and pituitary tissues were dissected from each fish and stored at −80°C in RNAlater for RNA extraction, with these central tissues archived for potential future study and not included in the present analysis. All animal handling and manipulation procedures were conducted in accordance with the University of Waikato Animal Ethics Protocol 1149.

### 2.2.4 : qPCR Experimental Design

Due to the lack of an assembled *R. leporina* genome, primers were designed using database sequences from *Paralichthys olivaceus* (Japanese flounder), a closely related flatfish species. qPCR primer design was conducted by Dr. Steve Bird (University of Waikato). All qPCR assay preparation, validation, and experimental work were performed by the author. Primers were commercially synthesized to enable reliable amplification of target gene sequences while allowing flexibility to optimise assay conditions.

### 2.2.5 : Gonadal Tissue Sampling for qPCR

Following completion of the experimental phase and euthanasia, each fish was dissected, and a small section (~10 mm × 10 mm) of ovarian tissue was excised from the central region of the gonad. Subsections were prepared using a sterile scalpel on RNase-free foil to produce smaller sections suitable for both histological staging and RNA extraction, with all steps performed under strict precautions to minimise RNA degradation. Tissue sections designated for RNA extraction were transferred into RNase-free microcentrifuge tubes containing RNAlater, temporarily stored on ice during the sampling process, and subsequently transferred to −80°C for long-term storage, with samples used for qPCR analysis remaining unfixed throughout storage.

### 2.2.6 : RNA Extraction

RNA was extracted using the Direct-zol RNA Miniprep Kit (Zymo Research), following a modified protocol optimised for ovarian tissue samples. Frozen tissue samples were thawed, and individual tissue fragments (~5 mm × 5 mm) were processed as follows:

- Each sample was placed into bead tubes containing a 30:70 ratio of small to medium stainless-steel beads along with 800 µL of TRIzol reagent.

- Samples were homogenized using a Precellys Evolution homogenizer (Hard setting).
- Homogenates were centrifuged at 6000 rpm for 60 seconds, and the resulting supernatant was mixed with an equal volume of 100% ethanol before being transferred into Zymo-Spin 11012 columns.
- Columns were centrifuged (6000 rpm, 60 seconds), washed with 400 µL of RNA wash buffer, and centrifuged again.
- DNA digestion was performed by applying 80 µL of DNase I master mix (5 µL DNase I, 75 µL digestion buffer) to each column, incubating at room temperature for 15 minutes.
- Columns were washed twice with Direct-zol RNA pre-wash (400 µL each), followed by 700 µL of RNA wash buffer, with centrifugation at 6000 rpm after each step.
- RNA was eluted into RNase-free tubes by adding 50 µL of DNase-free water and centrifuging for 120 seconds at 6000 rpm.

RNA concentration and purity were assessed using a NanoDrop Microvolume. Spectrophotometer (1 µL sample volume). RNA yield (ng/µL) and purity ratios (A260/A280) for all samples are provided in Appendix B. Agarose gel electrophoresis was also performed to confirm RNA integrity and assess extraction quality (Figure 2.3). Samples failing to meet quality or concentration thresholds were re-extracted to ensure sufficient RNA quality for qPCR analysis. No inhibition testing was conducted at the extraction stage. All RNA samples were immediately converted into cDNA for stable long-term storage prior to downstream qPCR analysis.

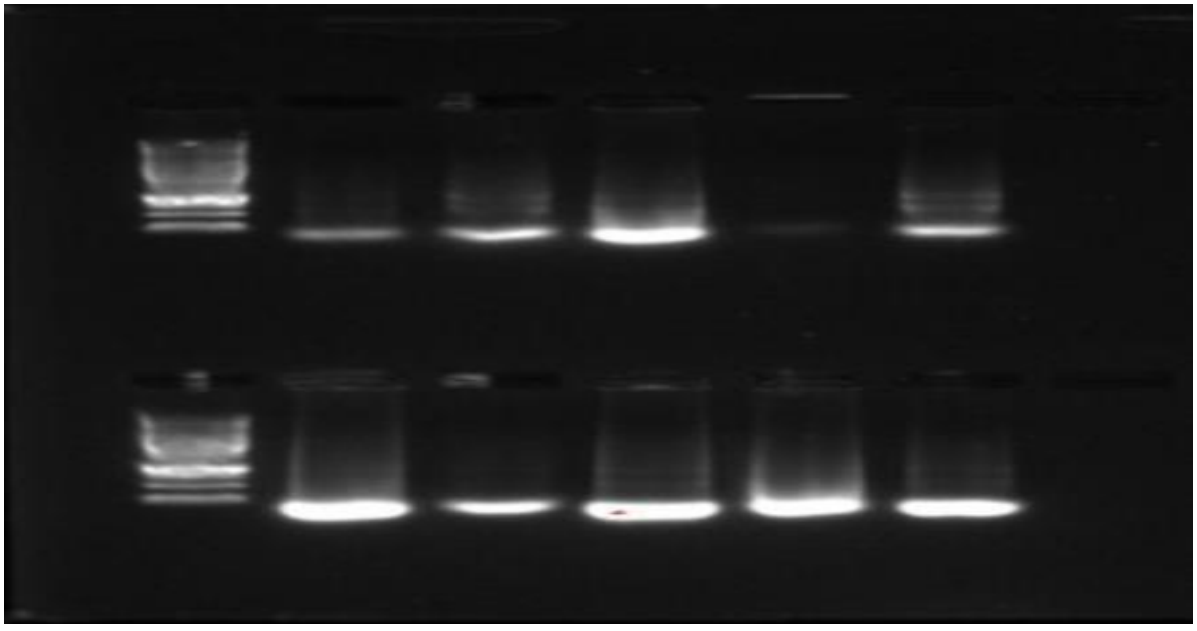

*Figure 2.3: The initial gel Electrophoresis Trace used to assess contamination during the RNA extraction process.*

### 2.2.7 : Reverse Transcription (cDNA Synthesis)

Following RNA extraction, reverse transcription was performed using the Quantabio qScript XLT cDNA Supermix kit to generate complementary DNA (cDNA) for downstream qPCR analysis. The 5X reaction buffer supplied in this kit includes optimized concentrations of $MgCl_2$, dNTPs (dATP, dCTP, dGTP, dTTP), recombinant RNase inhibitor, qScript reverse transcriptase, random primers, oligo(dT) primers, and stabilizers. This formulation allows for unbiased conversion of the extracted RNA pool into cDNA (Table 2.1).

The total reaction volume for each cDNA synthesis was 20 µL, consisting of 4 µL of Supermix, a calculated volume of RNA template, and RNase-free water. RNA input volumes were determined based on sample concentration measurements obtained during extraction (see Appendix B). For samples with low RNA yield, the maximum RNA input volume was capped at 16 µL.

*Table 2.1: Formula used for cDNA synthesis using Quantabio qScript XLT cDNA Supermix*

| Component | Volume |
|---|---|
| Supermix | 4 µL |
| RNA | 2 µL / (RNA concentration [ng/µL] / 1000) |
| RNase-free water | Adjusted to bring total volume to 20 µL |

Reaction mixtures were prepared in 0.2 mL RNase-free PCR tubes, gently vortexed, and centrifuged (6000 rpm for 60 seconds) to ensure complete mixing. The reverse transcription reaction was performed using a SimpliAmp Thermal Cycler under the thermal cycling conditions specified in Table 2.2.

*Table 2.2: Reverse transcription thermal cycling protocol*

| Step | Temperature | Time |
|---|---|---|
| Primer annealing | 25°C | 5 min |
| Reverse transcription | 42°C | 60 min |
| Enzyme inactivation | 85°C | 5 min |
| Hold | 4°C | ∞ |

### 2.2.8 qPCR Assay Design and Primer Validation

qPCR analysis targeted one gene of interest (*cyp19a1a*) and two reference genes (*tbp* and *rpl18*). All reactions were performed as singleplex reactions; no multiplexing was conducted.

qPCR assays were validated prior to experimental analysis to confirm amplification efficiency and specificity. The target genes, corresponding accession numbers, amplicon lengths, and validated amplification efficiencies are summarised in Table 2.3.

*Table 2.3: qPCR target genes, accession numbers, amplicon lengths, and assay efficiencies*

| Gene Target | Accession Number | Amplicon Length (bp) | Assay Efficiency (%) |
|---|---|---|---|
| *tbp* | XM_020098792 | 170 | 92 |
| *rpl18* | XM_020093129 | 176 | 90 |
| *cyp19a1a* | AB017182 | 142 | 91 |

In silico specificity screening was performed for all primers using NCBI Primer-BLAST and BLASTn to confirm sequence specificity against the intended gene targets. Due to the lack of an assembled *R. leporina* genome, primers were aligned against orthologous sequences from *Paralichthys olivaceus* (Japanese flounder), a closely related flatfish species. The predicted primer binding locations for each target gene are summarised in Table 2.4.

*Table 2.4: Primer binding locations for each gene target*

| Gene Target | Forward Primer Location | Reverse Primer Location |
|---|---|---|
| *tbp* | 715–737 bp | 856–837 bp |
| *rpl18* | 175–197 bp | 350–327 bp |
| *cyp19a1a* | 675–699 bp | 844–825 bp |

Amplicon binding sites were confirmed for each primer pair, with high sequence identity across all targets and no gaps observed in alignments. The *cyp19a1a* reverse primer aligned to AB017182.1 (837–856 bp, 90% identity), while *rpl18* primers aligned to XM_020093129.1 (forward: 175–197 bp, 96% identity; reverse: 327–349 bp, 96% identity). The *tbp* primers aligned to XM_020098792.1 (forward: 683–699 bp, 94% identity; reverse: 825–844 bp, 90% identity). A full summary of these alignments is presented in Appendix A, tables A1-A5.

The primer sequences used for qPCR amplification are shown in Table 2.5. All primers were synthesized by Macrogen (Seoul, South Korea), with purification performed via desalting prior to shipment. No modifications were made to the oligonucleotide sequences.

### 2.2.9 : qPCR Reaction Conditions

qPCR amplification was performed using PerfeCTa SYBR® Green FastMix (Quantabio, USA), which contains optimized reaction buffer components, including $MgCl_2$, dNTPs, AccuStart II Taq DNA polymerase, SYBR Green I dye, enzyme stabilizers, and proprietary performance-enhancing additives.

The reaction mix for each sample had a total volume of 20 µL, composed of 12 µL master mix and 8 µL cDNA template. cDNA was diluted 1:10 prior to addition. Primer working stocks were diluted 1:10 before use.

qPCR reactions were performed in MIC tubes and plates (Bio Molecular Systems, Australia), and thermal cycling was conducted on a Mic qPCR Cycler (Bio Molecular Systems). Each assay included at least 22 samples per plate, with paired technical replicates for each sample, plus no-template controls (NTC) and inter-plate calibrators (IPC). Sample 5 was designated as the IPC for plate normalization across runs within each gene assay.

Thermal cycling parameters are shown in Table 2.7. The annealing temperature was 60°C for all assays, except for the *tbp* assay, which was run at 59°C.

Each reaction underwent 40 amplification cycles to ensure full amplification and reliable fluorescence quantification. Each qPCR run was performed manually and took approximately 55 minutes to complete. Table 2.5 lists the primer sequences used for qPCR amplification.

*Table 2.5: Primer sequences used for qPCR analysis*

| Primer Target | Primer Direction | Sequence (5′–3′) |
|---|---|---|
| *cyp19a1a* | Forward | TCCTGGATGTTCCGATCAATGAG |
| *cyp19a1a* | Reverse | TCCTGGAATGCCGTCTTGTG |
| *rpl18* | Forward | CAGGAAAGAGCCAAAGAGTCAGG |
| *rpl18* | Reverse | ACATCTTCATCTTACGGATCAGGC |
| *tbp* | Forward | TGGGCTGTAAACTAGACTTGAAGAC |
| *tbp* | Reverse | CGACTGATCCTCGCTCTTGG |

*Table 2.6: qPCR reaction setup*

| Component | Volume (µL) | Dilution | Included in Master Mix? |
|---|---|---|---|
| Forward Primer | 1 | 1:10 | ✓ |
| Reverse Primer | 1 | 1:10 | ✓ |
| FastMix | 10 | n/a | ✓ |
| cDNA | 8 | 1:10 | ✗ |

*Table 2.7: qPCR thermal cycling parameters*

| Step | Temperature (°C) | Duration (s) |
|---|---|---|
| Denaturation | 95 | 15 |
| Annealing | 60* | 30 |
| Extension | 72 | 30 |
| Melt Curve | 95 | n/a |

### 2.2.10 qPCR Primer and Protocol Validation

Before the final qPCR runs were performed to obtain data for gene expression analysis, each primer set was experimentally validated to ensure both the specificity and reliability of the qPCR assays.

Several primer sets were designed and synthesized by Macrogen for each gene target. Initial test runs were conducted on these primer pairs to evaluate their amplification specificity, melt curve profiles, and potential formation of primer-dimers.

Figure A1 displays the validation testing for *tbp* primer sets. Four primer sets were compared for their performance, with Primer Set 3 (shown in purple) selected based on optimal melt curve specificity and absence of primer-dimer formation.

Figure A2 shows the validation of *rpl18* primer sets. Two primer sets were evaluated, and Primer Set 2 (blue) was selected due to its more consistent melt peak and reduced variability in melting temperature across replicates.

Figure A3 presents the validation for the *cyp19a1a* primer sets. Two candidate primer pairs were assessed, and Primer Set 2 (red) was selected, exhibiting consistent amplification and high specificity at the expected melt temperature.

Following primer selection, annealing temperatures were further optimized for each assay

using replicated test samples. Figure A4 shows the *rpl18* assay tested at 62°C, while Figure A5 displays the same assay at 60°C. The 60°C condition was chosen based on reduced variability and improved specificity.

For the *tbp* assay, Figures A6 and A7 show the annealing temperature validation at 61°C and 59°C, respectively. While both temperatures produced acceptable melt profiles, 59°C was ultimately chosen to maximize specificity, despite slightly higher intra-sample variability.

For the *cyp19a1a* assay, testing at 60°C produced strong and specific amplification with minimal variability across replicates. This annealing condition was therefore used for the final qPCR analysis.

The finalized primer sets and optimized thermocycling protocols developed through this validation process formed the foundation for all subsequent gene expression quantification.

### 2.2.11: Final qPCR Runs

Each plate used for the final qPCR analysis consisted of 20 biological samples, a no- template control (NTC), and an inter-plate calibrator (IPC). All samples and controls were performed in duplicate, and final Ct values for each sample were averaged across replicates. Sample 5 was selected as the IPC based on its high cDNA quality and stable expression observed throughout prior validation tests. Each qPCR plate was dedicated to a single gene assay.

The final qPCR runs demonstrated acceptable primer specificity and low intra-plate and inter-plate variability, providing confidence in the robustness of the data for downstream expression analysis.

In a subset of samples, initial qPCR runs produced no detectable amplification due to low template abundance, with cycle thresholds failing to reach detection limits at the standard cDNA dilution. These samples were therefore re-analysed using undiluted cDNA rather than the standard dilution, which successfully restored detectable amplification across all assays. Because both reference and target genes were treated identically for each sample and downstream analysis was based on relative expression, this adjustment is not expected to introduce systematic bias into the comparative results.

### 2.2.12 : qPCR Data Analysis

qPCR data acquisition and primary quality control were performed using micPCR Software V2.12.7 (Bio Molecular Systems), which was used to automatically calculate Ct values, assay efficiency, and inter-plate variability diagnostics, with melt-curve analysis conducted for each run to confirm amplification specificity and the absence of primer–dimer formation. Replicate consistency was assessed using the standard deviation between technical duplicates, and any sample displaying greater than 0.5 Ct deviation between replicates was rerun according to pre-defined quality control criteria, with no-template controls included on every plate to monitor contamination.

Inter-plate normalization was performed using an internal positive control (IPC; Sample 5) included on every plate for each gene assay, with IPC values used to correct minor between-plate variation. Relative gene expression of *cyp19a1a* was quantified using the ΔΔCt method with normalization to two reference genes, tbp and rpl18, which were selected based on prior validation of their stability in teleost gonadal tissue (Faheem et al., 2018; Marcoli et al., 2023). Ct values from all runs were exported into Microsoft Excel (Microsoft 365, Version 2401), and all ΔCt, ΔΔCt, and downstream statistical analyses were performed externally rather than within the micPCR software environment.

Statistical analyses were selected based on sample size and the structure of the experimental design, with pairwise comparisons of relative gene expression between treatment groups and sampling days performed using unpaired one-tailed t-tests with unequal variance where a directional biological response to treatment was expected, and comparisons involving oocyte developmental stage analysed using the non-parametric Kruskal–Wallis test due to small sample sizes and non-normal distribution of expression values across stages. All statistical tests were conducted using relative log2-transformed ΔΔCt values, with statistical significance assessed at $p \leq 0.05$, and the full Ct dataset for all assays provided in Appendix Table B3.

### 2.2.13 : Oocyte Classification and Measurement

Ovarian development was classified based on the most advanced cohort of oocytes present in each biopsy sample, following criteria adapted from Ellis-Smith (2022). Classification was informed by gross morphological and histological features, including oocyte size, translucency, presence of yolk granules or lipid droplets, and the position of the germinal vesicle.

Fish were assigned to one of three developmental stages:

- **Previtellogenic (PVO):** Early-stage oocytes that have been recruited from oogonia but have not yet begun active vitellogenesis. Fresh samples of these oocytes contain a central germinal vesicle and translucent cytoplasm which lacks obvious intracellular inclusions. The nucleus is comparatively large relative to the overall oocyte size and the entire follicle typically appears noticeably smaller than subsequent stages.

- **Vitellogenic (VIT):** Oocytes undergoing active vitellogenesis, marked by the accumulation of yolk granules and possibly some lipid inclusions. This stage is driven by estradiol-induced hepatic vitellogenin synthesis and results in greater oocyte opacity and grainy appearance of the oocyte along with an obvious increase in size compared to PVO.

- **Final oocyte maturation (FOM):** The terminal stage of oocyte development prior to ovulation, characterized by a physiological shift from yolk accumulation to the completion of the first meiotic division. Visual hallmarks include germinal vesicle migration toward the periphery of the oocyte, yolk coalescence with a more translucent appearance, obvious lipid droplets and a further increase in size. This transition is regulated by maturation-inducing progestins and prepares the oocyte for ovulation.

To assess oocyte diameter, biopsy samples were dispersed in Petri dishes and treated with Serra's clearing solution. Digital images were captured under an Olympus SZ61 stereo microscope and paired with a 2.0 mm micrometer slide for scale calibration. Oocyte diameters were measured using ImageJ software, with two perpendicular measurements taken for each oocyte to account for shape asymmetry. The average of these two values was used to calculate individual oocyte diameters. Up to 50 oocytes were measured per fish to ensure representative sampling of each individual's ovarian profile.
These classification and measurement procedures were used to explore relationships between developmental stage, *cyp19a1a* gene expression, and visual gonadal metrics. Oocyte classification and measurement data can be found in the Appendix Table B4.

## 2.3: qPCR Data Analysis Results

### 2.3.1 : Fold changes in *cyp19a1a* expression

This section presents the results of the qPCR analysis of ovarian *cyp19a1a* expression in *Rhombosolea leporina* following administration of exogenous GnRHa. Changes in gene expression are reported as normalized Log2 fold changes relative to baseline wild-type levels and are presented across treatment doses and sampling time points. The results first describe baseline expression prior to hormonal induction (Day 0), followed by the acute transcriptional response at Day 1 and the short-term response observed at the conclusion of the experiment on Day 5.

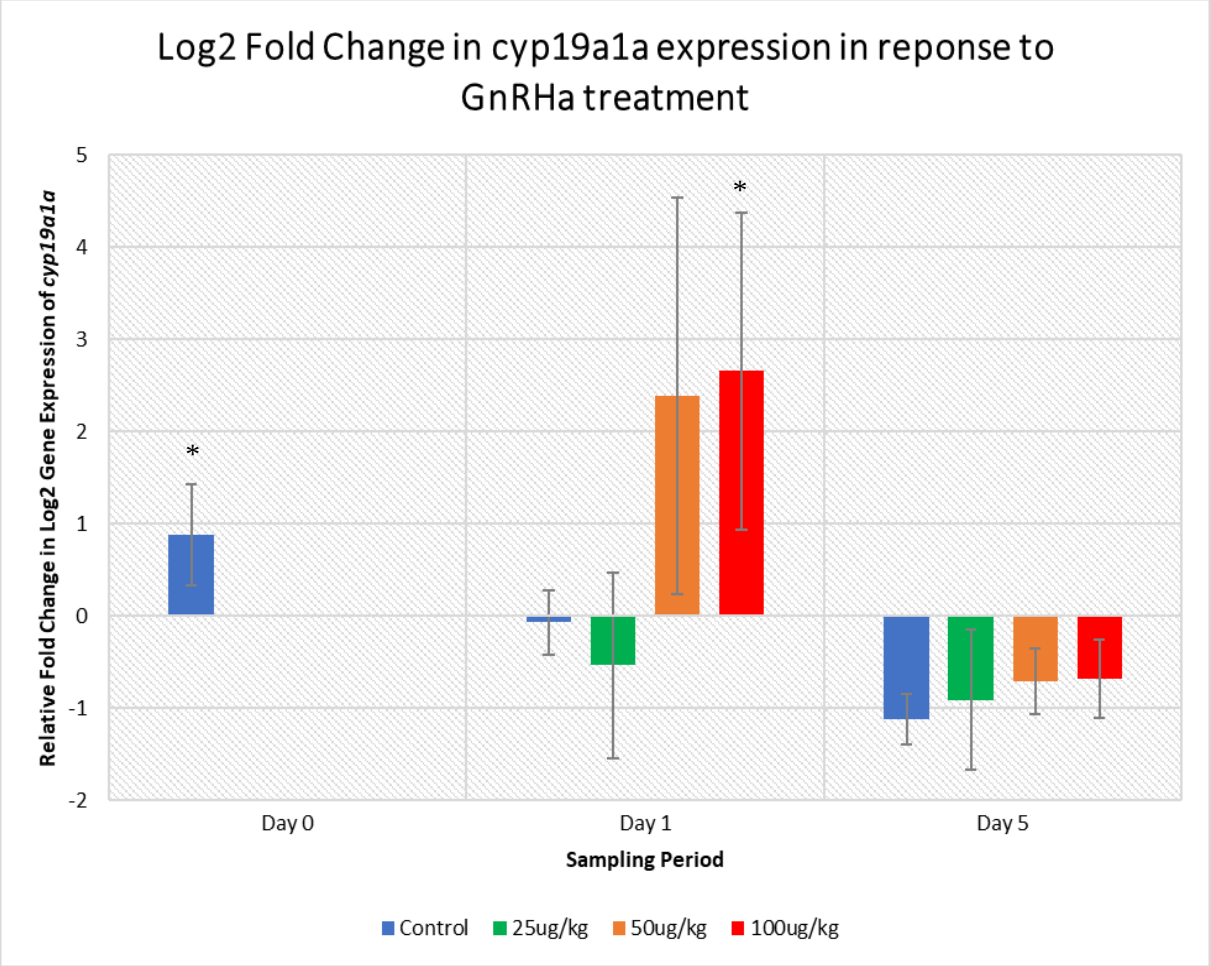


*Figure 2.4: Average log2-normalized relative fold change in cyp19a1a expression in R. leporina across GnRHa dosage treatments over the 5-day experimental period, with asterisks indicating a significant within-treatment difference between Day 1 and Day 5 ($p \leq 0.05$).*

### 2.3.2 : Baseline Expression Prior to Hormonal Induction (Day 0)

An initial set of baseline samples ($n$ = 5) was collected on Day 0 prior to GnRHa treatment to represent wild-type expression levels in fish minimally exposed to the aquaculture system. These individuals were sampled directly after arrival from the wild, with limited acclimation

time, providing a reference for natural *cyp19a1a* expression.

The average normalized relative fold expression of *cyp19a1a* on Day 0 was 0.88 ± 1.22 (SD). Individual values ranged from −0.58 to 2.40, indicating natural variability in baseline aromatase expression among wild-caught individuals**.**

### 2.3.3 : Acute Expression Response at Day 1 Post-GnRHa Treatment

On Day 1 post-treatment, gene expression of *cyp19a1a* exhibited a dose-dependent response to GnRHa administration (Figure 2.4)

The 100 µg/kg treatment group ($n$ = 4) displayed the highest average expression, with a normalized relative Log2 fold change of 2.65 (SD = 3.44). The 50 µg/kg treatment ($n$ = 3) showed a slightly lower mean expression of 2.38 (SD = 3.72). Statistical comparison using unpaired one-tailed t-tests with unequal variance revealed that neither the 100 µg/kg nor 50 µg/kg treatments were significantly different from the Day 1 control group ($n$ = 4), with p-values of 0.10 and 0.18, respectively.

The 25 µg/kg treatment group ($n$ = 4) demonstrated the lowest gene expression among treated groups, with a mean normalized Log2 fold change of −0.53 (SD = 2.01). The Day 1 control group exhibited a mean expression of −0.07 (SD = 0.70). No significant difference was observed between the 25 µg/kg treatment and control ($p$ = 0.34).

Pairwise comparisons between treatment groups showed no statistically significant differences at the 0.05 level, though trends were observed:

- 50 µg/kg vs. 100 µg/kg: $p$ = 0.46
- 50 µg/kg vs. 25 µg/kg: $p$ = 0.15
- 100 µg/kg vs. 25 µg/kg: $p$ = 0.08

Overall, mean *cyp19a1a* expression tended to increase with higher GnRHa dosage on Day 1, with higher average values observed in the 50 µg/kg and 100 µg/kg groups relative to lower doses and controls (Figure 2.4); however, this pattern was highly variable and was not supported by statistically significant differences between treatment groups. Substantial intra-group variability was present, with individuals exhibiting either strong or minimal transcriptional responses to GnRHa. The highest individual expression values were observed in single fish from the 100 µg/kg (normalized fold change 6.27) and 50 µg/kg (4.62) groups, while only one individual within the 25 µg/kg group showed elevated expression (2.25), with remaining individuals clustered near or below baseline levels.

### 2.3.4 : Sustained Expression Response at Day 5 Post-GnRHa Treatment

By Day 5, *cyp19a1a* expression declined across all treatment groups, including controls, with mean expression values falling below zero relative to Day 0 baseline. The control group exhibited the lowest expression (−1.11 ± 0.61), followed by the 25 µg/kg group (−0.91 ± 0.31). The 50 µg/kg and 100 µg/kg groups showed comparatively higher expression at −0.71 ± 0.70 and −0.68 ± 0.11, respectively. Although a slight positive trend with increasing GnRHa dose remained, overall expression was suppressed in all groups by Day 5.

Paired comparisons of Day 1 and Day 5 expression were conducted for each group. The control group declined from −0.07 to −1.11 ($p = 0.03$). The 25 µg/kg group showed a reduction from −0.53 to −0.91 ($p = 0.31$), and the 50 µg/kg group from 2.37 to −0.71 ($p = 0.07$). The 100 µg/kg group declined from 2.65 to −0.68 ($p = 0.03$).

### 2.3.5 : Expression of *cyp19a1a* in relation to ovarian development.

The highest mean *cyp19a1a* expression was observed in FOM-stage fish, with a mean $\log_2$ expression of approximately 1.41. Expression was lower in VIT-stage fish, averaging around 0.83, and was lowest in PVO-stage fish, with a mean of approximately −1.85 (Figure 2.5).

Although this trend suggests a progressive increase in *cyp19a1a* expression across advancing oocyte stages, a Kruskal–Wallis test indicated that these differences were not statistically significant ($H = 1.22$, $p = 0.545$). This outcome may reflect substantial individual variability and limited statistical power. As such, the results are presented descriptively to illustrate the observed stage-associated variation in *cyp19a1a* expression.

Notably, the ordering of expression levels across developmental stages aligns with established roles of aromatase and estradiol in promoting vitellogenesis and supporting late-stage oocyte maturation. Although not significant, the clear directional trend from suppressed expression in PVO-stage fish to elevated expression in FOM-stage fish provides supporting evidence that hormonal responsiveness to GnRHa may be stage-dependent. Further investigation with larger sample sizes could help clarify whether *cyp19a1a* expression reliably predicts or reflects oocyte developmental state following induction.

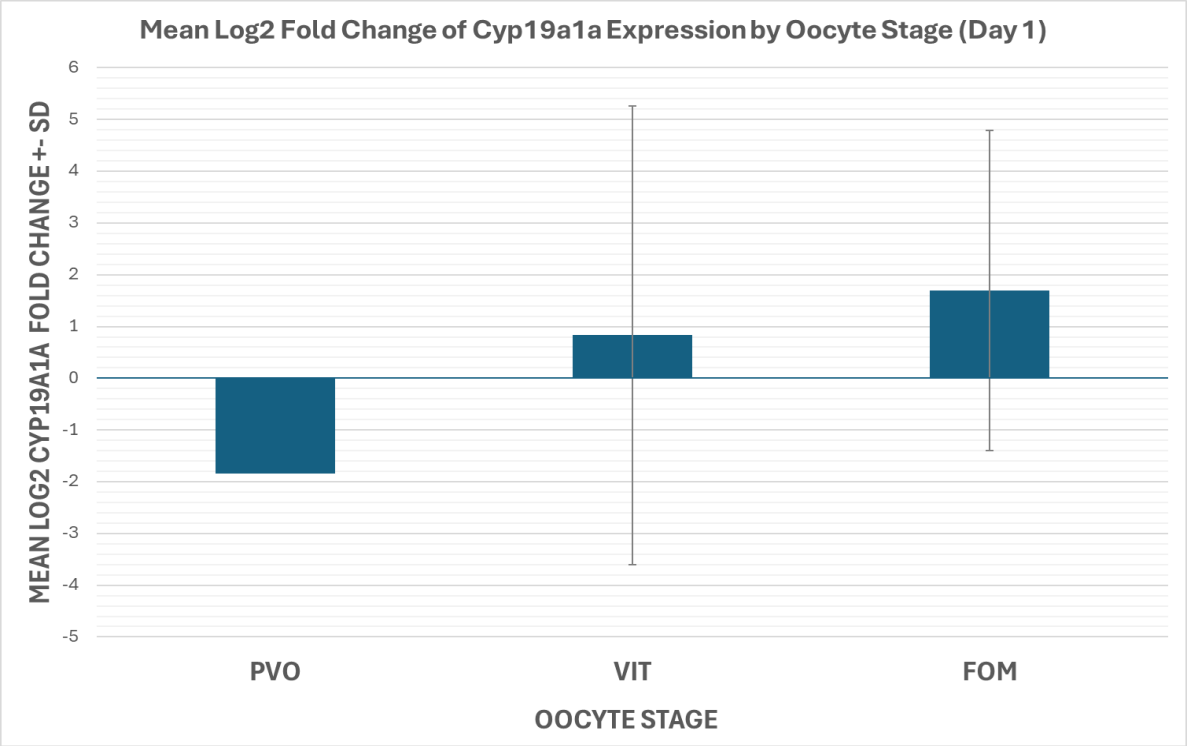


*Figure 2.5: Mean $Log_2$-normalized fold change in ovarian cyp19a1a expression across oocyte developmental stages (PVO, VIT, FOM) in R. leporina at 24 hours post- GnRHa injection. Only treated individuals sampled on Day 1 are included.*

## 2.4: Discussion

### 2.4.1: Key Findings

This study aimed to evaluate whether exogenous GnRH analog (GnRHa) treatment influences ovarian *cyp19a1a* gene expression in *Rhombosolea leporina*. As *cyp19a1a* encodes ovarian aromatase, the rate-limiting enzyme in $E_2$ biosynthesis, its expression provides a useful indicator of steroidogenic activity during oocyte development. This work represents the first examination of ovarian *cyp19a1a* expression in *R. leporina* and contributes baseline molecular data for this species in an aquaculture context.

Following GnRHa administration, mean *cyp19a1a* expression showed higher average values in the 50 µg/kg and 100 µg/kg treatment groups on Day 1 relative to baseline; however, these differences were not statistically significant and were accompanied by substantial inter-individual variability. By Day 5, expression levels had declined across all groups, including controls.

Collectively, the results indicate that while *R. leporina* is capable of mounting a short-term transcriptional response to GnRHa, the response was highly variable and transient under the conditions of this study, limiting its reliability for consistent induction at the doses tested.

### 2.4.2 : Acute Activation of *cyp19a1a* Expression and Early BPG Axis Stimulation

The short-term upregulation of *cyp19a1a* observed at 24 hours is consistent with early-stage BPG axis activation following GnRHa injection. GnRHa binds to pituitary GnRH receptors and primarily induces luteinizing hormone (LH) release, which plays a key role in stimulating final oocyte maturation (FOM). Some species may also exhibit FSH release, though this is not the primary mechanism of action (Zohar & Mylonas, 2001). This study focused on *cyp19a1a* as a marker of vitellogenesis rather than FOM, so downstream events such as ovulation or progestin induction were not assessed.

Although statistical significance was not observed, the ~2.5–3-fold increase in *cyp19a1a* expression suggests that GnRHa administration may induce transient activation of steroidogenic pathways in some individuals. Short-term aromatase upregulation may transiently elevate estradiol ($E_2$) synthesis, which could stimulate hepatic vitellogenin production and support early oocyte growth in hormonally responsive fish. However, substantial variability between individuals prevents firm conclusions regarding the reliability of this endocrine stimulation.

Notably, *cyp19a1a* upregulation was dose-dependent, with minimal change observed in the 25 µg/kg group. This suggests that *R. leporina* may require higher GnRHa doses to adequately stimulate pituitary output. For example, Berlinsky et al. (1996) reported that winter flounder required ≥50 µg/kg GnRHa to induce gonadal development, with lower doses proving ineffective. Similarly, in Senegalese sole (*Solea senegalensis*), low GnRHa doses (e.g., 5 µg/kg) failed to induce effective reproductive activation, indicating a clear dose threshold for endocrine responsiveness (Agulleiro et al., 2006). This potential threshold sensitivity may reflect variation in pituitary GnRH receptor density or the pituitary's gonadotropin reserve capacity at the time of induction, as has been described in other fish species. Sustained-release GnRHa studies have demonstrated that doses below a species-specific threshold often fail to induce significant gonadotropin release, whereas doses at or above this threshold result in reliable endocrine activation without receptor desensitisation (Zohar & Mylonas, 2001).

### 2.4.3 : Rapid Regression of Expression and Limitations of Single GnRHa Injection

By Day 5, *cyp19a1a* expression had declined across all treatment groups, including controls, indicating that the stimulatory effect of GnRHa was not sustained. This transient response is consistent with previous flatfish studies, including winter flounder (*Pseudopleuronectes americanus*) and southern flounder (*Paralichthys lethostigma*), where injection-based GnRHa delivery typically induces only short-lived endocrine activation lasting approximately 24–72 hours (Denson et al., 2007; Guzmán et al., 2009), as well as in Senegalese sole (*Solea senegalensis*), where single low-dose injections failed to produce sustained reproductive activation (Agulleiro et al., 2006). In contrast, sustained-release GnRHa implants have demonstrated more consistent success by prolonging pituitary activation and supporting ongoing steroidogenesis across multiple marine teleost species (Selvaraj et al., 2021).

A single GnRHa injection is therefore unlikely to maintain elevated $E_2$ levels over the extended period required to support vitellogenesis, which is a metabolically intensive process that depends on continuous aromatase activity over several weeks (Ramos-Júdez et al., 2022). While sustained-release formulations may extend endocrine stimulation beyond injection-based methods, their effect is still generally limited to one to two weeks (Guzmán et al., 2009). Nevertheless, prior work in *R. leporina* suggests that such delivery systems can improve reproductive outcomes and help overcome developmental arrest in wild-caught broodstock (Ellis-Smith, 2022).

### 2.4.4 : Inter-Individual Variability and Non-Responders

Marked inter-individual variability in *cyp19a1a* expression was observed across all treatments, including apparent non-responders who exhibited minimal changes despite GnRHa administration. Such variability is widely documented in captive flatfish, where differences in gonadal stage, spawning history, genetic background, and endocrine sensitivity produce inconsistent responses to hormonal induction (Luckenbach, 2005; Watanabe et al., 2005; Ramos-Júdez et al., 2022).

The high variability observed likely reflects underlying biological heterogeneity among individuals, compounded by the limited replication available in this early stage broodstock investigation. In addition, some fish appeared to contain atretic follicles alongside healthy vitellogenic oocytes. These fish also had variable *cyp19a1a* expression which aligned with the range of values observed in fish without atresia. Nonetheless, the presence of atretic

oocytes may indicate the physiological effects of capture stress. Non-invasive ovarian staging tools such as ultrasound or visual gonadosomatic indices may help reduce this variability in future work by targeting hormonally responsive developmental windows (Næve et al., 2018). This interpretation is supported by the results of the oocyte stage analysis, which showed that fish at more advanced ovarian stages tended to exhibit higher *cyp19a1a* expression following GnRHa injection, although this pattern was not statistically significant.

### 2.4.5 : Stress Effects and HPI-BPG Crosstalk

The observed decline in *cyp19a1a* expression within controls suggests that factors beyond GnRHa treatment influenced aromatase regulation. Handling stress and environmental disturbance likely activated the hypothalamic-pituitary-interrenal (HPI) axis, elevating plasma cortisol, which is known to suppress the BPG axis in teleosts via feedback inhibition at multiple levels (Pankhurst & Van der Kraak, 1997; Haddy & Pankhurst, 1999). Cortisol levels as low as 10–30 ng/mL have been associated with measurable reproductive suppression in fish under experimental conditions).

Mechanistically, elevated cortisol may inhibit hypothalamic GnRH release, suppress pituitary gonadotropin secretion, and directly downregulate ovarian aromatase expression, ultimately reducing both $E_2$ synthesis and oocyte development (Schreck et al., 2001). Thus, even minor chronic stress could have contributed to expression variability and regression, emphasizing the need for strict environmental control during broodstock management and experimentation (Murugananthkumar & Sudhakumari., 2022).

### 2.4.6 : *cyp19a1a* Expression in Relation to Ovarian Developmental Stage

Analysis of *cyp19a1a* expression across ovarian developmental stages did not reveal a statistically significant difference although mean expression values varied between groups. Expression was highest in females at final oocyte maturation (FOM), followed by those in the vitellogenic (VIT) stage, with the lowest expression observed in previtellogenic (PVO) individuals. However, all stages exhibited substantial inter-individual variability, and overlapping ranges limited the ability to draw firm conclusions regarding stage-dependent regulation.

Notably, the ordering of expression levels across developmental stages aligns with established roles of aromatase and estradiol in promoting vitellogenesis and supporting late-stage oocyte maturation. Although not significant, the clear directional trend from suppressed

expression in PVO-stage fish to elevated expression in FOM-stage fish provides supporting evidence that hormonal responsiveness to GnRHa may be stage-dependent. Further investigation with larger sample sizes could help clarify whether *cyp19a1a* expression reliably predicts or reflects oocyte developmental state following induction.

This variability likely reflects the asynchronous nature of oocyte development in batch-spawning flatfish such as *R. leporina*, where multiple oocyte cohorts at different stages may coexist within the ovary (Koverman, 2018; Ellis-Smith, 2022). In such cases, aromatase expression may reflect the cumulative steroidogenic activity across overlapping cohorts, rather than being restricted to the most advanced oocytes present at sampling. Consequently, elevated *cyp19a1a* expression in FOM-stage fish may reflect the development of multiple cohorts of oocytes at different stages of vitellogenesis rather than direct involvement in final maturation.

This interpretation aligns with established steroidogenic dynamics in flatfish and other teleosts. During vitellogenesis, increased aromatase activity supports estradiol ($E_2$) synthesis, promoting hepatic vitellogenin production for yolk accumulation (Nagahama & Yamashita, 2008; Zohar & Mylonas, 2001). In classical salmonid models that have synchronous ovarian development with a single cohort of oocytes, $E_2$ production typically declines at the end of vitellogenesis in favour of progestin synthesis, particularly 17,20β-dihydroxy-4-pregnen-3-one (17,20β-P), the primary maturation-inducing steroid (MIS), increases. This shift is mediated by elevated pituitary LH secretion and upregulation of ovarian *20β-hsd*, which collectively drive final oocyte maturation through germinal vesicle breakdown and ovulation (Weltzien et al., 2004; Nagahama & Yamashita, 2008).

Although this maturational steroid shift is well described in other flatfish, the absence of these measurements in the present study limits evaluation of this FOM marker. Future research incorporating both aromatase and progestin pathway markers such as *20β-hsd* would allow more definitive resolution of the endocrine transitions underlying oocyte maturation in *R. leporina*.

The observed trend of increasing *cyp19a1a* expression from PVO to VIT to FOM suggests that oocyte developmental stage may influence hormonal responsiveness, even though the results were not statistically significant. This reinforces the possibility that GnRHa-induced aromatase upregulation is stage-dependent and highlights the value of integrating ovarian staging into future broodstock induction protocols.

### 2.4.7 : Implications for Broodstock Management and Hormonal Induction

Taken together, these findings highlight both the potential and limitations of single-dose GnRHa injection for managing reproductive dysfunction in *R. leporina*. While higher GnRHa doses may produce short-term stimulation of steroidogenic activity, sustained reproductive improvement likely requires longer-duration endocrine support via implants or repeated dosing (Guzmán et al., 2009). An essential action of GnRHa treatment is the stimulation of pituitary LH release and its downstream effect on MIS-mediated induction of FOM. To fully understand the efficacy of hormonal induction on reproduction in this species, it will be necessary to further characterize its effects on FOM using markers such as gonadal ovarian 20β-hsd expression.

Moreover, effective broodstock management will require careful integration of hormonal induction with optimized environmental control, stress minimization, and accurate ovarian staging to better synchronize hormonal interventions with underlying reproductive readiness (Murugananthkumar & Sudhakumari., 2022; Næve et al., 2020). The observed association between higher *cyp19a1a* expression and advanced oocyte stage supports the value of incorporating staging assessments prior to treatment, enabling selection of individuals most likely to respond to induction. The development of such integrated protocols represents a key step in establishing reliable captive breeding programs for *R. leporina* and related flatfish species.

# Chapter 3 – Developing a Visual Gonadosomatic Index

### 3.1: Experimental Aims

The development of a non-invasive, reliable method for assessing gonadal maturation in *R. leporina* would represent a significant advantage for broodstock management in aquaculture. Current methods for evaluating sexual development in teleosts, such as gonadal biopsy or post-mortem GSI calculation, are either invasive or lethal. These approaches can induce stress, compromise gamete quality, or reduce broodstock viability, all of which are major constraints when working with wild-caught fish during domestication efforts.

This study explores the feasibility of a novel Visual Gonadosomatic Index (VGSI), a non-lethal method based on photographic imaging of the internal gonads through the semi-translucent ventral surface of *R. leporina*. Given the species' flattened morphology and comparatively superficial gonadal position in relation to the body-wall, it is hypothesized that a backlit visual assessment of the ovary could offer practical insights into reproductive status. To evaluate the VGSI concept, a series of morphometric measurements were obtained from backlit photographs of live female flounder. These were compared against established reproductive markers including oocyte diameter and developmental stage. The goal was to determine whether any visual metrics, such as gonad area or length relative to body dimensions, were significantly associated with reproductive maturation and therefore useful as predictive indicators in a hatchery context.

### 3.2: Literature Review

#### 3.2.1: The Gonadosomatic Index in Reproductive Assessment

A comprehensive understanding of reproductive physiology is essential for effective fishery management, conservation, and the development of captive breeding programmes in aquaculture. Gonadal development reflects a species' adaptive reproductive strategy, shaped by ecological pressures such as energy availability (Wootton, 1985), environmental seasonality (Munro et al., 1990), and reproductive competition (Essington et al., 2000). In aquaculture settings, reproductive dysfunctions often arise when wild-caught broodstock are held under artificial conditions that disrupt these natural cues (Poortenaar et al., 2001; Imanaga et al., 2014).

Fecundity, defined as the number of ripening oocytes in a female prior to spawning, is a key indicator of reproductive potential (Bagenal, 1978). It correlates strongly with body mass, with gonadal weight typically increasing as spawning approaches (Buckley et al., 1991; Bromage et al., 1990). However, fecundity is not strictly quantitative. Larger oocytes tend to yield higher fertilisation success (Kjørsvik et al., 2003), stronger larvae (Kohn & Symonds., 2012), and better-quality eggs overall (Jeuthe et al., 2013; Stuart et al., 2020), creating a trade-off between egg number and egg quality (Duarte & Alcaraz., 1989).

Several fecundity indices have been developed to accommodate different reproductive strategies. For example, batch fecundity reflects the number of eggs spawned per ovulation event, while annual potential fecundity estimates the number of oocytes that could develop in a given season, irrespective of actual spawning (Hunter et al., 1985; Hunter, 1992). In batch-spawning species, later batches often show diminished oocyte yields (Fitzhugh et al., 2012). For fish that fail to undergo final oocyte maturation in captivity, relative fecundity indices based on oocyte counts per unit body mass can still provide useful insights (Contreras-Sanchez et al., 1998; Rasines et al., 2012; Fakriadis et al., 2020).

Gonadal development can be evaluated using either microscopic or macroscopic techniques. Microscopic staging relies on ovarian biopsies and histological or morphological classification of oocyte development (Ellis-Smith, 2022). Macroscopic assessments typically involve the gonadosomatic index (GSI), calculated as the ratio of gonad weight to total (or somatic) body weight (Brown-Peterson and Warren, 2002). In practice, these approaches are often used together to improve diagnostic resolution (Murua et al., 2003).

Despite its utility, traditional GSI requires euthanasia, which limits its application in broodstock management. This constraint has driven interest in non-invasive alternatives that can approximate gonadal status without compromising fish viability. This is the rationale for exploring visual indices such as VGSI.

### 3.2.2 : Gonadosomatic Trends in Flatfish

In *R. leporina*, the spawning season typically extends from September to November. Colman (1973) reported that total fecundity increases with body size, ranging from approximately 250,000 eggs in 30 cm females to over 1.25 million eggs in individuals measuring 45 cm. However, this relationship was more strongly correlated with ovary weight than with body length alone, and considerable variation in fecundity was observed among fish of similar size and gonadal mass.

Comparable findings have been reported in other flatfish species. In *Pseudopleuronectes*

*americanus* (winter flounder), the size of mature females was positively associated with gonadosomatic index (GSI), egg size, and overall gamete viability (Buckley et al., 1991). Notably, females that spawned later in the season produced smaller eggs with reduced larval survival, although GSI values remained relatively stable across the spawning window. In *Psettodes erumei* (Indian halibut), seasonal fluctuations in GSI values were not observed in females (Yoshikawa et al., 2012), indicating possible species-specific differences in reproductive investment and timing.

Further evidence for GSI-based reproductive monitoring comes from studies on *Achirus lineatus* (Lined sole), where seasonal patterns of gonadal development were tracked using a combination of GSI values and histological staging (Oliveira and Fávaro, 2010). Female *A. lineatus* exhibited sexual size dimorphism, with larger average and maximum body sizes than males, a likely outcome of fecundity-driven selective pressures. Similar patterns were reported in first-generation ($F_1$) *Platichthys flesus* (European flounder), where female GSI values increased significantly during the three months preceding the spawning season and peaked during the reproductive period. In contrast, male *P. flesus* showed a bimodal GSI pattern, with a pronounced early-season peak followed by regression and a secondary rise just before spawning (Aydin et al., 2023). These findings highlight the possibility of asynchronous gonadal development between sexes in batch-spawning flatfish.

GSI profiling has also been used to estimate spawning periods in other teleost species. Texeira et al. (2010) combined GSI measurements with oocyte staging to determine the timing of reproductive activity in *Lutjanus analis* (Mutton Snapper), demonstrating the value of integrating macroscopic and microscopic indicators for seasonal characterisation.

In *R. leporina*, a unique morphological trait may facilitate a novel, non-lethal approach to reproductive assessment. The dorsoventrally flattened body and superficial location of the gonads enable internal structures to be illuminated using a backlighting technique. Individual fish can be placed over a lit surface, allowing the gonads to be visualised and photographed through the ventral body wall. This method permits rapid, non-invasive analysis with minimal handling stress. The current study evaluates this imaging approach as the basis for a Visual Gonadosomatic Index (VGSI), intended to provide a practical, non-destructive alternative for assessing ovarian development in *R. leporina* broodstock.

## 3.3: Visual Gonadosomatic Imaging Methods

To evaluate the feasibility of a Visual Gonadosomatic Index (VGSI) as a non-invasive reproductive assessment tool, live imaging was conducted on anaesthetized *R. leporina* using a backlighting technique (Figure 3.1). Fish were gently placed in a shallow plastic tub positioned over a ridged LED strip-light, which illuminated internal anatomical structures through the translucent ventral body wall. Photographs were taken from a consistent height (~30 cm above the fish) using a 48MP wide-angle camera (Redmi Note 10). Each image included a metal ruler for internal scale calibration and was captured under identical lighting and background conditions to minimise environmental variability.

The resulting images were analysed using ImageJ software (v1.54h). Two types of visual indices were developed: one based on relative gonad area (Visual Size Gonadosomatic Index, VSGSI), and another based on relative gonad length (Visual Length Gonadosomatic Index, VLGSI). Both indices were calculated by comparing the size or length of the visible gonad to the corresponding total fish dimension in the same image. This ratio-based approach allowed comparisons across fish of different sizes while accounting for the biological relationship between somatic growth and reproductive development (Table 3.1).

*Figure 3.1: Ventral photographs of R. leporina showing the female gonad on the left and the male gonad on the right, with internal structures illuminated from below using a backlighting setup.*

To reduce analytical error, several standardized rules were applied. External fins were excluded from fish length and area measurements due to inconsistent extension across images, and gonad measurements were limited to visible, illuminated structures. Each metric was measured in triplicate per fish, with average values used for final calculations. If high variability was observed among replicates, measurements were repeated until consistency was achieved, using a coefficient of variation (CV) threshold of <10%.

### 3.3.1 : Size GSI Methodology

The Visual Size Gonadosomatic Index (VSGSI) was calculated by measuring the two-dimensional area of the illuminated gonad and the corresponding external area of the fish body, excluding fins, using the same individuals maintained under the identical holding and experimental conditions as those used in the gene expression trials described in Chapter 2. Using the freehand polygon selection tool in ImageJ, both the gonad and body outline were traced manually (Figure 3.2). Each measurement was repeated three times, and average values were used in downstream analysis. If replicate values differed substantially (CV > 10%), all three measurements were repeated to ensure accuracy and consistency.

The final VSGSI value for each fish was calculated as follows:

**VSGSI = (Average Gonad Area) / (Average Body Area)**

This index provided a standardized representation of internal gonad development relative to somatic size and was compared statistically to oocyte diameter, fish weight, and histological maturity stage using correlation and regression analysis as described above, to determine whether this non-invasive size-based metric could meaningfully reflect reproductive status and assist in decision-making in broodstock management (Figure 3.3).

*Figure 3.2: ImageJ-based analysis of internal gonad area used to calculate the Visual Size Gonadosomatic Index (VSGSI) in R. leporina. The highlighted region (outlined in red and shaded in blue) denotes the manually traced ovarian tissue used for gonad area measurement relative to total body area.*

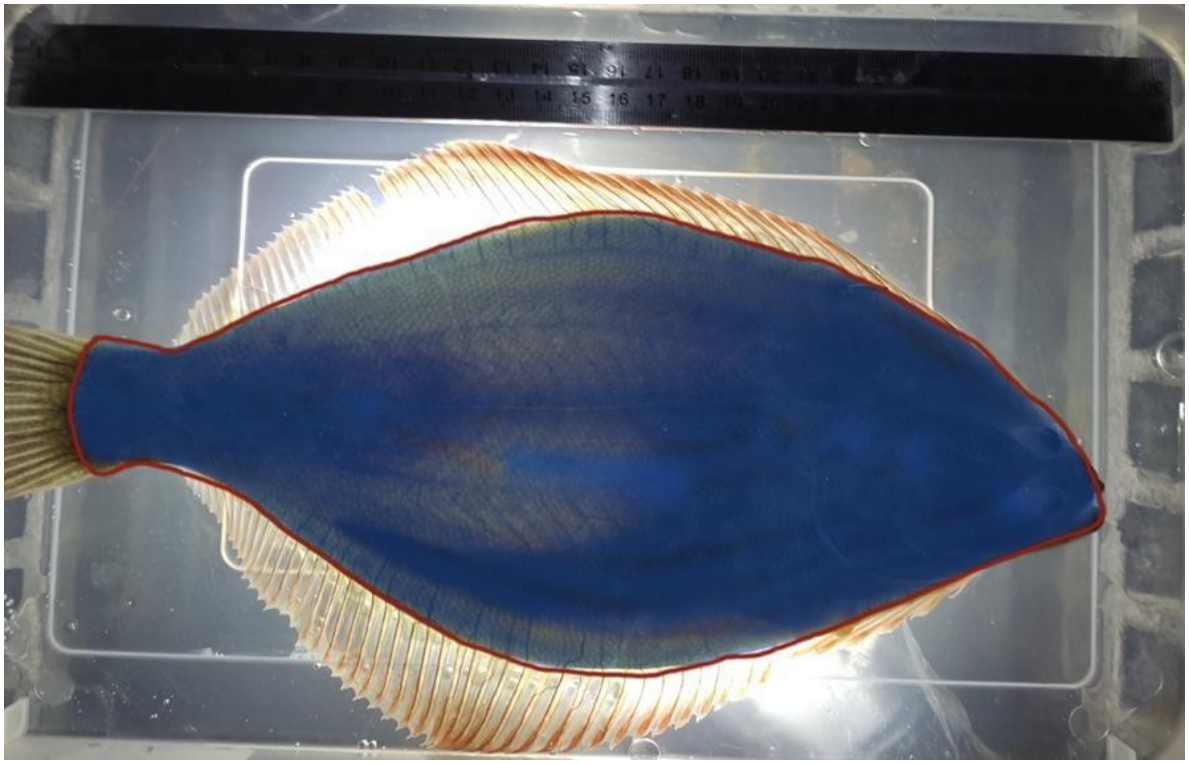

*Figure 3.3: ImageJ-based analysis of external body area used to calculate the Visual Size Gonadosomatic Index (VSGSI) in R. leporina. The highlighted region (outlined in red and shaded in blue) denotes the traced external body area used for normalization of gonad area measurements, with fins excluded from the analysis.*

### 3.3.2 : Length GSI Methodology

The Visual Length Gonadosomatic Index (VLGSI) was developed to provide a non-invasive estimate of gonadal development based on linear proportions. This index was calculated by comparing the visible length of the gonad to the total length of the fish using standardized backlit images analysed in ImageJ (Figure 3.4).

Measurements were taken using the freehand line selection tool. Gonad length was measured from the anterior margin of the body cavity, consistently anchored to the posterior edge of the gill plate, to the most posterior visible extent of the illuminated gonad. This standardised method ensured that consistent anatomical landmarks were used across all individuals.

Total body length was measured along the midline axis of the fish, from the tip of the snout to the base of the caudal peduncle. External fins were excluded from this measurement to minimise variation caused by inconsistent fin extension.

Each measurement was performed three times per image, and the average value was used for both gonad length and total body length. If substantial variability was observed among replicate measurements (CV >10%), all three were repeated to ensure consistency.

The VLGSI was calculated as:

**VLGSI = (Average Gonad Length) / (Average Body Length)**

This ratio-based metric was then compared to biological indicators of reproductive status, including oocyte diameter and histological maturation stage (Figure 3.5).

*Figure 3.4: ImageJ-based measurement of internal gonad length used to calculate the Visual Length Gonadosomatic Index (VLGSI) in R. leporina. The highlighted red line denotes the manually traced visible gonad length measured from the posterior edge of the gill plate to the most posterior illuminated extent of the gonad.*

*Figure 3.5: ImageJ-based measurement of total external body length used to calculate the Visual Length Gonadosomatic Index (VLGSI) in R. leporina. The highlighted red line denotes the traced body length measured along the midline from the tip of the snout to the base of the caudal peduncle.*

### 3.3.3 : VGSI Statistical Analysis

All statistical analyses for VGSI metrics were performed using Microsoft Excel (Microsoft 365, Version 2401). Prior to analysis, all VGSI, oocyte diameter, body weight, and gene expression datasets were screened for obvious outliers and data-entry errors. Linear regression and Pearson correlation analyses were used to assess relationships between VGSI metrics (VSGSI and VLGSI) and continuous biological variables including fish weight, mean oocyte diameter, and $\log_2$-normalised *cyp19a1a* expression. One-way analysis of variance (ANOVA) was applied to test for differences in VSGSI, VLGSI, and oocyte diameter among pooled maturation stages (PVO, VIT, FOM), with Tukey's post-hoc tests used where appropriate to resolve pairwise differences. Statistical significance was accepted at $p \leq 0.05$. All tests were two-tailed. Sample sizes varied among analyses due to tissue availability, successful imaging, and gene expression subsampling and are reported with each result.

### 3.3.4 : Hydrated Oocyte Morphology

Photographic analysis revealed that female *R. leporina* at the final hydrated stage of sexual maturation exhibited visibly translucent gonads under backlighting. This distinct morphological change provided a visual indicator of imminent ovulation, typically within a few days. If validated, the appearance of this feature may offer a simple, non-invasive cue for identifying females imminently ready for stripping (Figure 3.6).

*Figure 3.6: Backlit ventral image of a female R. leporina showing a presumed hydrated ovary, identified by the increased translucency of the ovarian tissue relative to surrounding structures. This visual appearance is characteristic of the peri-ovulatory stage immediately preceding ovulation.*

*Table 3.1: Overview of ImageJ-based measurements and formulas used to calculate the Visual Gonadosomatic Indices (VGSI) in R. leporina.*

| GSI Technique | Measurements (via ImageJ) | Formula |
|---|---|---|
| Visual Length GSI (VLGSI) | - Gonad length (anterior to posterior)<br>- Fish length (snout to caudal peduncle, excluding fins) | **Gonad Length / Total Length** |
| Visual Size GSI (VSGSI) | - Gonad area<br>- Body area (excluding fins) | **Gonad Area / Total Body Area** |

## 3.4: Visual GSI Results

### 3.4.1: Evaluating VSGSI against Fish Weight

The validity of VGSI metrics was assessed by examining their relationships with established indicators of reproductive development, including fish weight, oocyte diameter, and histological maturation stage. This analysis was to determine whether VGSI measurements could function as non-invasive proxies for ovarian development and provide insight into reproductive readiness for hormonal induction.

To assess whether somatic mass could serve as a proxy for reproductive condition, regression analysis was conducted between Visual Size Gonadosomatic Index (VSGSI; gonad area relative to body area) and fish weight (Figure 3.7). A statistically significant positive association was observed ($R^2 = 0.2273$, $r = 0.477$, $p = 0.0044$, $n = 34$), indicating that heavier individuals tended to exhibit proportionally larger gonads. However, the modest coefficient of determination indicates that body weight explained only approximately 23% of the variance in gonad size.

This limited explanatory power likely reflects structural confounding whereby larger but reproductively undeveloped individuals may have comparable mass to shorter, gravid fish. Consequently, although body weight exhibited a weak positive association with gonadal development, it lacks sufficient precision for reliable broodstock staging or selection. In contrast, direct morphological metrics such as VGSI provide a more biologically informative and functionally relevant assessment of gonadal development in *R. leporina*.

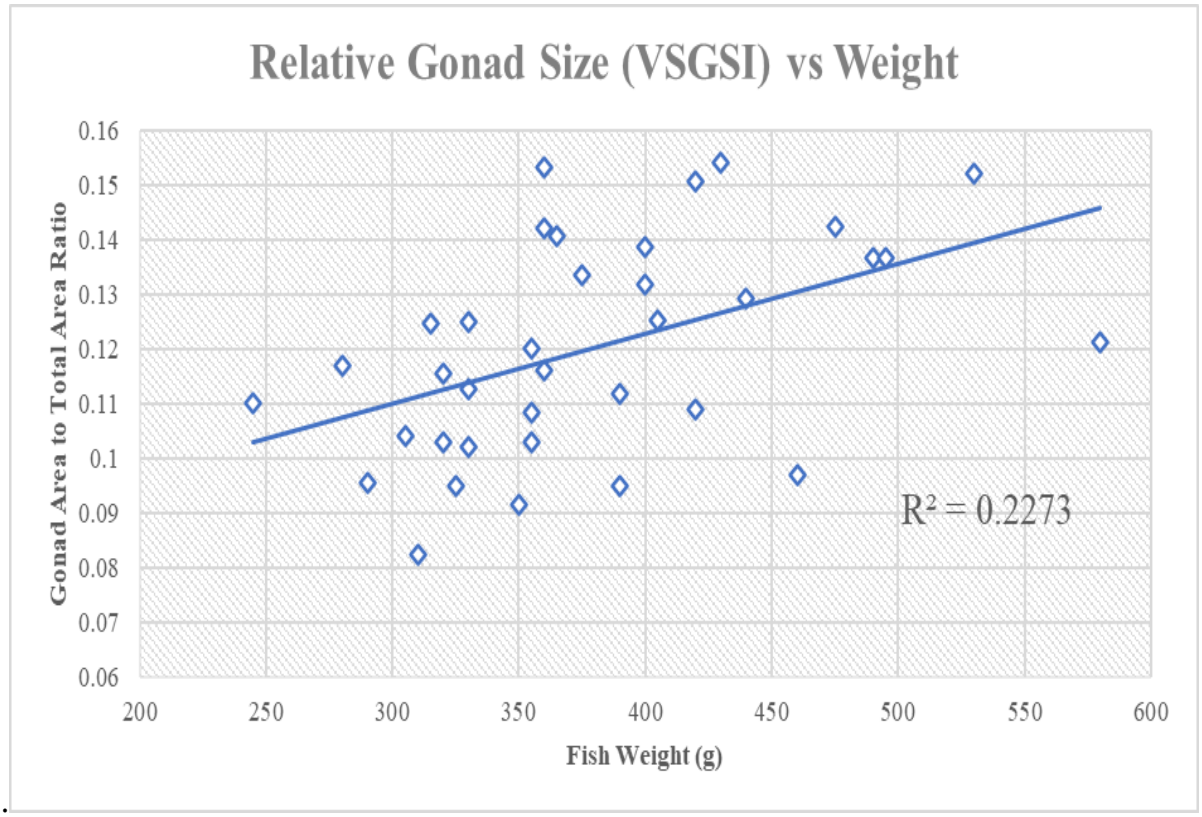


*Figure 3.7: Relationship between VSGSI and fish weight in R. leporina (n = 34). A weak but significant positive association was observed ($R^2$ = 0.227, $p$ = 0.004).*

### 3.4.2 : Evaluating VLGSI against Fish Weight

A second analysis was conducted to evaluate whether heavier individuals also exhibited proportionally longer gonads by examining the relationship between Length GSI (gonad length relative to body length) and fish weight in *R. leporina* (Fig. 3.8). The association was weak ($R^2$ = 0.0812, r = 0.285, $p$ = 0.1020, n = 34) and did not reach statistical significance. While the trend was positive, indicating that heavier fish may have slightly longer gonads relative to body length, the variability in body shape and tissue composition likely limited the strength of this association. These findings reinforce that fish weight alone does not reliably reflect gonadal development and is not a suitable proxy for selecting broodstock based on Length GSI.

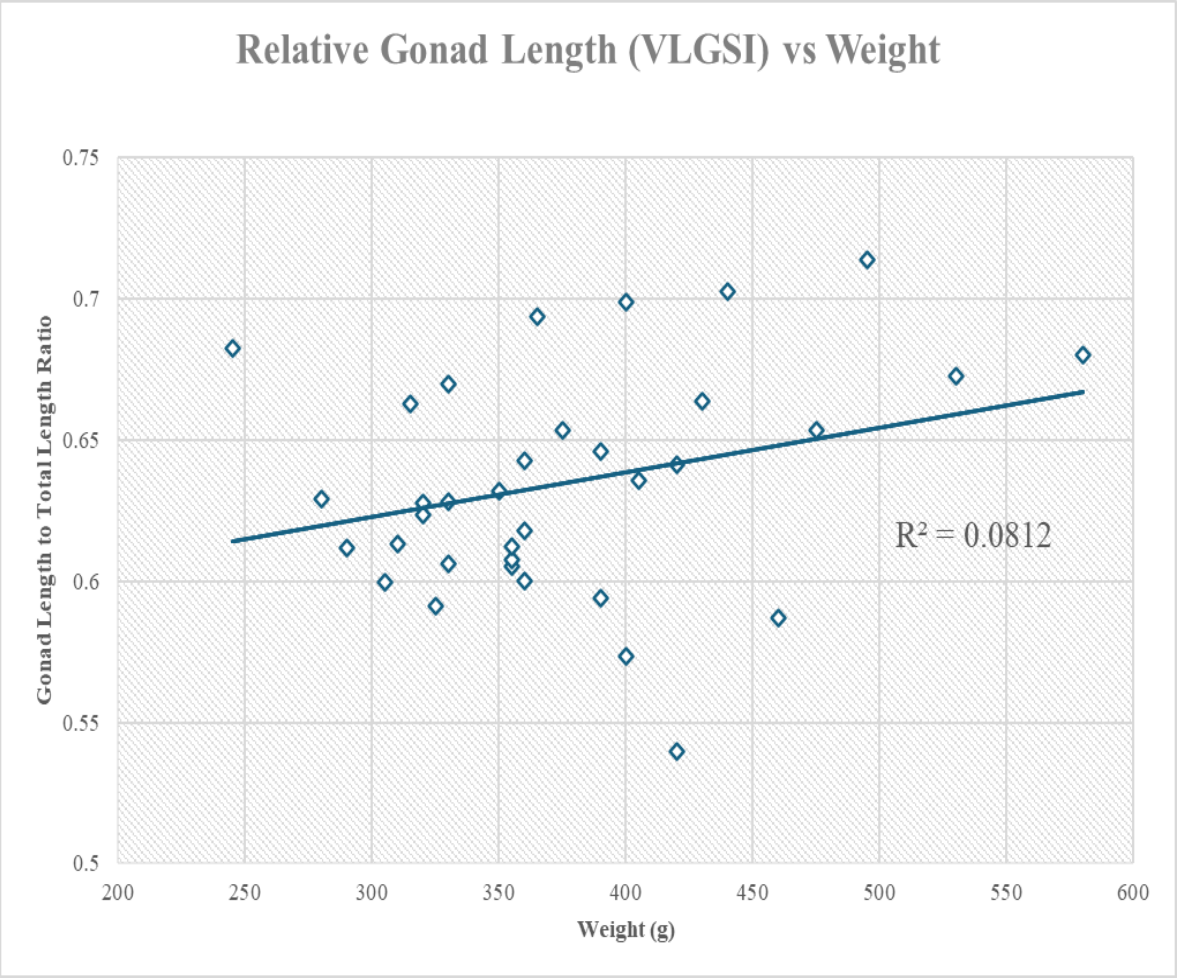


*Figure 3.8: Relationship between VLGSI and fish weight in R. leporina (n = 34). A weak positive correlation was observed ($R^2 = 0.081$, $p = 0.102$), but the result was not statistically significant.*

### 3.4.3 : Relationship Between VGSI Metrics and Oocyte Diameter

To assess whether VGSI could serve as a non-lethal proxy for reproductive maturity in *R. leporina*, oocyte developmental stages were first validated against mean oocyte diameter. A one-way ANOVA confirmed a highly significant difference in oocyte size across the three maturation stages ($F = 23.71$, $p < 0.0001$), with a clear progressive increase from previtellogenic (PVO) to vitellogenic (VIT) and final oocyte maturation (FOM) (Fig. 3.9). Post-hoc Tukey testing revealed that all pairwise comparisons were statistically significant ($p < 0.012$), confirming that mean oocyte diameter reliably identifies each developmental stage. These findings establish oocyte diameter as a robust biological reference point for assessing reproductive maturity in this species and provide a strong benchmark for evaluating the predictive utility of non-lethal VGSI metrics.

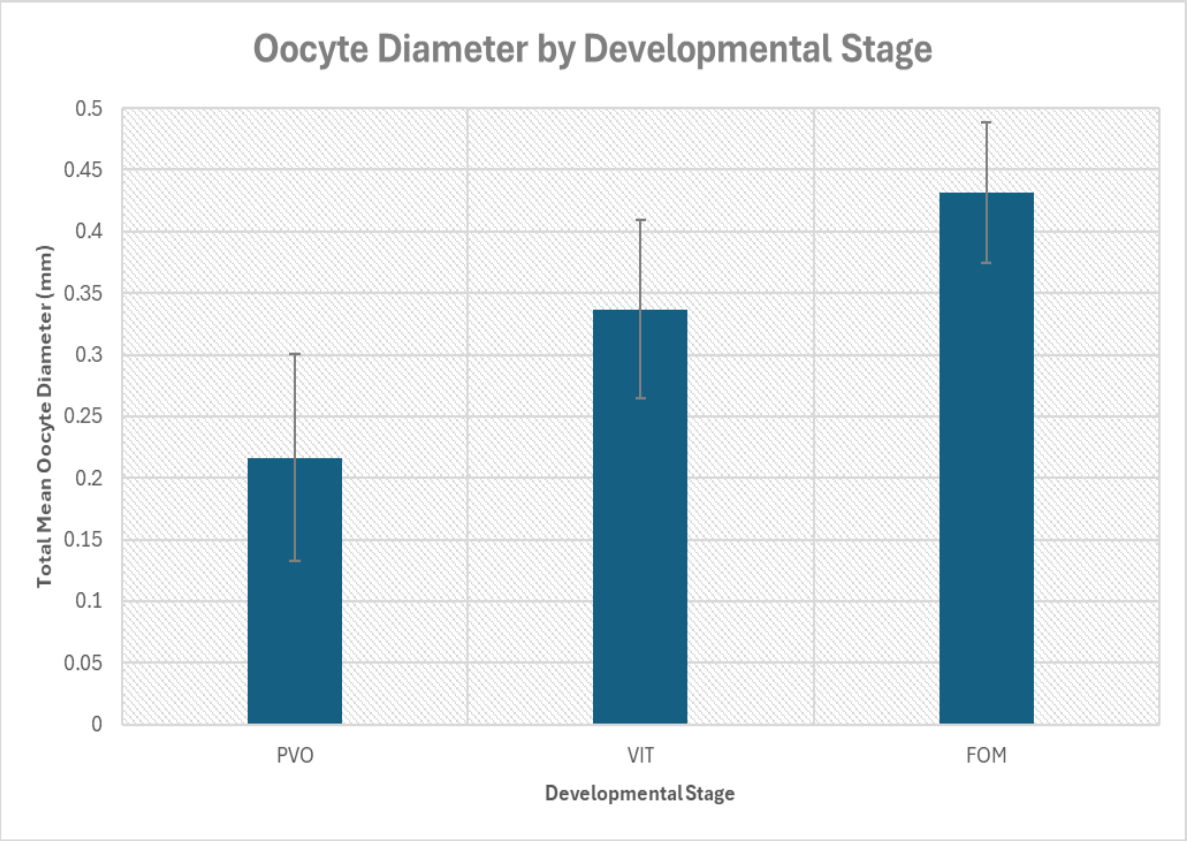


*Figure 3.9: Total mean oocyte diameter across histologically identified developmental stages in R. leporina. Error bars represent standard deviation.*

A regression was conducted to examine whether fish weight in *R. leporina* could predict the mean oocyte diameter (Fig. 3.10). The relationship was negligible ($R^2 = 0.0041$, $r = 0.064$, $p = 0.72$, $n = 34$), indicating no meaningful association. This suggests that heavier fish do not necessarily have larger or more developed oocytes, and fish weight alone is not a useful predictor of reproductive maturation at the cellular level.

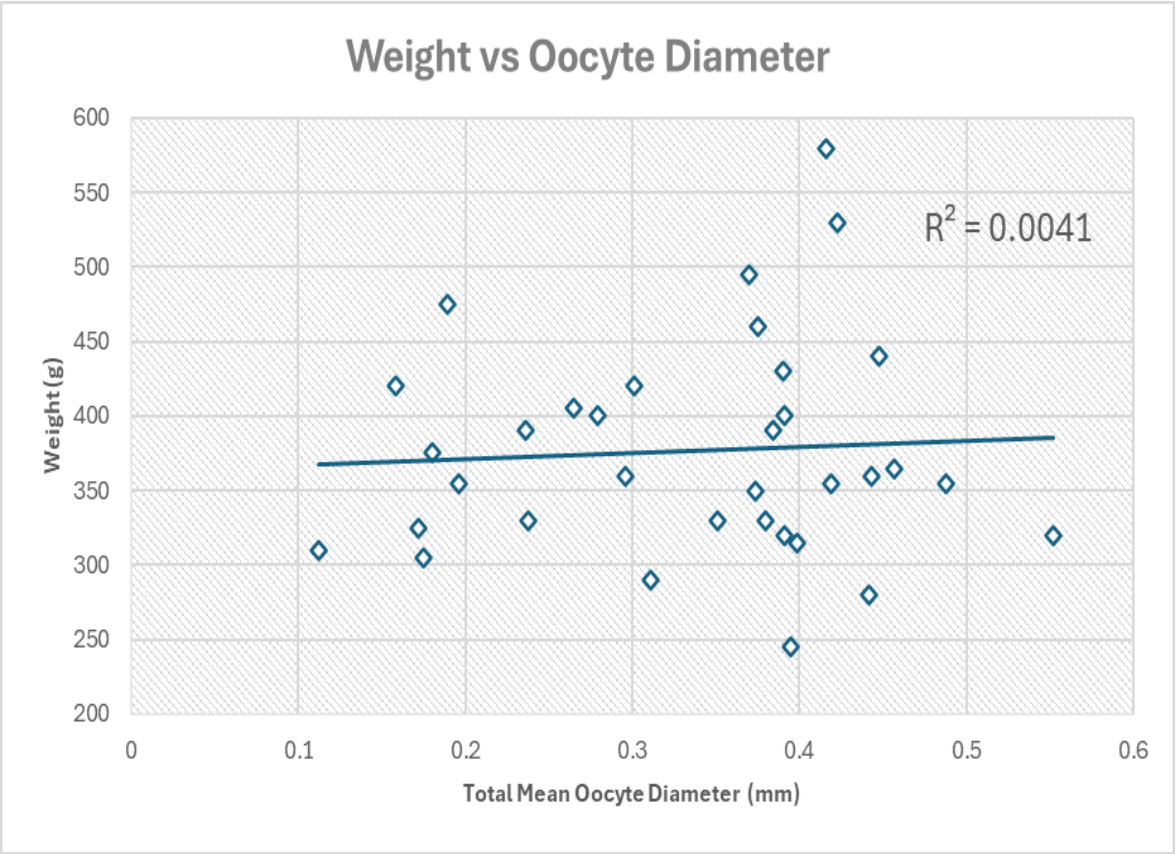


*Figure 3.10: Relationship between total mean oocyte diameter and initial fish weight in R. leporina (n = 34). No significant association was observed ($R^2 = 0.0041$, $p = 0.72$).*

With this biological progression established, the relationship between oocyte stage and Size GSI was examined. To assess whether the Size GSI metric could predict oocyte diameter, a linear regression was performed (Fig. 3.11). The analysis revealed no discernible association ($R^2 = 0.0082$, $r = 0.091$, $p = 0.611$, $n = 34$), indicating that Size GSI was not a reliable predictor of oocyte development in *R. leporina*. Despite the rationale that increasing gonad area should correspond to later stages of oogenesis, the results suggest substantial variability and limited predictive power using this method alone. These results may indicate that VSGSI is more reflective of overall fish size or body condition than of true reproductive advancement.

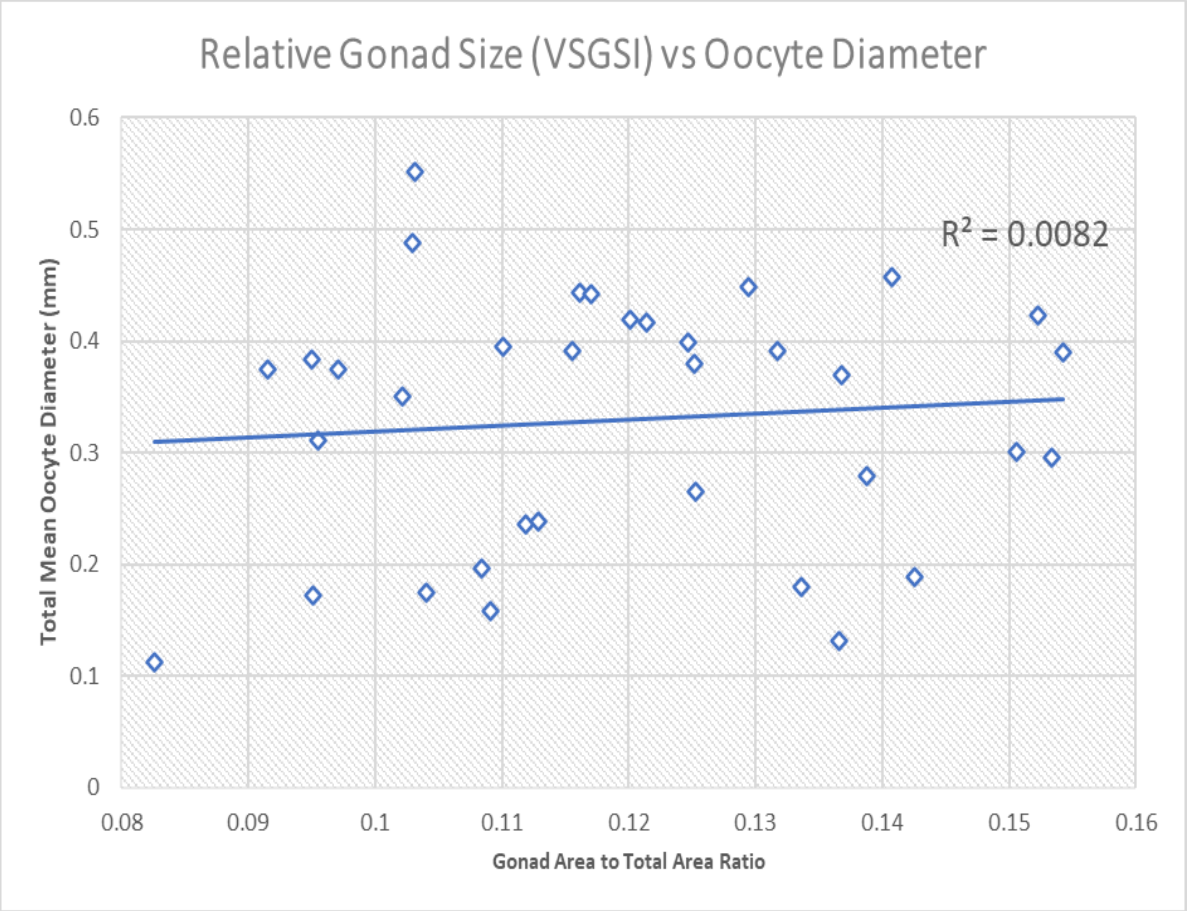


*Figure 3.11: Relationship between VSGSI and mean oocyte diameter in R. leporina (n = 34). No significant association was observed ($R^2 = 0.0082$, $p = 0.611$).*

A modest positive association was found between Length GSI and mean oocyte diameter in *R. leporina* (r = 0.440, $R^2 = 0.1936$, $p = 0.0090$; Fig. 3.12), suggesting a statistically significant relationship. While overall variability remains high, this result indicates that the ratio of gonad length to body length may serve as a viable, non-invasive proxy for assessing ovarian development. In contrast to Size GSI, which showed negligible predictive ability (Fig. 3.11), Length GSI appears to align more closely with physiological indicators of maturation, supporting its potential application in broodstock selection and hormone treatment timing.

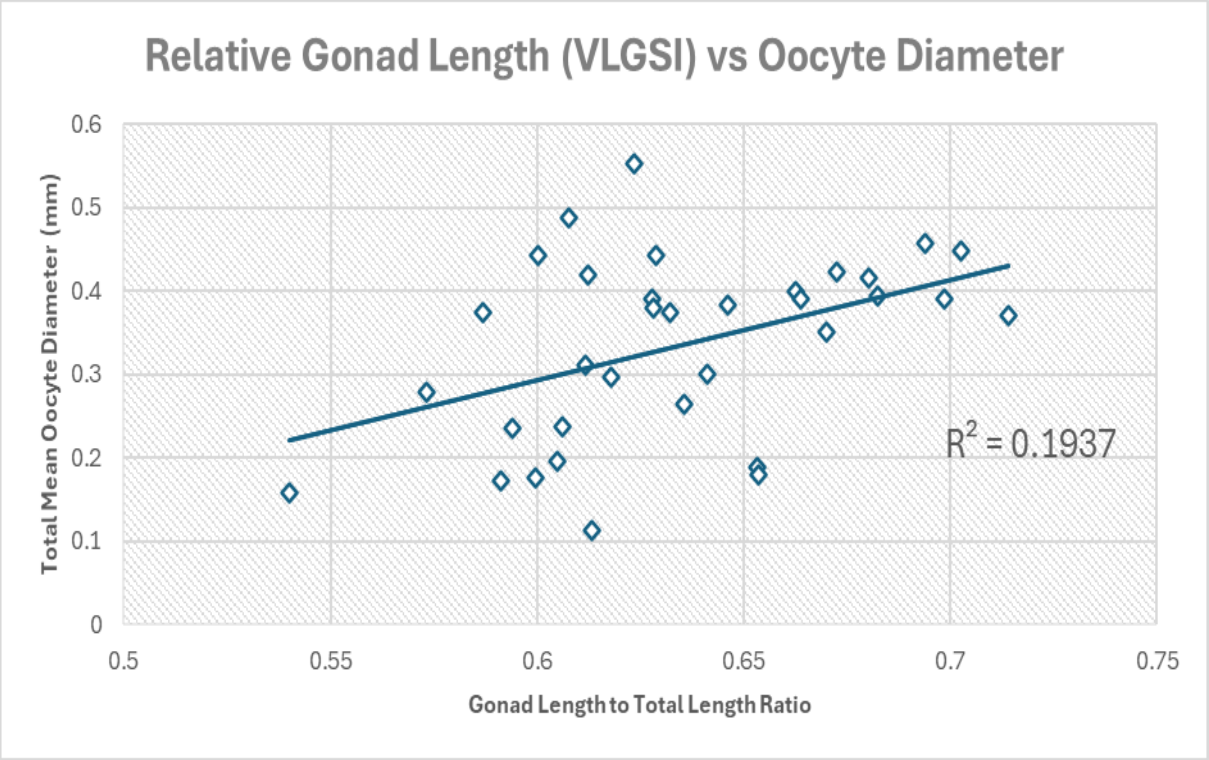


*Figure 3.12: Relationship between VLGSI and mean oocyte diameter in R. leporina (n = 34). A small positive association was observed ($R^2 = 0.1937$, $p = 0.009$), indicating that Length GSI may have predictive value for assessing gonadal maturation*

### 3.4.4 : Evaluating VGSI against Maturation Stage

The Size GSI (VSGSI) did not show a clear or consistent trend across the pooled oocyte maturation stages in *R. leporina* (Fig. 3.13). While fish in the vitellogenic (VIT) stage exhibited a marginally higher mean VSGSI than those in the previtellogenic (PVO) and final oocyte maturation (FOM) stages, the differences were modest and not statistically significant (ANOVA: F = 1.17, $p = 0.325$). Mean values were relatively close across all three stages, and the overlapping error bars highlight considerable within-stage variability. Rather than indicating progressive gonadal development, VSGSI values appeared to fluctuate slightly without forming a reliable trend aligned with maturation progression.

This lack of resolution may be due to biological variability, inconsistencies in gonad shape or proportional growth across individuals, or the inherent imprecision of using two-dimensional measurements to capture volumetric changes in gonad structure. In particular, the increasingly translucent and irregular morphology of hydrated ovaries may have impaired accurate boundary identification in photographs, further contributing to measurement noise. While VSGSI may still provide a rough indication of reproductive status, these findings suggest limited value as a standalone proxy for maturity in this species under the current methodology.

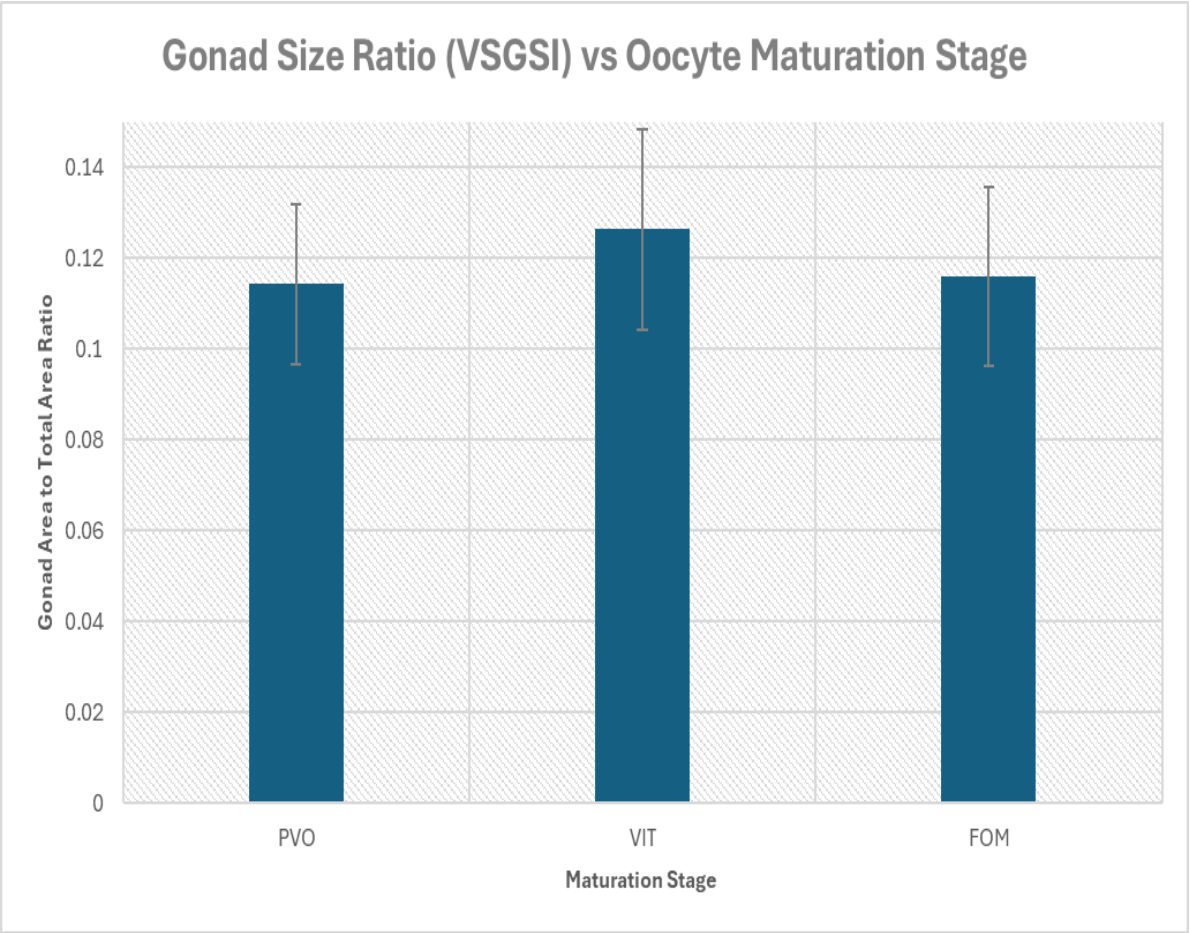


*Figure 3.13: Mean Size GSI (VSGSI) across identified oocyte maturation stages (PVO, VIT, FOM) in R. leporina. Error bars represent standard error.*

The Length GSI (VLGSI) showed a weak upward trend across the pooled oocyte maturation stages in *R. leporina*, with mean values increasing from the previtellogenic (PVO) to final oocyte maturation (FOM) stage (Fig. 3.14). Fish in the FOM stage exhibited the highest average VLGSI, followed by those in the vitellogenic (VIT) stage, while PVO fish displayed the lowest values. Despite this progression, the overall differences were not statistically significant (one-way ANOVA: $F = 2.94$, $p = 0.069$), although they approached the threshold for significance. The overlapping standard error bars suggest that individual variation remains substantial, and the apparent trend should be interpreted with caution.

While the VLGSI may reflect longitudinal gonad development more accurately than area-based estimates, this result indicates only a limited association with the maturation stage. Possible contributors to the observed variability include anatomical differences between individuals and subtle distortions in gonad orientation or compression during imaging. Regardless, the length-based index may retain some value as a coarse proxy for developmental progression, especially when used in conjunction with other indicators.

VLGSI may function best as a repeatable, non-lethal metric for tracking progression within individuals over time, rather than between groups.

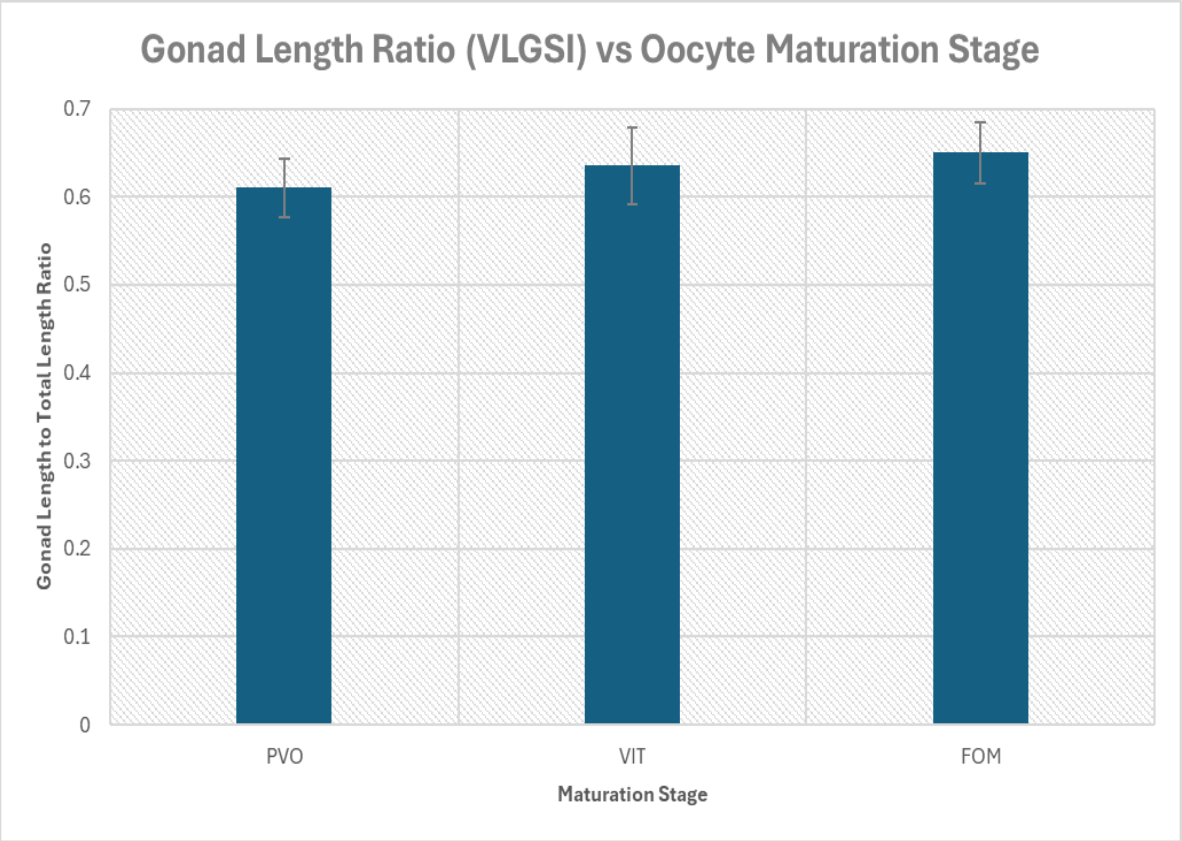


*Figure 3.14: Mean Length GSI (VLGSI) across identified oocyte maturation stages (PVO, VIT, FOM) in R. leporina. Error bars represent standard error.*

### 3.4.5 : VGSI as a Predictor of Aromatase Activity

A Pearson correlation using Size GSI (VSGSI) revealed a strong, statistically significant positive relationship between VSGSI and $\log_2$-transformed *cyp19a1a* expression ($r = 0.710$, $p = 0.021$, $n = 10$), suggesting that individuals with larger relative gonad areas exhibit higher aromatase activity following GnRHa treatment.

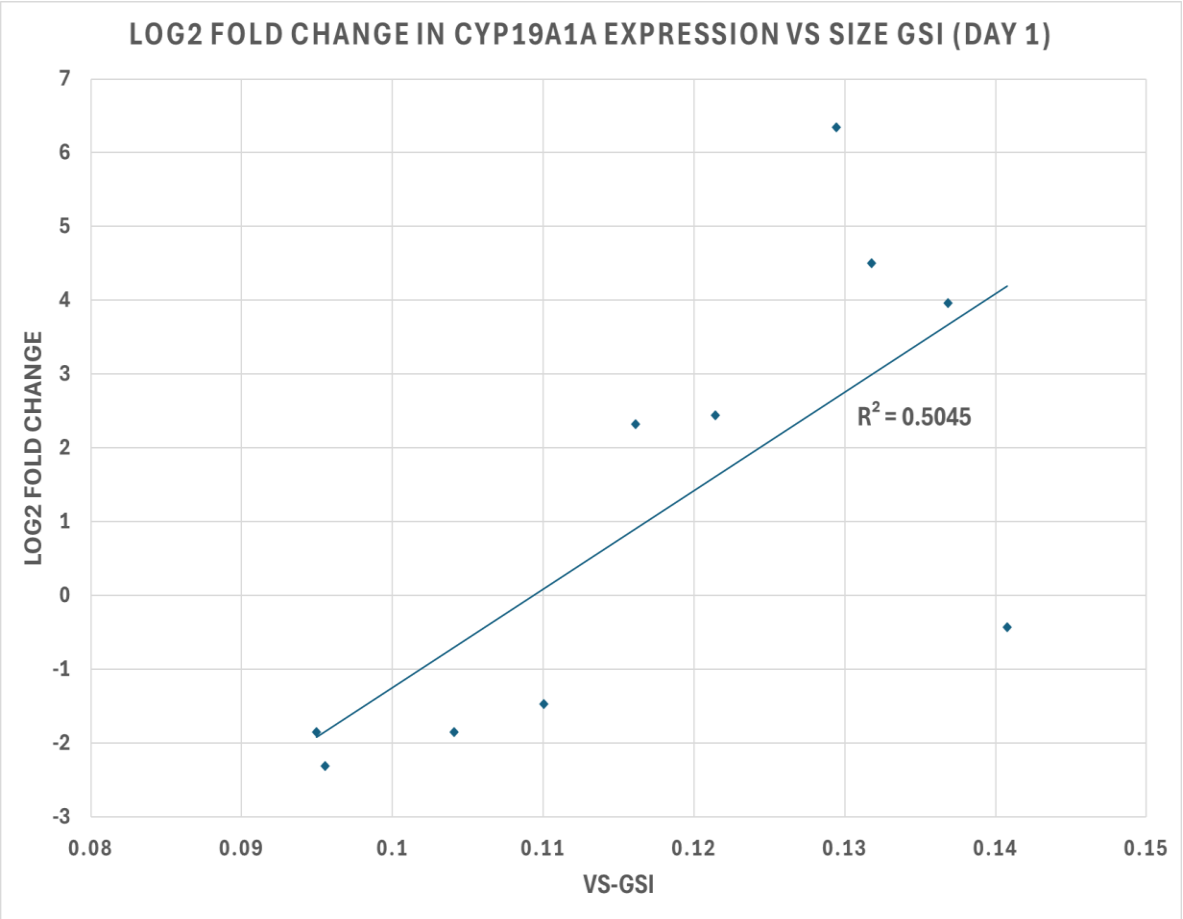


*Figure 3.15: Correlation between VSGSI and $log_2$-transformed cyp19a1a expression in GnR R. leporina (n = 10) 24 hours post-GnRHa injection. A significant positive association was observed (r = 0.710, p = 0.021).*

The Length GSI (VLGSI) by contrast, showed a moderate but non-significant positive correlation with *cyp19a1a* expression (r = 0.584, *p* = 0.076, n = 10), indicating a possible relationship between gonad elongation and steroidogenic activation that merits further study. The dual correlations with oocyte diameter and gene expression strengthen the case for using VGSI as a practical, non-lethal indicator of reproductive readiness in *R. leporina*.

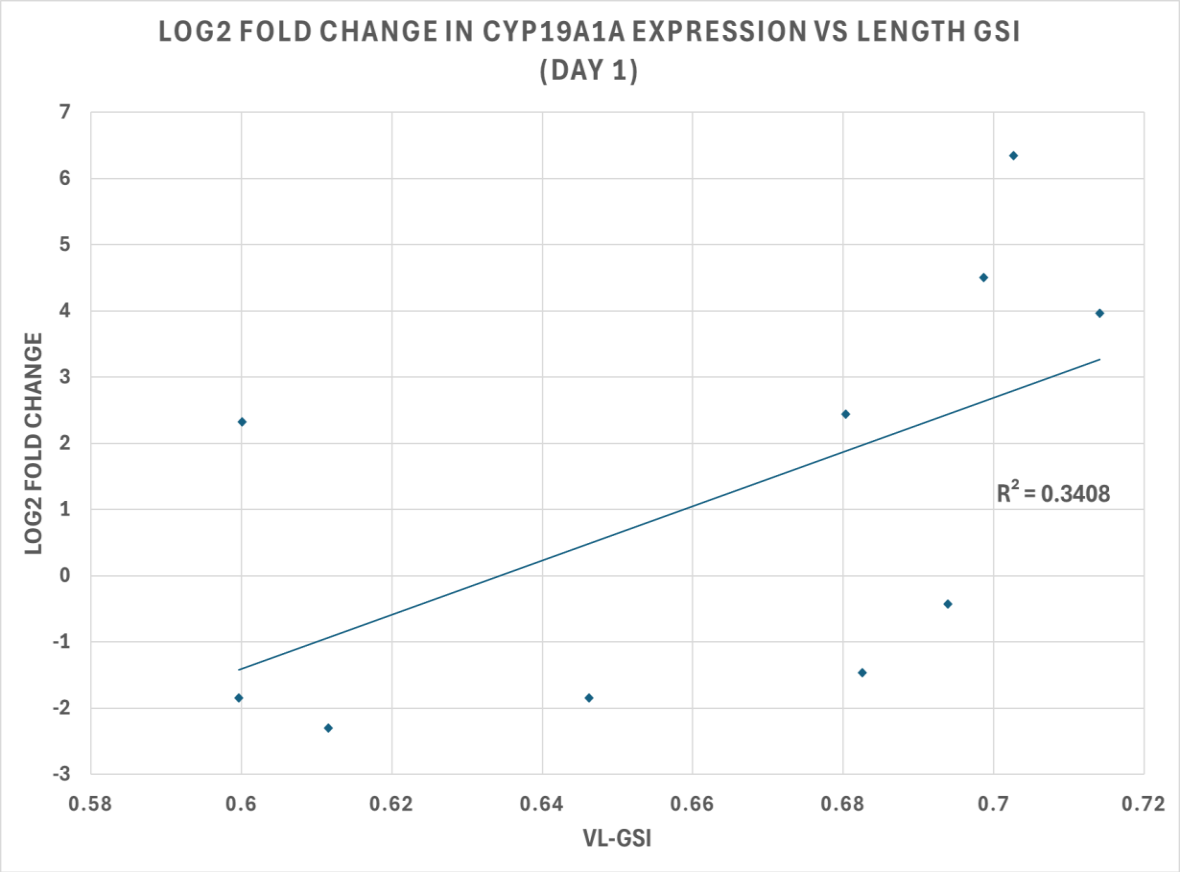


*Figure 3.16: Correlation between VLGSI and $log_2$-normalised cyp19a1a expression in R. leporina (n = 10) 24 hours post-GnRHa injection. A moderate positive association was observed (r = 0.584, p = 0.076).*

## 3.5: Discussion of Visual GSI Performance in *R. leporina*

This chapter presents a pilot evaluation of two non-lethal Visual Gonadosomatic Index (VGSI) metrics, an area-based index (VSGSI) and a length-based index (VLGSI), as exploratory tools for assessing gonadal maturation in *Rhombosolea leporina*. Developed from standardized backlit photographs, these indices were intended to provide a minimally invasive and low-cost method of estimating reproductive status suitable for hatchery environments. Given the limited sample size (n = 34), the present study should be interpreted as a preliminary validation focused on feasibility and biological relevance rather than on the establishment of definitive operational thresholds.

Although strong predictive relationships between VGSI values and conventional reproductive markers were not consistently observed, the findings nonetheless provide important insight into the strengths and constraints of visual gonadal assessment. The VLGSI exhibited a statistically significant but moderate correlation with mean oocyte diameter ($R^2$ = 0.1937, p = 0.009), indicating that relative gonad length is associated with ovarian development but is not sufficiently precise for reliable prediction at the individual level.

Mean VLGSI values also increased modestly across maturation stages, from 0.61 in previtellogenic (PVO) fish to 0.65 in final oocyte maturation (FOM) fish, representing an increase of approximately 6.5 percent. However, this trend did not reach statistical significance ($p = 0.069$). This pattern suggests a potential longitudinal expansion of the gonads with progressive oocyte development, although substantial inter-individual variability limits interpretive confidence. In contrast, the VSGSI showed no meaningful association with histological staging ($R^2 = 0.0082$, $p = 0.611$), indicating that two-dimensional gonad area alone is a poor proxy for reproductive maturation in this species. While these outcomes are constrained by limited statistical power, they establish a useful baseline against which future refinements of non-lethal assessment methods can be evaluated.

Interestingly, despite the weak association between VSGSI and traditional morphological and histological markers, a strong positive correlation was observed between VSGSI and $\log_2$-transformed *cyp19a1a* expression following GnRHa treatment ($r = 0.710$, $R^2 = 0.5045$, $p = 0.021$). This result suggests that relative gonad area may align more closely with underlying steroidogenic activity than with static histological staging. The VLGSI similarly showed a positive, although non-significant, correlation with *cyp19a1a* expression ($r = 0.584$, $R^2 = 0.3408$, $p = 0.076$). Together, these findings imply that VGSI measurements may reflect dynamic physiological processes that are not captured by morphological staging alone, particularly in hormonally stimulated broodstock. This distinction highlights an important conceptual difference between structural maturity and endocrine responsiveness, which may not always coincide spatially or temporally.

One of the most promising attributes of the VGSI approach lies in its potential for repeatability. Because imaging is non-lethal and low stress, VGSI enables repeated measurements on the same individuals over time. While neither VLGSI nor VSGSI appears sufficiently accurate to stage fish reliably from a single image, their primary utility may lie in tracking within-individual changes in gonad morphology across sequential timepoints. Such longitudinal monitoring could be particularly valuable in experimental trials involving hormonal induction, photoperiod manipulation, or stress-response assessment, where relative temporal change is often more informative than absolute maturity state. However, this longitudinal application remains unvalidated, and it is not yet known whether VGSI values remain consistent or biologically meaningful within individuals across extended time periods. The repeatability and within-fish sensitivity of these indices must therefore be explicitly tested before they can be confidently applied in routine broodstock management.

Direct lethal validation of VGSI estimates against gonad mass and gravimetric

gonadosomatic index was not undertaken in the present study. VGSI imaging was conducted opportunistically on broodstock already allocated to the GnRHa gene expression experiment, and additional sacrifice for method validation was not ethically or logistically justified. As a result, correlations with gonad mass were inferred indirectly through histological staging, oocyte diameter, and molecular markers rather than through direct gravimetric measurements. This represents an important limitation of the present validation and should be explicitly addressed in future targeted VGSI trials designed specifically for method calibration.

Several technical and biological factors likely contributed to the limited predictive power of the current VGSI formulations. Both indices rely on two-dimensional projections of three-dimensional structures, meaning that variation in gonad depth, opacity, and orientation can substantially influence measurement values. Hydrated ovaries introduced additional analytical noise due to their increased translucency under backlighting, which complicated accurate delineation of gonad margins. Furthermore, lateral swelling, asymmetry, and non-uniform gonad morphology likely obscured relationships between VGSI values and true gonadal volume. These sources of error are inherent to planar imaging approaches and must be accounted for in future methodological refinement.

Despite these challenges, the flattened morphology of *R. leporina* remains uniquely well suited to visual assessment relative to most teleosts. The superficial positioning of the ovaries beneath the ventral body wall enables high-resolution internal imaging that would be impractical in species with deeper visceral cavities. Future work should prioritize optimization of gonad-specific dimensions that are less sensitive to body shape variation, such as longitudinal gonad length or maximum visible gonad width, rather than relying on whole-body proportional metrics. Incorporation of pixel-based size estimation, volumetric reconstruction, or three-dimensional modelling may further improve measurement accuracy. Standardized imaging setups, consistent fish positioning, and automated tracing algorithms would also reduce observer bias and improve reproducibility. Machine learning approaches may ultimately provide a pathway toward automated detection of subtle morphological changes associated with reproductive progression.

Looking forward, the most practical and impactful application of VGSI lies in its capacity for tracking reproductive changes within individual fish over time. Rather than serving as a diagnostic tool for single timepoint staging, VGSI offers a minimally invasive method for detecting relative shifts in gonadal morphology across the reproductive cycle. This capacity is particularly well suited to research contexts involving hormonal induction, seasonal

photoperiod manipulation, or environmental stress exposure, where understanding within-fish progression is more informative than between-fish comparisons. Repeated VGSI imaging could, for example, be used to assess whether specific treatments accelerate or delay ovarian development in broodstock, providing a continuous, non-destructive alternative to biopsy or lethal sampling.

In summary, this pilot study demonstrates that VGSI, particularly the length-based metric, holds promise as a low-cost, repeatable technique for monitoring gonadal development in *R. leporina*. Although predictive power remains limited at single timepoints, its value as a longitudinal monitoring tool is both biologically meaningful and practically applicable. The observed associations between VGSI metrics and aromatase expression strengthen this conclusion by highlighting the relevance of these visual indices to underlying steroidogenic activity. Given the trends observed with *cyp19a1a* expression, future validation efforts should also examine whether VGSI correlates with expression of 20β-hsd, the key progestin synthesis enzyme involved in final oocyte maturation. If confirmed, this would further enhance the capacity of VGSI to predict physiological readiness for hormone-induced spawning. With continued refinement, increased standardisation, and validation against endocrine and histological benchmarks, VGSI may ultimately contribute to more precise, ethical, and scalable reproductive management strategies in flatfish aquaculture. Comparable non-lethal approaches using ultrasound imaging have already been applied for gonadal staging in teleost broodstock to support reproductive management without sacrificing fish (Næve et al., 2018).

# Chapter 4 – Discussion

### 4.1: Interpreting GnRHa Effects on *cyp19a1a* Expression

This study examined ovarian *cyp19a1a* expression in R. leporina following administration of varying GnRHa doses. One day after injection, a dose-related trend was observed, with relative expression quantified using the ΔΔCt method and expressed as $\log_2$ fold change relative to the Day 0 baseline. Expression was highest in the 100 µg/kg group ($\log_2$ fold change = +2.65), followed by the 50 µg/kg group (+2.38), while the 25 µg/kg group showed reduced expression (−0.53). When compared directly against the Day 1 control group ($\log_2$ = −0.07), none of the treatment groups differed significantly (p = 0.10, 0.18, and 0.34, respectively). Although not statistically significant, this pattern suggests that higher GnRHa doses may transiently stimulate the steroidogenic pathway involved in estrogen synthesis. This response is consistent with the established role of GnRHa in activating the brain–pituitary–gonadal axis through stimulation of luteinizing hormone and follicle-stimulating hormone release, which in turn regulates aromatase activity and estradiol production (Kagawa et al., 2003; Moulik et al., 2016). The absence of a response at 25 µg/kg likely reflects insufficient pituitary stimulation, a pattern also reported in other flatfish species treated with low-dose LHRH-a (Poortenaar and Pankhurst, 1998). High inter-individual variability among reproductively impaired broodstock is likely to further obscure clear dose effects.

A near-significant difference between the 100 µg/kg and 25 µg/kg groups ($p$ = 0.08) suggests that increased sample sizes could resolve the current ambiguity. However, gene expression alone cannot confirm endocrine activation. Follow-up studies should measure plasma E2 levels and include additional markers such as *fshb*, *lhb*, and *gpα* to assess activation of the full reproductive axis (Nyuji et al., 2020). The return to baseline by Day 5 indicates that a single injection does not provide sustained stimulation. Longer-acting delivery systems such as Ovaplant or recombinant gonadotropins (rFSH, rLH) may offer more consistent results (Guzmán et al., 2009; Ramos-Júdez et al., 2022). However, as the latter are species specific, they are only likely to be a viable option with the existence of a profitable industry.

By Day 5, *cyp19a1a* expression had declined across all groups, confirming that the stimulatory effect of GnRHa was short-lived. This pattern suggests rapid hormonal clearance and the influence of captivity-induced reproductive suppression, as observed in other species (Akhtar et al., 2017; Nargesi et al., 2023). A single intramuscular injection appears insufficient to maintain reproductive activation in *R. leporina*. Notably, many studies

employing injection-based delivery incorporate repeated booster doses to sustain endocrine stimulation over time. For example, wild-caught greater amberjack (*Seriola dumerili*) were successfully induced to spawn 22 times across 15 GnRHa injections, demonstrating that repeat injections can prolong gonadal responsiveness and support sequential reproductive events (Fernández-Palacio et al., 2013).

Sustained-release systems such as Ovaplant have been shown to prolong elevated LH and FSH levels and improve fecundity in flatfish (Guzmán et al., 2009; Kuradomi et al., 2017). However, prolonged gonadotropin exposure does not ensure oocyte maturation and ovulation unless adequate levels of maturation-inducing steroids like 17α,20β-dihydroxyprogesterone (MIS) are also produced (Nagahama, 1997). As this study did not measure MIS or the expression of its biosynthetic enzyme *20β-hsd*, the full stimulatory effect of GnRHa on oogenesis could not be determined, limiting conclusions about functional readiness. Although elevated *cyp19a1a* expression reflects estrogenic activation during vitellogenesis, it does not confirm progression to FOM, which requires a preovulatory LH surge and production of MIS. Incorporating such protocols into *R. leporina* culture may help overcome the transient effects of injection-based treatments.

The apparent link between oocyte maturity and aromatase expression on Day 1 further supports the need for proper staging prior to induction. Fish with more advanced oocytes exhibited higher *cyp19a1a* expression, consistent with studies in Southern Flounder, where follicles larger than 500 µm were necessary for final maturation (Berlinsky et al., 1996). While fish at early stages of ovarian development may express basal aromatase for differentiation (Luckenback et al., 2005), their capacity to respond to exogenous stimulation is limited. These results strengthen the argument for excluding immature females from hormonal protocols until late vitellogenesis is confirmed. This is typically assessed by ovarian biopsy and microscopic measurement of oocyte diameter, a method that is invasive, stressful, and time consuming, hence the value of a non-invasive VGSI. By Day 5, the relationship between oocyte maturity and *cyp19a1a* expression had dissipated, reinforcing the need for sustained hormonal delivery and careful broodstock selection based on follicle development.

### 4.2: Visual GSI Discussion

This study evaluated the feasibility of using visual gonadosomatic index (VGSI) metrics as a non-lethal method for monitoring reproductive development in *R. leporina*. Two indices were developed using standardised backlit imaging of the ventral surface: Length GSI (gonad length relative to fish length) and Size GSI (gonad area relative to body area). The goal was to provide a minimally invasive alternative to lethal sampling or repeated biopsies in broodstock management.

Among the two metrics, Length GSI showed the strongest association with reproductive stage, displaying a significant correlation with mean oocyte diameter ($R^2 = 0.1937$, $p = 0.009$). Mean Length GSI increased across histological stages, from 0.61 in previtellogenic fish to 0.65 in those undergoing final oocyte maturation, though this trend did not reach significance ($p = 0.069$). Size GSI showed no meaningful relationship with maturation ($R^2 = 0.0082$, $p = 0.611$), likely due to confounding factors such as gonad translucency, hydration, and irregular morphology. In late-stage females, hydrated ovaries become more transparent and lose turgidity, making boundaries harder to distinguish and reducing image contrast under backlighting. This effect has been quantified by Peer et al. (2012), who demonstrated that ovary percentage water content is a strong predictor of reproductive stage based on visual characteristics, including color and translucency. Combined with the lateral swelling typical of maturation, these issues likely biased two-dimensional area estimates (Emerson et al., 1990; Hunter & Macewicz, 2003). High inter-individual variability and the projection of complex 3D structures into 2D space likely further reduced predictive utility.

Despite its poor correlation with oocyte diameter or histological stage, the significant positive association between Size GSI and *cyp19a1a* expression ($R^2 = 0.5045$, $r = 0.710$, $p = 0.021$) suggests that this metric may reflect active vitellogenic processes within the ovary. Elevated *cyp19a1a* levels indicate increased aromatase activity and estradiol synthesis, both of which support yolk protein production during vitellogenesis. Therefore, even though Size GSI lacks morphological precision, it may still capture underlying steroidogenic activation. A similar, though weaker, trend was observed between Length GSI and *cyp19a1a* expression ($R^2 = 0.3408$, $r = 0.584$, $p = 0.076$), indicating that both visual metrics could be sensitive to physiological changes not visible through traditional staging alone. This supports the idea that VGSI may be useful not just as a morphological proxy but also as a physiological marker for reproductive activation, especially in combination with gene expression data.

If future studies can demonstrate correlations between VGSI and additional endocrine markers such as *20β-hsd*, which governs MIS production, VGSI could become a non-invasive predictor of imminent final oocyte maturation (FOM). This would significantly enhance its utility for guiding hormone treatment timing and refining broodstock induction protocols. Despite these limitations, VGSI may have potential for longitudinal monitoring. Its non-lethal and repeatable nature makes it well-suited for tracking individual reproductive trajectories over time, such as during hormonal or environmental manipulation. In this context, trends in Length GSI may serve as early indicators of ovarian development. However, for precise staging or hormone induction decisions, VGSI lacks sufficient resolution. In contrast, ultrasound-based GSI estimates have achieved much higher accuracy in species like Atlantic salmon, Hilsa shad, and Turbot, often with $R^2$ values exceeding 0.9 (McGarvey et al., 2021; Naeve et al., 2018). Emerging methods such as three-dimensional ultrasound imaging systems, like the OSIS platform which has achieved high segmentation fidelity for ovarian structures (Royo et al., 2024), and species-specific ordinal regression models, offering improved accuracy for classifying reproductive stages under noisy or variable data conditions (Cao et al., 2021), represent promising tools for enhancing reproductive assessment.
Future refinement should focus on improving imaging protocols and metric selection. Internal ovarian dimensions such as visible width or longitudinal expansion may prove more robust than body-wide ratios. Standardising lighting, positioning, and camera setup will also improve consistency. Validation against histology or gravimetric GSI remains essential for confirming the reliability of imaging-derived reproductive metrics. In channel catfish, ultrasound-based assessments of ovarian development were corroborated by both histological profiles and gravimetric GSI, demonstrating that internal imaging metrics can reliably reflect maturation status when calibrated against biological benchmarks (Novelo et al., 2011; Guitreau et al., 2012). Automated image analysis and machine learning may further reduce subjective variability. While current VGSI models are not suitable for diagnostic classification, the technique remains a promising foundation for non-invasive broodstock monitoring in flatfish aquaculture.

### 4.3: Synthesis

Together, these findings highlight the complementary roles of physiological staging, hormonal treatment, and non-lethal assessment tools in addressing reproductive dysfunction in *R. leporina*. While *cyp19a1a* expression offers a molecular window into estrogenic activity, its utility as a predictive marker depends on the female's developmental stage, only individuals nearing FOM showed transcriptional responsiveness to GnRHa. This reinforces the need for accurate, pre-treatment staging to avoid ineffective inductions in immature fish. VGSI, particularly the size-based metric, emerged as a promising morphological proxy for this readiness. Despite its poor alignment with oocyte diameter, its strong correlation with *cyp19a1a* suggests that visible changes in gonad area may reflect underlying steroidogenic processes. This is significant because it suggests a potential role for VGSI not just in morphometric classification, but in anticipating endocrine activation.

When used in tandem, these tools offer a practical framework: VGSI enables non-invasive, repeated assessment of maturation over time, while gene expression assays can confirm steroidogenic competence after induction. Together, they may guide more targeted broodstock selection, improving the timing and efficacy of hormone treatments.

Such an integrated approach combining imaging and molecular diagnostics may ultimately help overcome the transient, inconsistent results of single-dose GnRHa protocols and improve spawning reliability in captive flatfish aquaculture.

### 4.4: Gene Expression Limitations and Recommendations

This study provides preliminary insight into how *cyp19a1a* responds to GnRHa in *R. leporina*, but several limitations affect the strength and generalizability of the findings. The most significant constraint was the small sample size across treatment groups, which, combined with high inter-individual variability, reduced statistical power. Although the 100 µg/kg dose produced the highest average expression on Day 1, the difference was not statistically significant. As a result, evidence for a dose-dependent response remains inconclusive and should be re-evaluated with increased replication.

The biological scope was also limited. While *cyp19a1a* is a well-characterised component of estrogen synthesis, it does not indicate final oocyte maturation. The absence of downstream markers such as *lhb*, *20βhsd*, or morphological outcomes like hydration and ovulation limits interpretation. Plasma estradiol (E2) was not measured, preventing confirmation that gene expression translated into hormonal output (Kagawa et al., 2003). Additionally, pituitary markers such as *gnrh-r*, *fshb*, and *lhb* were not assessed, making it unclear whether ovarian

responses originated from full BPG axis activation. Future work should include plasma steroid measurements, and additional histological staging to validate physiological relevance. The study did not sample within the first 24 hours post-injection, a period when endocrine gene expression can be highly dynamic. In teleosts, even brief disruption of *cyp19a1a* has been shown to impair reproductive function within days, indicating that early responses are both rapid and biologically relevant (Villeneuve, 2016). Without early timepoints, transient peaks in expression may have been missed. Future studies should prioritise tighter temporal resolution during this window to better capture initial endocrine activation.

The short-lived expression peaks observed on Day 1 also point to a delivery limitation. A single intramuscular injection likely results in rapid clearance, producing only brief endocrine activation. This aligns with known pharmacokinetics of GnRHa and suggests that slow-release systems, such as Ovaplant, may provide more sustained stimulation. Direct comparisons between injection and implant approaches are needed to evaluate differences in response duration, gene expression persistence, and reproductive outcomes.

Dopaminergic inhibition may contribute to reproductive dysfunction in *R. leporina*, particularly in males. In *Solea senegalensis*, pimozide treatment enhanced spermatogenesis and amplified GnRHa-induced gonadotropin expression, confirming dopamine's inhibitory role in males, but not in females (Guzmán et al., 2011). Conversely, in *R. leporina* co-treatment with pimozide did not enhance ovulation or steroid levels beyond GnRHa alone, suggesting weak or absent dopaminergic inhibition (Poortenaar & Pankhurst, 2000). These findings highlight species- and sex-specific variation, warranting further testing of dopamine antagonists in *R. leporina*.

### 4.5: VGSI Limitations and Future Refinement

The Visual Gonadosomatic Index (VGSI) offers a non-lethal method for monitoring reproductive development in flatfish, but its diagnostic reliability was limited in this pilot study. Of the two indices tested, Length GSI showed a modest correlation with oocyte diameter, while Size GSI showed no predictive value.

In contrast, both metrics demonstrated stronger associations with molecular markers of reproductive activity. Specifically, Size GSI correlated significantly with ovarian *cyp19a1a* expression, explaining over 50% of the variation in transcriptional response. Length GSI also showed a moderately strong, though not statistically significant, association with gene expression. Performance was constrained by biological variability, small sample sizes, and imaging artefacts, particularly in translucent or underhydrated gonads where visual

boundaries were difficult to define.

These issues reflect a core limitation of VGSI: it relies on two-dimensional imaging to estimate complex three-dimensional structures. Hydration reduces contrast under backlighting, further obscuring gonad margins. Inconsistent image quality, fish positioning, and lighting conditions compound the problem, undermining metric consistency.

VGSI metrics were also not validated against benchmark methods such as histological staging or gravimetric GSI, leaving uncertainty about their biological relevance. In other species, calibrated non-invasive tools have achieved high accuracy. For example, ultrasound staging in lumpfish (*Cyclopterus lumpus*) aligned closely with histology and showed strong correlation ($r > 0.9$) with GSI and plasma sex steroids (Mlingi et al., 2023). Similarly, histologically validated GSI values have proven effective in small-bodied freshwater fish (Brewer et al., 2008). These findings underscore the need to calibrate visual indices against established biological benchmarks.

To improve VGSI utility, imaging protocols should be standardised for lighting, angle, and positioning. Internal ovarian metrics such as maximum gonad length or width may yield more reliable indicators than body-area ratios. Composite indices or pixel-based volumetric estimates could further enhance precision but must ultimately be validated against histology, gravimetric GSI, or observed spawning outcomes.

Despite current limitations, VGSI remains a promising tool for longitudinal monitoring. Its non-invasive nature allows repeated assessment of individual fish, enabling detection of developmental changes such as oocyte hydration or gonadal elongation over time. While it is not yet suitable for precise staging, the demonstrated correlation with aromatase expression indicates that VGSI may have value as an indicator of endocrine activation when used in combination with molecular data. Future work should prioritise refining the technique and evaluating its practical performance in hatchery settings.

### 4.6: Proposed Protocol for Hatchery Application

This study provides a foundation for refining hormone induction strategies in *R. leporina* by integrating morphological and molecular indicators of reproductive readiness. While further validation is required, the following protocol is proposed to support hatchery operations aiming to overcome spawning dysfunction in captive broodstock.

**Proposed Protocol Steps:**

1. **Initial Screening**
    a. Select female broodstock with a mean oocyte diameter of at least 0.35 mm,

indicating the onset of final oocyte maturation (FOM).

b. Staging should be performed via ovarian biopsy or histological confirmation during pre-conditioning.

2. **Non-Lethal Visual Assessment**
    a. Apply backlit imaging to monitor gonad morphology through the ventral surface.
    b. Use changes in gonad length and translucency as indicators of reproductive progression.
    c. Repeat imaging over time to track development, but do not rely on visual indices alone for treatment decisions.
3. **Hormonal Induction**
    a. Administer a slow-release GnRHa implant (e.g. Ovaplant) at 50 µg/kg body weight (based on Ellis-Smith 2022) or injection of 100 µg/kg (based on our results) followed by booster injection two days later.
    b. Treat only females confirmed to be in late vitellogenesis or FOM to maximise response likelihood and minimise unnecessary interventions and cost.
4. **Response Monitoring (In experimental context).**
    a. Collect blood samples 24–48 hours post-treatment to measure plasma estradiol (E2) as a proxy for endocrine activation.
    b. Where feasible, assess ovarian *cyp19a1a* and *20β-hsd* expression to verify steroidogenic response at the transcriptional level across critical stages of ovarian development.
    c. Visual GSI metrics may also assist in non-lethal tracking of treatment response, particularly when used in conjunction with molecular data.
5. **Spawning Management**
    a. Observe broodstock daily for signs of hydration and behavioural readiness.
    b. If tank-based spawning does not occur naturally then prioritise egg stripping when hydration is visually apparent or confirmed by backlighting/ultrasound/biopsy.

This protocol, while preliminary, outlines a biologically grounded approach to induced spawning in *R. leporina*. By targeting females at the appropriate stage of oocyte development and verifying hormonal response post-treatment, hatchery managers can reduce treatment failure and improve spawning reliability in early domestication programs.

### 4.7: Final Conclusions

This study evaluated two complementary approaches for improving reproductive performance in yellowbelly Flounder (*R. leporina*): hormonal induction using GnRHa and the development of a non-lethal Visual Gonadosomatic Index (VGSI) for broodstock monitoring.

GnRHa injections transiently stimulated ovarian *cyp19a1a* expression, particularly at the highest dose (100 µg/kg), indicating partial activation of the steroidogenic pathway during late vitellogenesis. However, this effect was short-lived, with expression declining by Day 5 across all groups. The absence of downstream maturation markers such as *lhb* and *20βhsd*, along with the lack of plasma estradiol or MIS measurements, limited conclusions about functional reproductive readiness. Small sample sizes and high individual variability further constrained statistical confidence. Future research should incorporate broader gene panels targeting the BPG axis, including *fshb*, *lhb*, *gpα*, and *20β-hsd*, alongside plasma profiling of estradiol and MIS to better characterise endocrine activation. Integrating these markers with sustained-release delivery systems such as Ovaplant or recombinant gonadotropins would help determine whether hormonal stimulation results in full reproductive competence rather than transient transcriptional responses.

VGSI, based on backlit imaging of the ventral gonads, represents a novel and minimally invasive method for assessing reproductive state in flatfish. While Length GSI showed a weak but significant correlation with oocyte diameter, overall performance was inconsistent, and Size GSI did not reflect maturity stage. However, Size GSI showed a statistically significant correlation with *cyp19a1a* expression, explaining over half of the observed variance, and Length GSI also showed a moderate association. These findings indicate that visual metrics may reflect transcriptional activity linked to reproductive development, even when histological resolution is limited. VGSI may still be useful for longitudinal monitoring of individual fish, particularly for detecting changes such as oocyte hydration or gonadal elongation during hormone trials. Further refinement of imaging protocols and a focus on ovarian-specific metrics will be necessary before VGSI can be applied as a diagnostic tool.

Together, these findings underscore both the potential and current limitations of GnRHa-based hormone induction and VGSI-based monitoring in *R. leporina*. The results highlight the importance of delivery method, timing, and broodstock selection for achieving predictable spawning outcomes. Continued development of complementary molecular and imaging approaches will be critical for enhancing reproductive success and supporting the commercial viability of *R. leporina* aquaculture.

# References


Ackefors, H., Huner, J., & Konikoff, M. (2017). *Introduction to the general principles of aquaculture*. CRC Press.

Agulleiro, M. J., Anguis, V., Cañavate, J. P., Martínez-Rodríguez, G., Mylonas, C. C., & Cerdà, J. (2006). Induction of spawning of captive-reared Senegal sole (*Solea senegalensis*) using different administration methods for gonadotropin-releasing hormone agonist. *Aquaculture*, 257(1–4), 511–524.

Ahmed, N., Bunting, S. W., Glaser, M., Flaherty, M. S., & Diana, J. S. (2017). Can greening of aquaculture sequester blue carbon? Ambio, 46, 468–477.

Akhtar, M. S., Ciji, A., Sarma, D., Rajesh, M., Kamalam, B. S., Sharma, P., & Singh, A. K. (2017). Reproductive dysfunction in females of endangered golden mahseer (*Tor putitora*) in captivity. *Animal Reproduction Science*, 182, 95–103.

Aydin, I., Firidin, Ş., Cebeci, A., Öztürk, R. Ç., Terzi, Y., Polat, H., & Küçük, E. (2023). Gonad development of Black Sea European flounder, Platichthys flesus, under culture conditions. Thalassas: *An International Journal of Marine Sciences*, 39, 1–6.

Ayling, T., & Cox, G. J. (1982). *Collins guide to the sea fishes of New Zealand*. Collins.

Bagenal, T. B. (1978). Aspects of fish fecundity. In T. B. Bagenal (Ed.), *Ecology of freshwater fish production* (pp. 75–101). Blackwell.

Berlinsky, D. L., King, V. W., Smith, T. I., Hamilton, R. D., Holloway, J., & Sullivan, C. V. (1996). Induced ovulation of southern flounder *Paralichthys lethostigma* using gonadotropin releasing hormone analogue implants. *Journal of the World Aquaculture Society*, 27(2), 143–152.

Berlinsky, D. L., King, W. V., Hodson, R. G., & Sullivan, C. V. (1997). Hormone induced spawning of summer flounder *Paralichthys dentatus*. *Journal of the World Aquaculture Society*, 28(1), 79–86.

Brewer, S. K., Rabeni, C. F., & Papoulias, D. M. (2008). Comparing histology and gonadosomatic index for determining spawning condition of small-bodied riverine fishes. *Ecology of Freshwater Fish*, 17(1), 54–58.

Bromage, N., Hardiman, P., Jones, J., Springate, J., & Bye, V. (1990). Fecundity, egg size and total egg volume differences in 12 stocks of rainbow trout, *Oncorhynchus mykiss* Richardson. *Aquaculture Research*, 21(3), 269–284.

Bromage, N., Porter, M., & Randall, C. (2001). The environmental regulation of maturation in farmed finfish with special reference to the role of photoperiod and melatonin. *Aquaculture*, 197(1–4), 63–98.

Brown-Peterson, N. J., & Warren, J. W. (2001). The reproductive biology of spotted seatrout, *Cynoscion nebulosus*, along the Mississippi Gulf Coast. *Gulf of Mexico Science*, 19(1), 7–16.

Buckley, L. J., Smigielski, A. S., Halavik, T. A., Caldarone, E. M., Burns, B. R., & Laurence, G. C. (1991). Winter flounder *Pseudopleuronectes americanus* reproductive success. II. Effects of spawning time and female size on size, composition and viability of eggs and larvae. *Marine Ecology Progress Series*, 74(2), 125–135.

Cao, J., Wang, X., Damiano, M. D., Zhou, C., & Zhu, J. (2021). A Bayesian multilevel ordinal regression model for fish maturity data: Difference in maturity ogives of skipjack tuna (*Katsuwonus pelamis*) between schools in the Western and Central Pacific Ocean. *Frontiers in Marine Science*, 8, 736462.

Colman, J. A. (1973). Spawning and fecundity of two flounder species in the Hauraki Gulf, New Zealand. *New Zealand Journal of Marine and Freshwater Research*, 7(1–2), 21–43.

Contreras-Sanchez, W. M., Schreck, C. B., Fitzpatrick, M. S., & Pereira, C. B. (1998). Effects of stress on the reproductive performance of rainbow trout (*Oncorhynchus mykiss*). *Biology of Reproduction*, 58(2), 439–447.

Denson, M. R., Jenkins, W. E., Berlinsky, D. L., & Smith, T. I. (2007). A comparison of human chorionic gonadotropin and luteinizing hormone releasing hormone analogue for ovulation induction in black sea bass *Centropristis striata* (Linnaeus, 1758). *Aquaculture Research*, 38(9), 918–925.

Duarte, C. M., & Alcaraz, M. (1989). To produce many small or few large eggs: A size-independent reproductive tactic of fish. *Oecologia*, 80, 401–404.

Edwards, P. (2015). Aquaculture environment interactions: Past, present and likely future trends. *Aquaculture*, 447, 2–14.

Ellis-Smith, B. G. (2022). Induced reproduction in pātiki (*Rhombosolea leporina*), a novel endemic aquaculture candidate (Master's thesis, University of Waikato, Hamilton, New Zealand).

Emerson, L. S., Walker, M. G., & Witthames, P. R. (1990). A stereological method for estimating fish fecundity. *Journal of Fish Biology*, 36(5), 721–730.

Essington, T. E., Quinn, T. P., & Ewert, V. E. (2000). Intra- and inter-specific competition and the

reproductive success of sympatric Pacific salmon. *Canadian Journal of Fisheries and Aquatic Sciences*, 57(1), 205–213.

Faheem, M., Jahan, N., Khaliq, S., & Lone, K. P. (2018). Validation of reference genes for expression analysis in a teleost fish (*Catla catla* Hamilton) exposed to an endocrine-disrupting chemical, bisphenol-A. *Rendiconti Lincei. Scienze Fisiche e Naturali*, 29, 13–22.

Fakriadis, I., Sigelaki, I., Papadaki, M., Papandroulakis, N., Raftopoulos, A., Tsakoniti, K., & Mylonas, C. C. (2020). Control of reproduction of greater amberjack *Seriola dumerili* reared in aquaculture facilities. *Aquaculture*, 519, 734880.

Fernández-Palacios, H., Schuchardt, D., Roo, J., Hernández-Cruz, C. M., & Izquierdo, M. (2015). Multiple GnRHa injections to induce successful spawning of wild caught greater amberjack (*Seriola dumerili*) matured in captivity. *Aquaculture Research*, 46(7), 1748–1759.

Fitzhugh, G. R., Shertzer, K. W., Kellison, G. T., & Wyanski, D. M. (2012). Review of size- and age-dependence in batch spawning: Implications for stock assessment of fish species exhibiting indeterminate fecundity. *Fishery Bulletin*, 110(4), 413–425

Garlock, T., Asche, F., Anderson, J., Bjørndal, T., Kumar, G., Lorenzen, K., Ropicki, A., Smith, M. D., & Tveterås, R. (2020). A global blue revolution: Aquaculture growth across regions, species, and countries. *Reviews in Fisheries Science & Aquaculture*, 28(1), 107–116.

Gjerde, B. (1984). Response to individual selection for age at sexual maturity in Atlantic salmon. *Aquaculture*, 38(3), 229–240.

Guitreau, A. M., Eilts, B. E., Novelo, N. D., & Tiersch, T. R. (2012). Fish handling and ultrasound procedures for viewing the ovary of submersed, nonanesthetized, unrestrained channel catfish. *North American Journal of Aquaculture*, 74(2), 182–187.

Guzmán, J. M., Ramos, J., Mylonas, C. C., & Mañanós, E. L. (2009). Spawning performance and plasma levels of GnRHa and sex steroids in cultured female Senegalese sole (*Solea senegalensis*) treated with different GnRHa-delivery systems. *Aquaculture*, 291(3–4), 200–209.

Guzmán, J. M., Cal, R., García-López, Á., Chereguini, O., Kight, K., Olmedo, M., ... & Mañanós, E. L. (2011). Effects of in vivo treatment with the dopamine antagonist pimozide and gonadotropin-releasing hormone agonist (GnRHa) on the reproductive axis of Senegalese sole (*Solea senegalensis*). *Comparative Biochemistry and Physiology Part A: Molecular & Integrative Physiology*, 158(2), 235–245.

Haddy, J. A., & Pankhurst, N. W. (1999). Stress-induced changes in concentrations of plasma sex steroids in black bream. *Journal of Fish Biology*, 55(6), 1304–1316.

Hamidoghli, A., Won, S., Lee, S., Lee, S., Farris, N. W., & Bai, S. C. (2020). Nutrition and feeding of olive flounder *Paralichthys olivaceus*: A review. *Reviews in Fisheries Science & Aquaculture*, 28(3), 340–357.

Helfrich, L. A., & Libey, G. S. (1991). Fish farming in recirculating aquaculture systems (RAS). Dept. Fisheries & Wildlife Sciences, Virginia Tech. Retrieved December 8, 2025 https://extension.rwfm.tamu.edu/wp-content/uploads/sites/8/2013/09/Fish-Farming-in-Recirculating-Aquaculture-Systems-RAS.pdf

Hunter, J. R., Lo, N. C., & Leong, R. J. (1985). Batch fecundity in multiple spawning fishes. *NOAA Technical Report NMFS*, 36, 67–77.

Hunter, J. R. (1992). Fecundity, spawning and maturity of female Dover sole *Microstomus pacificus*, with an evaluation of assumption and precision. *Fishery Bulletin*, 90, 101–128.

Hunter, J. R., & Macewicz, B. J. (2003). Improving the accuracy and precision of reproductive information used in fisheries. In O. S. Kjesbu, J. R. Hunter & P. R. Witthames (Eds.), Modern approaches to assess maturity and fecundity of warm- and cold-water fish and squids (pp. 57–68). Institute of Marine Research, Bergen, Norway.

Imanaga, Y., Nyuji, M., Amano, M., Takahashi, A., Kitano, H., Yamaguchi, A., & Matsuyama, M. (2014). Characterization of gonadotropin-releasing hormone and gonadotropin in jack mackerel (*Trachurus japonicus*): Comparative gene expression analysis with respect to reproductive dysfunction in captive and wild fish. *Aquaculture*, 428, 226–235.

Jeuthe, H., Brännäs, E., & Nilsson, J. (2013). Effects of egg size, maternal age and temperature on egg viability of farmed Arctic charr. *Aquaculture*, 408, 70–77.

Kagawa, H., Gen, K., Okuzawa, K., & Tanaka, H. (2003). Effects of luteinizing hormone, follicle-stimulating hormone, and insulin-like growth factor-I on aromatase activity and P450 aromatase gene expression in the ovarian follicles of red seabream, *Pagrus major*. *Biology of Reproduction*, 68(5), 1562–1568.

Kjørsvik, E., Hoehne-Reitan, K., & Reitan, K. I. (2003). Egg and larval quality criteria as predictive measures for juvenile production in turbot (*Scophthalmus maximus L.*). *Aquaculture*, 227(1–4), 9–20.

Kohn, Y. Y., & Symonds, J. E. (2012). Evaluation of egg quality parameters as predictors of

hatching success and early larval survival in hapuku (*Polyprion oxygeneios*). *Aquaculture*, 342, 42–47.

Koverman, R. (2018). Reproductive biology of yellowbelly flounder *Rhombosolea leporina* (Günther, 1862) and *Rhombosolea spp* (Doctoral dissertation, University of Waikato).

Kuradomi, R. Y., Foresti, F., & Batlouni, S. R. (2017). The effects of sGnRHa implants on *Piaractus mesopotamicus* female breeders: An approach addressed to aquaculture. Aquaculture International, 25, 2259–2273.

Luckenbach, J. A., Early, L. W., Rowe, A. H., Borski, R. J., Daniels, H. V., & Godwin, J. (2005). Aromatase cytochrome P450: Cloning, intron variation, and ontogeny of gene expression in southern flounder (*Paralichthys lethostigma*). *Journal of Experimental Zoology Part A: Comparative Experimental Biology*, 303(8), 643–656.

Morrison, M. A., Lowe, M. L., Parsons, D. M., Usmar, N. R., & McLeod, I. M. (2009). A review of land-based effects on coastal fisheries and supporting biodiversity in New Zealand. *New Zealand Aquatic Environment and Biodiversity Report*, 37, 1–100.

MacLeod, M. J., Hasan, M. R., Robb, D. H., & Mamun-Ur-Rashid, M. (2020). Quantifying greenhouse gas emissions from global aquaculture. *Scientific Reports*, 10(1), 11679.

Marcoli, R., Symonds, J. E., Walker, S. P., Battershill, C. N., & Bird, S. (2023). Characterising the physiological responses of Chinook salmon (*Oncorhynchus tshawytscha*) subjected to heat and oxygen stress. *Biology*, 12(10), 1342.

McGarvey, L. M., Ilgen, J. E., Guy, C. S., McLellan, J. G., & Webb, M. A. (2021). Gonad size measured by ultrasound to assign stage of maturity in burbot. *Journal of Fish and Wildlife Management*, 12(1), 241–249.

Memarzadeh, M., Britten, G. L., Worm, B., & Boettiger, C. (2019). Rebuilding global fisheries under uncertainty. *Proceedings of the National Academy of Sciences*, 116(32), 15985–15990.

Mlingi, F. T., Puvanendran, V., Burgerhout, E., Tveiten, H., Tomkiewicz, J., Kjørsvik, E., & Mommens, M. (2023). Ultrasonic imaging as a means of monitoring gonadal development in lumpfish (*Cyclopterus lumpus*). *Physiological Reports*, 11(18), e15811.

Moulik, S. R., Pal, P., Majumder, S., Mallick, B., Gupta, S., Guha, P., ... & Mukherjee, D. (2016). Gonadotropin and SF-1 regulation of *cyp19a1a* gene and aromatase activity during oocyte development in the rohu, *Labeo rohita*. *Comparative Biochemistry and Physiology Part A: Molecular & Integrative Physiology*, 196, 1–10.

Mungkung, R., Aubin, J., Prihadi, T. H., Slembrouck, J., van der Werf, H. M., & Legendre, M. (2013). Life cycle assessment for environmentally sustainable aquaculture management: A case study of combined aquaculture systems for carp and tilapia. *Journal of Cleaner Production*, 57, 249–256.

Munro, A. D., Scott, A. P., & Lam, T. J. (Eds.). (1990). *Reproductive seasonality in teleosts: Environmental influences* (pp. 1–11). Boca Raton: CRC Press.

Murua, H., Kraus, G., Saborido-Rey, F., Witthames, P. R., Thorsen, A., & Junquera, S. (2003). Procedures to estimate fecundity of marine fish species in relation to their reproductive strategy. *Journal of Northwest Atlantic Fishery Science*, 33, 33–54.

Murugananthkumar, R., & Sudhakumari, C. C. (2022). Understanding the impact of stress on teleostean reproduction. *Aquaculture and Fisheries*, 7(5), 553–561.

Mylonas, C. C., Zohar, Y., Pankhurst, N., & Kagawa, H. (2011). Reproduction and broodstock management. In M. Pavlidis & C. C. Mylonas (Eds.), *Sparidae* (pp. 95–131). Academic Press.

Mylonas, C. C., & Zohar, Y. (2009). Controlling fish reproduction in aquaculture. In G. Burnell & G. Allan (Eds.), *New technologies in aquaculture* (pp. 109–142). Woodhead Publishing.

Mylonas, C. C., Fostier, A., & Zanuy, S. (2010). Broodstock management and hormonal manipulations of fish reproduction. *General and Comparative Endocrinology*, 165(3), 516–534.

Næve, I. (2020). Development of non-invasive methods using ultrasound technology in monitoring of Atlantic salmon (*Salmo salar*) production and reproduction. Master's thesis, Norwegian University of Science and Technology, Trondheim, Norway.

Næve, I., Mommens, M., Arukwe, A., & Kjørsvik, E. (2018). Ultrasound as a noninvasive tool for monitoring reproductive physiology in female Atlantic salmon (*Salmo salar*). *Physiological Reports*, 6(9), e13640.

Nagahama, Y. (1997). 17α, 20β-Dihydroxy-4-pregnen-3-one, a maturation-inducing hormone in fish oocytes: Mechanisms of synthesis and action. *Steroids*, 62(1), 190–196.

Nagahama, Y., & Yamashita, M. (2008). Regulation of oocyte maturation in fish. *Development, Growth & Differentiation*, 50(Suppl. 1), S195–S219.

Nyuji, M., Hongo, Y., Yoneda, M., & Nakamura, M. (2020). Transcriptome characterization of BPG axis and expression profiles of ovarian steroidogenesis-related genes in the Japanese sardine.

BMC Genomics, 21(1), 668.

Nargesi, E. A., Falahatkar, B., Żarski, D., & Gorouhi, D. (2023). The effectiveness of Ovaprim, Ovopel, and their combinations in artificial reproduction of common rudd *Scardinius erythrophthalmus* under controlled conditions. *Theriogenology*, 199, 114–120.

Novelo, N., Kuenz, D., Green, C. C., & Tiersch, T. R. (2011). Ultrasonic monitoring of channel catfish ovarian development. In T. R. Tiersch & C. C. Green (Eds.), *Cryopreservation in aquatic species* (2nd ed., pp. 134–144). World Aquaculture Society.

Oliveira, E. C. D., & Fávaro, L. F. (2010). Reproduction of the flatfish *Achirus lineatus* (Pleuronectiformes: Achiridae) in Paranaguá Bay, state of Paraná, a subtropical region of Brazil. *Zoologia* (Curitiba), 27, 523–532.

Pankhurst, N. W., & Van der Kraak, G. (1997). Effects of stress on reproduction and growth of fish. In G. K. Iwama, A. D. Pickering, J. P. Sumpter, & C. B. Schreck (Eds.), *Fish stress and health in aquaculture* (pp. 73–93). Cambridge University Press.

Peer, A. C., Selckmann, G. M., & Miller, T. J. (2012). A standardized method and analytical approach for predicting female reproductive stage in teleosts by using ovary color and female characteristics. *Transactions of the American Fisheries Society*, 141(4), 1036–1044.

Poortenaar, C. W., Hooker, S. H., & Sharp, N. (2001). Assessment of yellowtail kingfish (*Seriola lalandi*) reproductive physiology as a basis for aquaculture development. Aquaculture, 201(3–4), 271–286.

Poortenaar, C. W., & Pankhurst, N. W. (2000). Potential for dopamine inhibition of GtH release in greenback flounder *Rhombosolea tapirina*: indirect assessment by measurement of gonadal steroids and ovulation. *In Proceedings of the International Symposium on the Reproductive Physiology of Fish*.

Ramos-Júdez, S., Giménez, I., Gumbau-Pous, J., Arnold-Cruañes, L. S., Estévez, A., & Duncan, N. (2022). Recombinant Fsh and Lh therapy for spawning induction of previtellogenic and early spermatogenic arrested teleost, the flathead grey mullet (*Mugil cephalus*). *Scientific Reports*, 12, 6563.

Rasines, I., Gómez, M., Martín, I., Rodríguez, C., Mañanós, E., & Chereguini, O. (2012). Artificial fertilization of Senegalese sole (*Solea senegalensis*): Hormone therapy administration methods, timing of ovulation and viability of eggs retained in the ovarian cavity. *Aquaculture*, 326, 129–135.

Ritchie, H., & Roser, M. (2023). The world population is changing: For the first time there are more people over 64 than children younger than 5. Our World in Data. https://ourworldindata.org/population-age-structure

Royo, P., Muñoz, E., Romero, J. E., Manjón, J. V., Roig, C., Fernández-Delgado, C., ... & Pellicer, A. (2024). Three-dimensional ultrasound-based online system for automated ovarian follicle measurement. arXiv. https://arxiv.org/abs/2407.18818

Schreck, C. B., Contreras-Sanchez, W., & Fitzpatrick, M. S. (2001). Effects of stress on fish reproduction, gamete quality, and progeny. In B. G. Muir & S. K. Leong (Eds.), *Reproductive biotechnology in finfish aquaculture* (pp. 3–24). Elsevier.

Schulz, R. W., & Henk, J. (1999). Puberty in male fish: Concepts and recent developments with special reference to the African catfish (*Clarias gariepinus*). *Aquaculture*, 177(1–4), 5–12.

Schulz, R. W., & Miura, T. (2002). Spermatogenesis and its endocrine regulation. *Fish Physiology and Biochemistry*, 26, 43–56.

Selvaraj, S., Chidambaram, P., Ezhilarasi, V., Kumar, P. P., Samuel Moses, T. L. S., Antony, C., & Ahilan, B. (2021). A review on the reproductive dysfunction in farmed finfish. *Annual Research & Review in Biology*, 36(10), 65–81.

Senarat, S., Kettratad, J., Kangwanrangsan, N., Jiraungkoorskul, W., Amano, M., Shimizu, A., Plumley, F. G., & Tipdomrongpong, S. (2019). The sbGnRH–GTH system in the female short mackerel, *Rastrelliger brachysoma* (Bleeker, 1851), during breeding season: Implications for low gamete production in captive broodstock. *Fish Physiology and Biochemistry*, 45, 1–18.

Stuart, K. R., Armbruster, L., Johnson, R., & Drawbridge, M. A. (2020). Egg diameter as a predictor for egg quality of California yellowtail (*Seriola dorsalis*). *Aquaculture*, 522, 735154.

Subasinghe, R., Soto, D., & Jia, J. (2009). Global aquaculture and its role in sustainable development. *Reviews in Aquaculture*, 1(1), 2–9.

Taranger, G. L., Carrillo, M., Schulz, R. W., Fontaine, P., Zanuy, S., Felip, A., Weltzien, F. A., Dufour, S., Karlsen, Ø., Norberg, B., & Andersson, E. (2010). Control of puberty in farmed fish. *General and Comparative Endocrinology*, 165(3), 483–515.

Teixeira, S. F., Duarte, Y. F., & Ferreira, B. P. (2010). Reproduction of the fish *Lutjanus analis* (mutton snapper; Perciformes: Lutjanidae) from Northeastern Brazil. *Revista de Biología Tropical*, 58(3), 791–800.

Villeneuve, D. L. (2016). Adverse outcome pathway on aromatase inhibition leading to reproductive dysfunction (in fish). *OECD Series on Testing and Assessment*, No. 232. https://doi.org/10.1787/5jln7vnpxzs1-en

Wedemeyer, G. (1996). Physiology of fish in intensive culture systems. Springer Science & Business Media.

Wallace, P., Pierce, H., & Paul, N. (2003). Pūawaitanga o te Ringa - *Fruits of your busy hands*. Christchurch City Libraries. https://christchurchcitylibraries.com/Maori/Puawaitanga/Puawaitanga.pdf

Watanabe, W. O., Benetti, D. D., Feeley, M. W., Davis, A. D., & Phelps, R. P. (2005). Status of artificial propagation of mutton, yellowtail, and red snapper (family *Lutjanidae*). In C. J. Walters & T. D. Mosher (Eds.), *American Fisheries Society Symposium* (Vol. 46, pp. 517–540). AFS.

Weltzien, F. A., Andersson, E., Andersen, Ø., Shalchian-Tabrizi, K., & Norberg, B. (2004). The brain–pituitary–gonad axis in male teleosts, with special emphasis on flatfish (*Pleuronectiformes*). *Comparative Biochemistry and Physiology Part A: Molecular & Integrative Physiology*, 137(3), 447–477.

Wootton, R. J. (1985). Energetics of reproduction. In P. Tytler & P. Calow (Eds.), Fish energetics: *New perspectives* (pp. 231–254). Springer.

Yoshikawa, N., Mammaran, T., Bavoh, E. M., Ridzwan, A. R., Tanaka, M., & Tagawa, M. (2012). Gonadal development of the primitive flatfish *Psettodes erumei* in Kota Kinabalu, Sabah, Malaysia. *Aquaculture Science*, 60(4), 475–483.

Zohar, Y., & Mylonas, C. C. (2001). Endocrine manipulations of spawning in cultured fish: From hormones to genes. In B. G. Muir & S. K. Leong (Eds.), *Reproductive biotechnology in finfish aquaculture* (pp. 99–136). Elsevier.

Zohar, Y., Muñoz-Cueto, J. A., Elizur, A., & Kah, O. (2010). Neuroendocrinology of reproduction in teleost fish. *General and Comparative Endocrinology*, 165(3), 438–455.

# Appendices

## Appendix A – qPCR Assay Methods and Validation

*Table A1: In silico alignment summary: cyp19a1a reverse primer*

| Alignment Information | Details |
|---|---|
| Gene Target | *cyp19a1a* (reverse) |
| Reference Sequence ID | AB017182.1 |
| Query Sequence | TCC TGGA ATGC CGTC TTGTG |
| Subject Sequence | TCC TGG ACT GCC GCT TGTG |
| Alignment Range | 837–856 |
| Identity | 90% |
| Gaps | 0% |
| E-value | 29 |
| Score | 24.3 bits (12) |

*Table A2: In silico alignment summary: rpl18 forward primer*

| Alignment Information | Details |
|---|---|
| Gene Target | *rpl18* (forward) |
| Reference Sequence ID | XM_020093129.1 |
| Query Sequence | CAG GAA GAG GCC AAG AGT CAG G |
| Subject Sequence | CAG GAA GAG GCC AAG AGC CAG G |
| Alignment Range | 175–197 |
| Identity | 96% |
| Gaps | 0% |
| E-value | 0.003 |
| Score | 38.2 bits (19) |

*Table A3: In silico alignment summary: rpl18 reverse primer*

| Alignment Information | Details |
|---|---|
| Gene Target | *rpl18* (reverse) |
| Reference Sequence ID | XM_020093129.1 |
| Query Sequence | CAT CTT CAT CTT ACG GAT CAG GC |

| | |
|---|---|
| Subject Sequence | CAT CTT CAT CTT ACG AAT CAG GC |
| Alignment Range | 327–349 |
| Identity | 96% |
| Gaps | 0% |
| E-value | 0.003 |
| Score | 38.2 bits (19) |

*Table A4: In silico alignment summary: tbp forward primer*

| Alignment Information | Details |
|---|---|
| Gene Target | *tbp* (forward) |
| Reference Sequence ID | XM_020098792.1 |
| Query Sequence | AAA CTA GAC TTG AAG AC |
| Subject Sequence | AAA CTT GAC TTG AAG AC |
| Alignment Range | 683–699 |
| Identity | 94% |
| Gaps | 0% |
| E-value | 14 |
| Score | 26.3 bits (13) |

*Table A5: In silico alignment summary: tbp reverse primer*

| Alignment Information | Details |
|---|---|
| Gene Target | *tbp* (reverse) |
| Reference Sequence ID | XM_020098792.1 |
| Query Sequence | CGA CTG ATC CTC GCT TGG |
| Subject Sequence | CGA CTG TGC TCT CAC TTC GG |
| Alignment Range | 825–844 |
| Identity | 90% |
| Gaps | 0% |
| E-value | 29 |
| Score | 24.3 bits (12) |

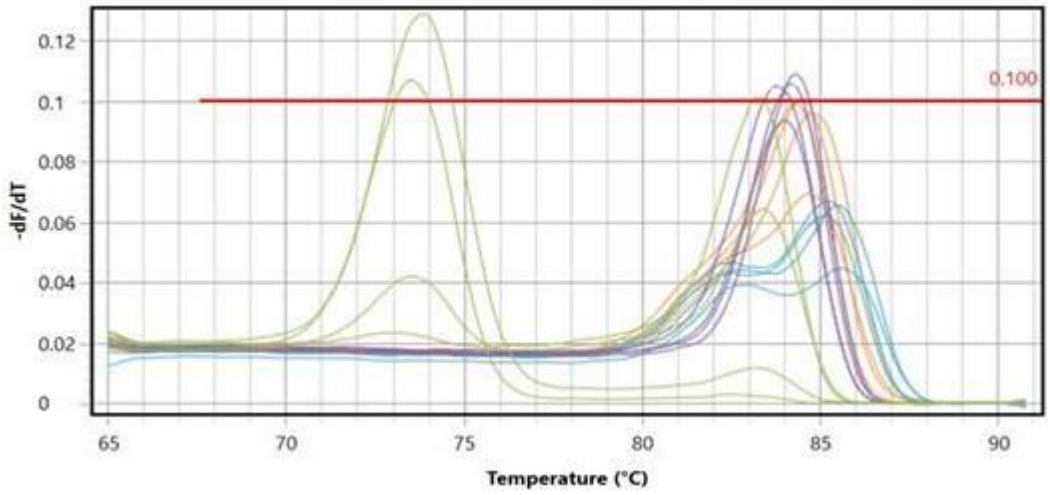


*Figure A1: Validation testing for tbp primer sets.*

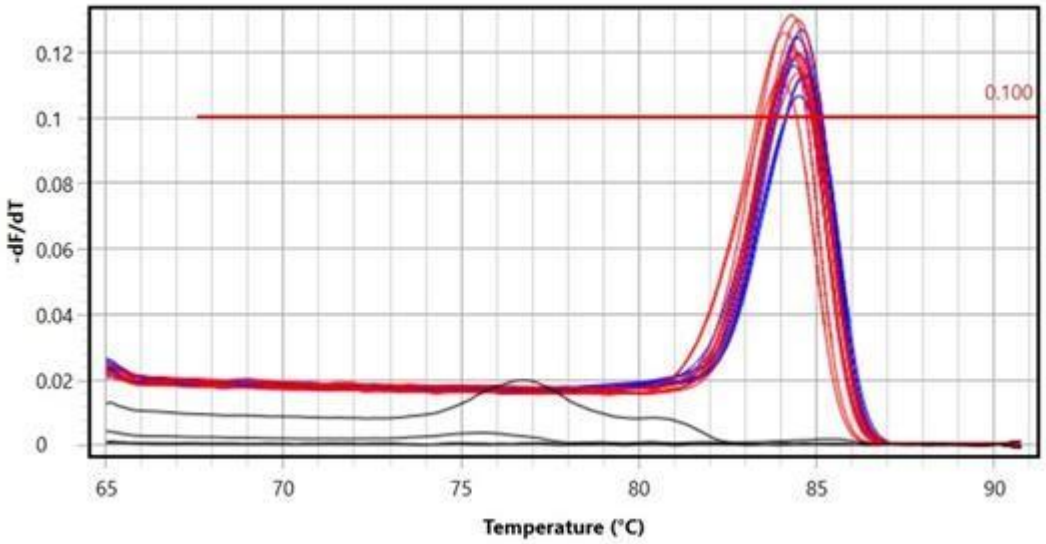


*Figure A2: Validation testing for rpl18 primer sets.*

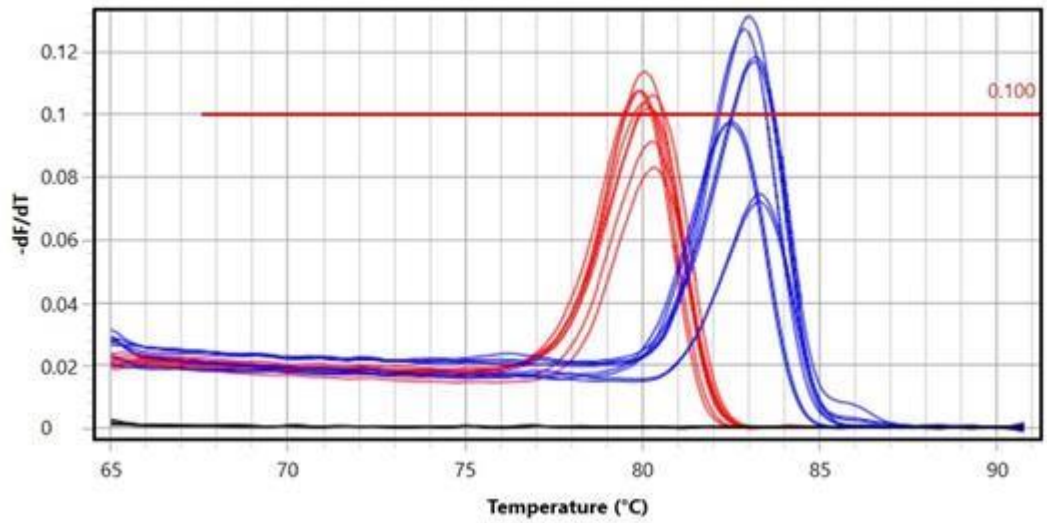


*Figure A3: Validation testing for cyp19a1a primer sets.*

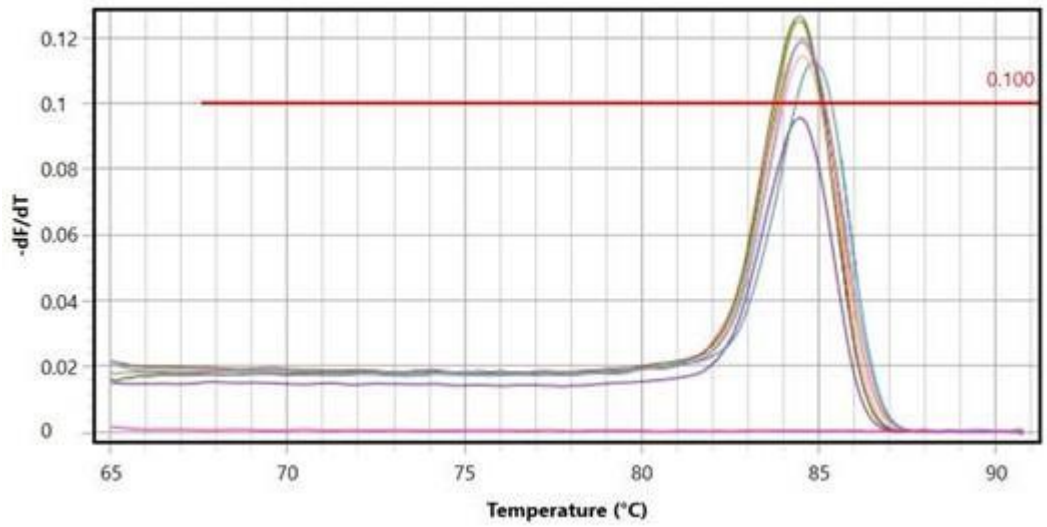


*Figure A4: rpl18 annealing temperature validation at 62°C.*

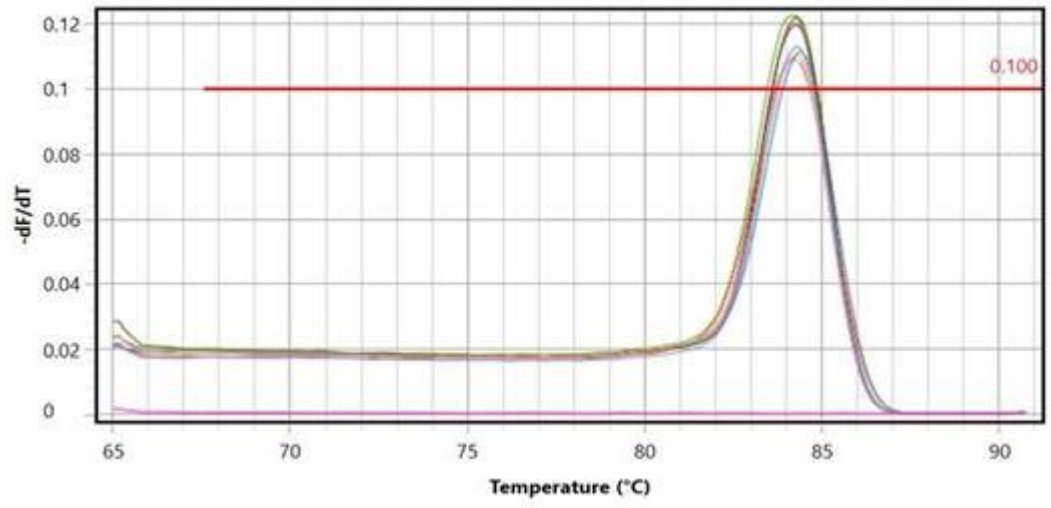


*Figure A5: rpl18 annealing temperature validation at 60°C.*

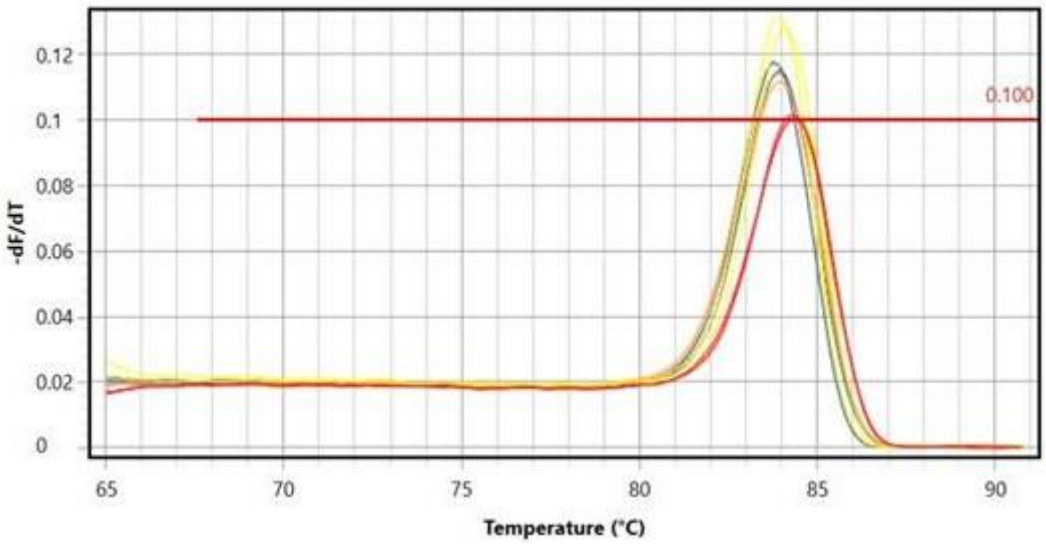


*Figure A6: tbp annealing temperature validation at 61°C.*

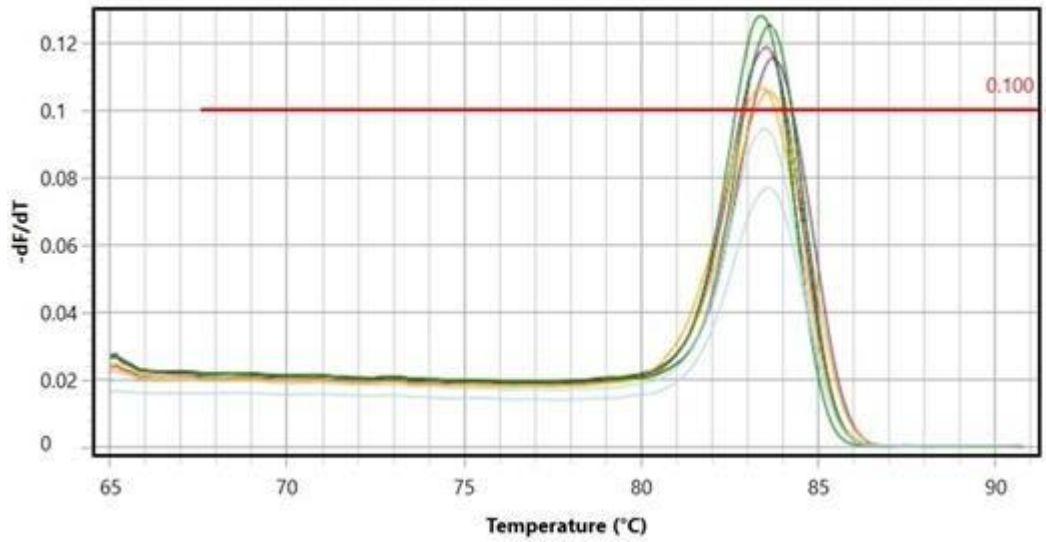


*Figure A7: tbp annealing temperature validation at 59°C.*

**Appendix B – Supplementary Figures and Results**

*Table B1: DeNovix® DS-11 spectrophotometer results showing the concentration and purity of RNA for each sample.*

| **Sample Name** | **A260** | **A260/A230** | **A260/A280** | **RNA Concentration: ng/uL** |
|---|---|---|---|---|
| GON1 | 3.89 | 2.12 | 1.98 | 12.86 |
| GON2 | 14.28 | 2.23 | 2.03 | 3.50 |
| GON3 | 6.47 | 1.85 | 2.02 | 7.72 |
| GON4 | 2.51 | 1.80 | 2.05 | 19.85 |
| GON5 | 2.93 | 1.93 | 2.02 | 17.01 |
| GON6 | 5.43 | 2.13 | 2.01 | 9.21 |
| GON7 | 3.30 | 1.55 | 2.01 | 15.11 |
| GON8 | 3.91 | 2.11 | 1.94 | 12.76 |
| GON10 | 4.92 | 2.11 | 1.98 | 10.16 |
| GON11 | 8.53 | 2.15 | 2.03 | 5.86 |
| GON12 | 9.37 | 2.09 | 2.02 | 5.33 |
| GON13 | 3.24 | 2.02 | 1.97 | 15.41 |
| GON14 | 8.10 | 2.04 | 1.97 | 6.17 |
| GON15 | 16.10 | 2.18 | 2.06 | 3.11 |
| GON16 | 24.69 | 2.25 | 2.10 | 2.02 |
| GON17 | 12.69 | 2.15 | 2.11 | 3.94 |
| GON18 | 8.46 | 2.21 | 2.03 | 5.91 |
| GON19 | 14.03 | 2.24 | 2.07 | 3.56 |
| GON20 | 24.00 | 2.27 | 2.09 | 2.08 |
| GON21 | 20.03 | 2.26 | 2.08 | 2.50 |
| GON22 | 8.50 | 2.00 | 2.00 | 5.88 |
| GON23 | 14.65 | 2.16 | 2.04 | 3.41 |
| GON24 | 10.73 | 2.15 | 2.00 | 4.66 |
| GON25 | 10.52 | 2.17 | 1.99 | 4.75 |
| GON26 | 14.68 | 2.22 | 2.03 | 3.41 |
| GON27 | 18.52 | 2.25 | 2.05 | 2.70 |
| GON28 | 16.58 | 2.23 | 2.04 | 3.01 |
| GON29 | 7.79 | 2.20 | 2.00 | 6.42 |

| | | | | |
|---|---|---|---|---|
| GON30 | 10.61 | 2.21 | 2.01 | 4.71 |
| GON31 | 21.59 | 2.25 | 2.06 | 2.32 |
| GON32 | 16.11 | 2.22 | 2.02 | 3.10 |
| GON33 | 27.22 | 2.04 | 2.09 | 1.84 |
| GON34 | 19.36 | 2.25 | 2.07 | 2.58 |
| GON35 | 72.97 | 2.19 | 2.02 | 0.69 |
| GON36 | 9.47 | 2.19 | 2.03 | 5.28 |
| GON37 | 92.91 | 2.26 | 2.06 | 0.54 |
| GON38 | 18.09 | 2.21 | 2.03 | 2.76 |
| GON39 | 37.30 | 2.21 | 2.02 | 1.34 |
| GON40 | 43.05 | 2.22 | 2.05 | 1.16 |
| GON41 | 24.50 | 2.28 | 2.04 | 2.04 |

*Table B2: Reagent volumes for qScript™ cDNA synthesis for each sample.*

| **Sample Name** | **RNA (µL)** | **Water (µL)** | **Supermix (µL)** | **Total (µL)** |
|---|---|---|---|---|
| GON1 | 12.8 | 3.2 | 4 | 20 |
| GON2 | 13.8 | 2.2 | 4 | 20 |
| GON3 | 7.7 | 8.3 | 4 | 20 |
| GON4 | 16.0 | 0 | 4 | 20 |
| GON5 | 16.0 | 0 | 4 | 20 |
| GON6 | 9.2 | 6.8 | 4 | 20 |
| GON7 | 16.0 | 0 | 4 | 20 |
| GON8 | 15.1 | 0.9 | 4 | 20 |
| GON10 | 10.1 | 5.9 | 4 | 20 |
| GON11 | 5.8 | 10.2 | 4 | 20 |
| GON12 | 5.3 | 10.7 | 4 | 20 |
| GON13 | 15.4 | 0.6 | 4 | 20 |
| GON14 | 6.2 | 9.8 | 4 | 20 |
| GON15 | 3.1 | 12.9 | 4 | 20 |
| GON16 | 2.0 | 14 | 4 | 20 |
| GON17 | 3.9 | 12.1 | 4 | 20 |
| GON18 | 5.9 | 10.1 | 4 | 20 |

| | | | | |
|---|---|---|---|---|
| GON19 | 3.6 | 12.4 | 4 | 20 |
| GON20 | 2.1 | 13.9 | 4 | 20 |
| GON21 | 2.5 | 13.5 | 4 | 20 |
| GON22 | 5.9 | 10.1 | 4 | 20 |
| GON23 | 3.4 | 12.6 | 4 | 20 |
| GON24 | 4.7 | 11.3 | 4 | 20 |
| GON25 | 4.8 | 11.2 | 4 | 20 |
| GON26 | 3.4 | 12.6 | 4 | 20 |
| GON27 | 2.7 | 13.3 | 4 | 20 |
| GON28 | 3.0 | 13 | 4 | 20 |
| GON29 | 6.4 | 9.6 | 4 | 20 |
| GON30 | 4.7 | 11.3 | 4 | 20 |
| GON31 | 2.3 | 13.7 | 4 | 20 |
| GON32 | 3.1 | 12.9 | 4 | 20 |
| GON33 | 4.0 | 12 | 4 | 20 |
| GON34 | 2.6 | 13.4 | 4 | 20 |
| GON35 | 5.8 | 10.2 | 4 | 20 |
| GON36 | 5.3 | 10.7 | 4 | 20 |
| GON37 | 2.1 | 13.9 | 4 | 20 |
| GON38 | 2.8 | 13.2 | 4 | 20 |
| GON39 | 1.3 | 14.7 | 4 | 20 |
| GON40 | 1.2 | 14.8 | 4 | 20 |
| GON41 | 1.5 | 14.5 | 4 | 20 |

*Table B3: qPCR Threshold values (Ct) for housekeeping and gene of interest of each sample.*

| **Sample Number** | **Treatment** | ***tbp* Ct (avg)** | ***rpl18* Ct (avg)** | ***cyp19a* Ct (avg)** |
|---|---|---|---|---|
| GON1 | Control | 23.08 | 20.03 | 30.02 |
| GON2 | Control | 20.85 | 17.04 | 26.92 |
| GON3 | Control | 21.21 | 17.96 | 25.06 |
| GON4 | Control | 22.24 | 19.08 | 26.96 |
| GON5 | Control | 21.34 | 17.45 | 26.15 |
| GON6 | 25 | 21.63 | 17.67 | 28.02 |

| | | | | |
|---|---|---|---|---|
| GON7 | Control | 28.28 | 22.41 | 32.26 |
| GON8 | 50 | 29.90 | 28.74 | 32.58 |
| GON10 | 100 | 28.70 | 27.31 | 29.61 |
| GON11 | 25 | 24.42 | 22.47 | 29.07 |
| GON12 | Control | 21.39 | 16.42 | 27.36 |
| GON13 | 25 | 22.61 | 18.04 | 29.74 |
| GON14 | 50 | 24.12 | 22.73 | 26.86 |
| GON15 | Control | 22.78 | 19.00 | 28.60 |
| GON16 | 100 | 21.10 | 16.56 | 24.33 |
| GON17 | 100 | 20.09 | 16.08 | 27.89 |
| GON18 | 50 | 20.07 | 16.11 | 27.89 |
| GON19 | 100 | 22.19 | 18.23 | 24.20 |
| GON20 | 25 | 19.33 | 14.47 | 27.15 |
| GON21 | Control | 20.94 | 17.40 | 27.89 |
| GON22 | Control | 19.68 | 16.06 | 27.71 |
| GON23 | Control | 19.19 | 15.62 | 26.02 |
| GON24 | 100 | 20.47 | 16.62 | 26.51 |
| GON25 | 100 | 20.25 | 16.76 | 26.22 |
| GON26 | 25 | 20.79 | 19.94 | 28.28 |
| GON27 | 50 | 18.66 | 15.12 | 25.24 |
| GON28 | 100 | 19.10 | 15.90 | 26.62 |
| GON29 | 50 | 20.40 | 17.61 | 28.45 |
| GON30 | 100 | 19.36 | 15.11 | 27.02 |
| GON31 | 50 | 18.94 | 15.23 | 25.88 |
| GON32 | 25 | 20.79 | 17.64 | 29.21 |
| GON33 | Control | 19.65 | 15.71 | 26.16 |
| GON34 | 100 | 23.99 | 19.92 | 29.20 |
| GON35 | Control | 18.79 | 15.80 | 25.70 |
| GON36 | 25 | 24.16 | 19.25 | 29.03 |
| GON37 | 25 | 21.06 | 17.30 | 30.35 |
| GON38 | Control | 21.29 | 16.84 | 28.70 |
| GON39 | 25 | 19.49 | 16.47 | 25.49 |

| | | | | |
|---|---|---|---|---|
| GON40 | 50 | 18.93 | 15.82 | 25.14 |
| GON41 | 100 | 19.48 | 15.79 | 27.17 |

*Table B4: Oocyte Development Stage, Mean Oocyte Diameter, and GnRHa Treatment for R. leporina*

| Sample # | Oocyte Stage | Mean Oocyte Diameter (mm) | GnRHa Treatment (µg/kg) |
|---|---|---|---|
| S12 | VIT | 0.351 | 0 |
| S15 | PVO | 0.189 | 0 |
| S21 | VIT | 0.375 | 0 |
| S22 | FOM | 0.488 | 0 |
| S23 | PVO | 0.18 | 0 |
| S33 | VIT | 0.334 | 0 |
| S35 | VIT | 0.2295 | 0 |
| S38 | FOM | 0.552 | 0 |
| S7 | VIT | 0.196 | 0 |
| S11 | FOM | 0.443 | 25 |
| S13 | FOM | 0.395 | 25 |
| S20 | VIT | 0.311 | 25 |
| S26 | FOM | 0.391 | 25 |
| S32 | VIT | 0.296 | 25 |
| S36 | FOM | 0.39 | 25 |
| S37 | VIT | 0.301 | 25 |
| S39 | VIT | 0.265 | 25 |
| S6 | FOM | 0.457 | 25 |
| S14 | FOM | 0.391 | 50 |
| S18 | PVO | 0.175 | 50 |
| S29 | FOM | 0.399 | 50 |
| S31 | VIT | 0.279 | 50 |
| S40 | FOM | 0.423 | 50 |
| S8 | PVO | 0.112 | 50 |
| S10 | FOM | 0.448 | 100 |
| S16 | FOM | 0.416 | 100 |

| | | | |
|---|---|---|---|
| S17 | FOM | 0.384 | 100 |
| S19 | VIT | 0.37 | 100 |
| S24 | FOM | 0.442 | 100 |
| S25 | VIT | 0.158 | 100 |
| S28 | VIT | 0.374 | 100 |
| S30 | VIT | 0.236 | 100 |
| S34 | VIT | 0.38 | 100 |
| S41 | VIT | 0.238 | 100 |

*Table B5: Day 1 body weight summary of R. leporina broodstock by GnRHa treatment group*

| **GnRHa Treatment (µg/kg)** | ***n*** | ***Mean Weight (g)*** | ***SD (g)*** | ***Min (g)*** | ***Max (g)*** |
|---|---|---|---|---|---|
| Control | 10 | 389.5 | 66.5 | 320 | 510 |
| 25 | 10 | 355.5 | 57.8 | 245 | 430 |
| 50 | 10 | 386.5 | 77.2 | 305 | 530 |
| 100 | 10 | 400.5 | 88.4 | 280 | 580 |

*Table B6: Mortality summary of R. leporina broodstock by GnRHa treatment group during the experimental period*

| **GnRHa Treatment (µg/kg)** | ***n*** | **Deaths** | **Survived** | **Mortality %** |
|---|---|---|---|---|
| Control | 10 | 1 | 9 | 10 |
| 25 | 10 | 1 | 9 | 10 |
| 50 | 10 | 2 | 8 | 20 |
| 100 | 10 | 0 | 10 | 0 |

*Table B7: Baseline normalized $log_2$ fold change in ovarian cyp19a1a expression (Day 0).*

| **Group** | **n** | **Mean $Log_2$ FC ± SD** |
|---|---|---|
| Baseline (Wild) | 5 | 0.88 ± 1.22 |

*Table B8: Day 1 normalized $log_2$ fold change in ovarian cyp19a1a expression following GnRHa treatment.*

| Treatment (µg/kg) | *n* | Mean $Log_2$ FC | SD | *p* vs Control |
|---|---|---|---|---|
| Control | 4 | -0.07 | 0.70 | — |
| 25 | 4 | -0.53 | 2.01 | 0.34 |
| 50 | 3 | 2.38 | 3.72 | 0.18 |
| 100 | 4 | 2.65 | 3.44 | 0.10 |

*Table B9: Day 5 normalized $log_2$ fold change in ovarian cyp19a1a expression following GnRHa treatment.*

| Treatment (µg/kg) | *n* | Mean $Log_2$ FC | SD | *p* (Day 1 vs Day 5) |
|---|---|---|---|---|
| Control | 5 | -1.11 | 0.61 | 0.03 |
| 25 | 5 | -0.91 | 0.31 | 0.31 |
| 50 | 4 | -0.71 | 0.70 | 0.07 |
| 100 | 6 | -0.68 | 0.11 | 0.03 |

*Table B10: Expression by Oocyte Developmental Stage (Day 1 Treated Only)*

| Stage | Mean $Log_2$ FC |
|---|---|
| PVO | -1.85 |
| VIT | 0.83 |
| FOM | 1.41 |

**Kruskal–Wallis** test across stages: H = 1.22, $p = 0.545$.

*Table B11: VGSI vs Fish Weight (Regression Summary)*

| VGSI Metric | r | $R^2$ | *p*-value | n |
|---|---|---|---|---|
| VSGSI vs Weight | 0.477 | 0.2273 | 0.0044 | 34 |
| VLGSI vs Weight | 0.285 | 0.0812 | 0.1020 | 34 |

*Table B12: Predictors of Mean Oocyte Diameter (Regression Summary)*

| Predictor Variable | r | $R^2$ | *p*-value | n |
|---|---|---|---|---|
| Fish Weight vs Oocyte Diameter | 0.064 | 0.0041 | 0.72 | 34 |
| VSGSI vs Oocyte Diameter | 0.091 | 0.0082 | 0.611 | 34 |
| VLGSI vs Oocyte Diameter | 0.440 | 0.1936 | 0.0090 | 34 |

*Table B13: Mean Oocyte Diameter by Developmental Stage*

| Oocyte Stage | n | Mean Diameter (mm) | SD (mm) |
|---|---|---|---|
| PVO | 10 | 0.2165 | 0.0837 |
| VIT | 11 | 0.3367 | 0.0723 |
| FOM | 11 | 0.4274 | 0.0641 |

**ANOVA:** $F = 23.71$, $p < 0.0001$
**Post-hoc Tukey:** all pairwise $p < 0.012$

*Table B14: Mean Size GSI (VSGSI) by Oocyte Stage*

| Oocyte Stage | n | Mean VSGSI | SE |
|---|---|---|---|
| PVO | 10 | 0.1142 | 0.0055 |
| VIT | 11 | 0.1262 | 0.0066 |
| FOM | 11 | 0.1158 | 0.0059 |

**One-way ANOVA:** $F = 1.17$, $p = 0.325$

*Table B15: Mean Length GSI (VLGSI) by Oocyte Stage*

| Oocyte Stage | n | Mean VLGSI | SE |
|---|---|---|---|
| ***PVO*** | 10 | 0.6104 | 0.0105 |
| ***VIT*** | 11 | 0.6355 | 0.0131 |
| ***FOM*** | 11 | 0.6499 | 0.0104 |

**One-way ANOVA:** $F = 2.94$, $p = 0.069$

*Table B16: Correlation Between VGSI Metrics and Aromatase Expression (Day 1)*

| VGSI Metric | r | p-value | n |
|---|---|---|---|
| VSGSI vs $\log_2$ cyp19a1a | 0.710 | 0.021 | 10 |
| VLGSI vs $\log_2$ cyp19a1a | 0.584 | 0.076 | 10 |

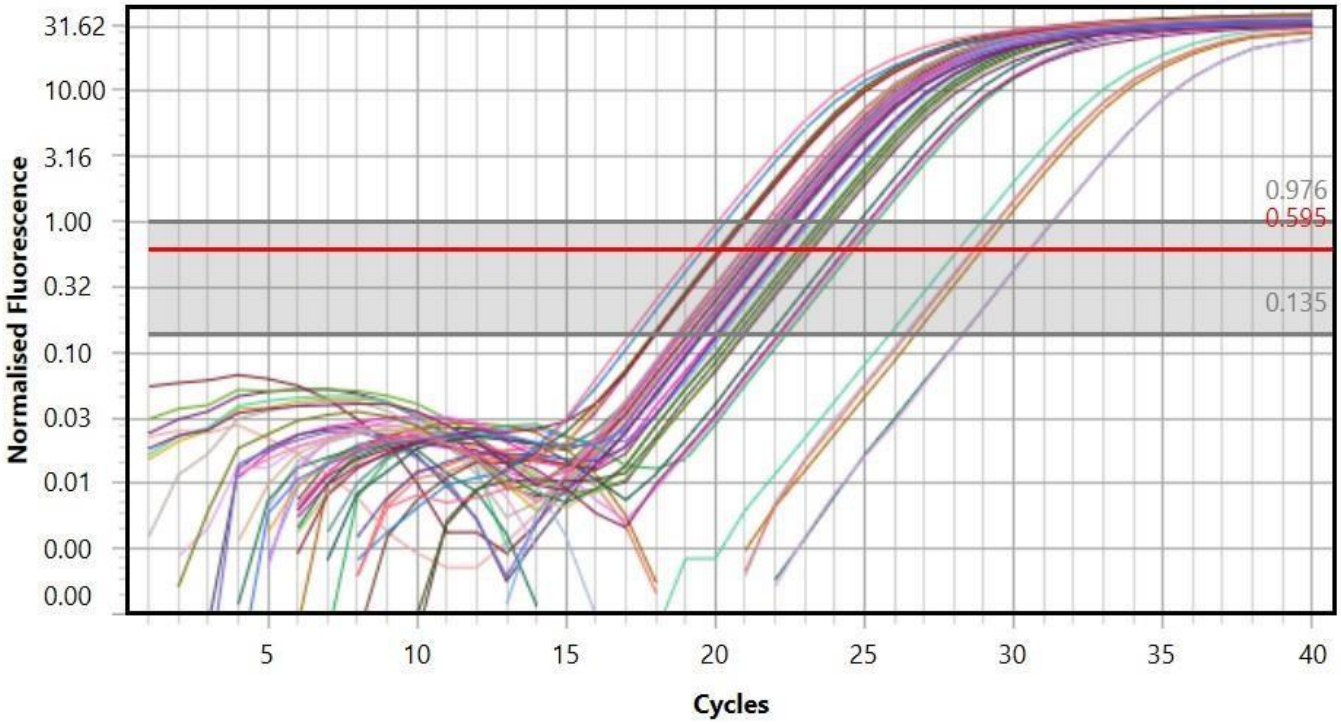


*Figure B1: Normalized Fluorescence of final tbp qPCR [Samples 1-21]*

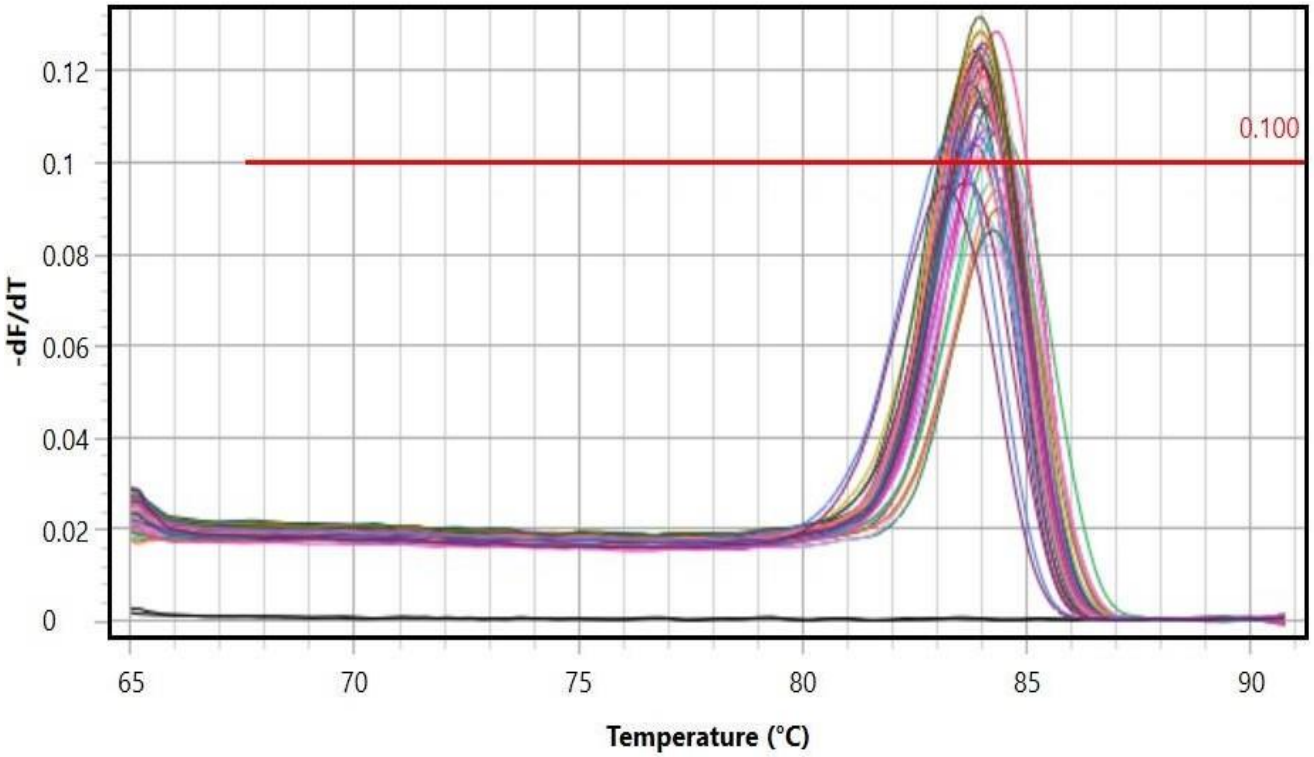


*Figure B2: Melt Curve analysis of final tbp qPCR [Samples 1-21]*

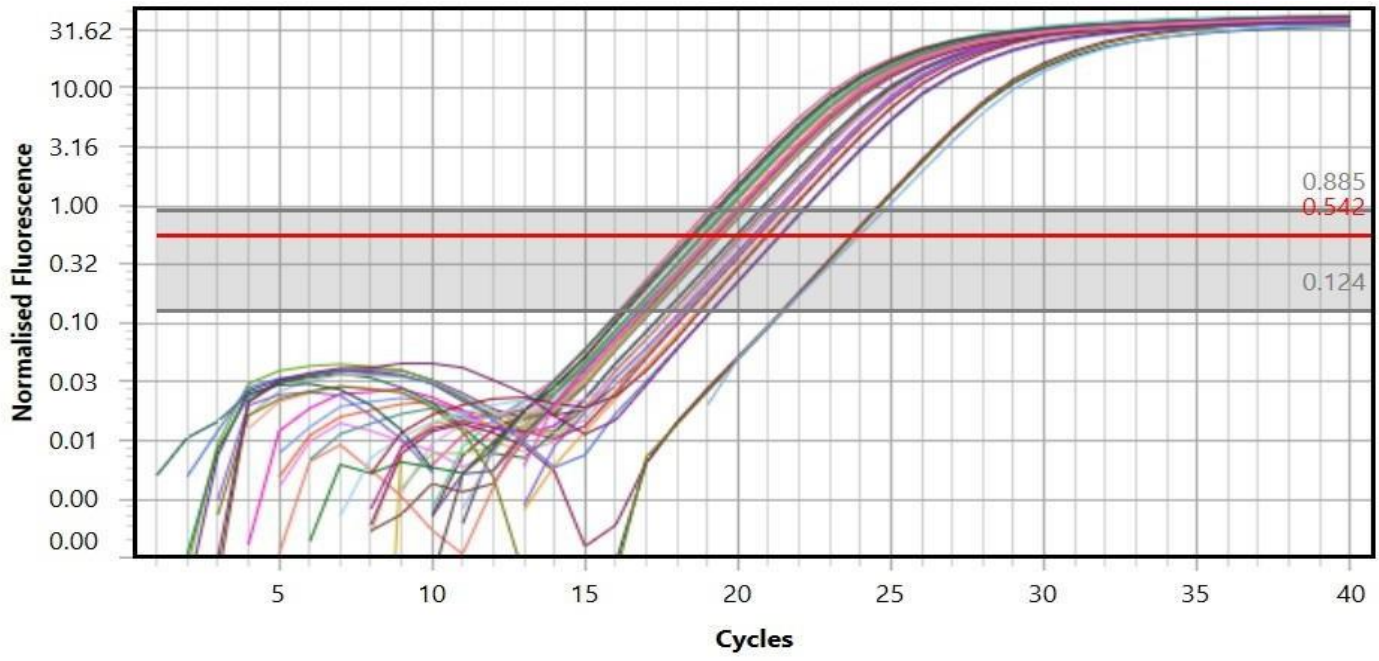


*Figure B3: Normalized Fluorescence of final tbp qPCR [Samples 22-42*

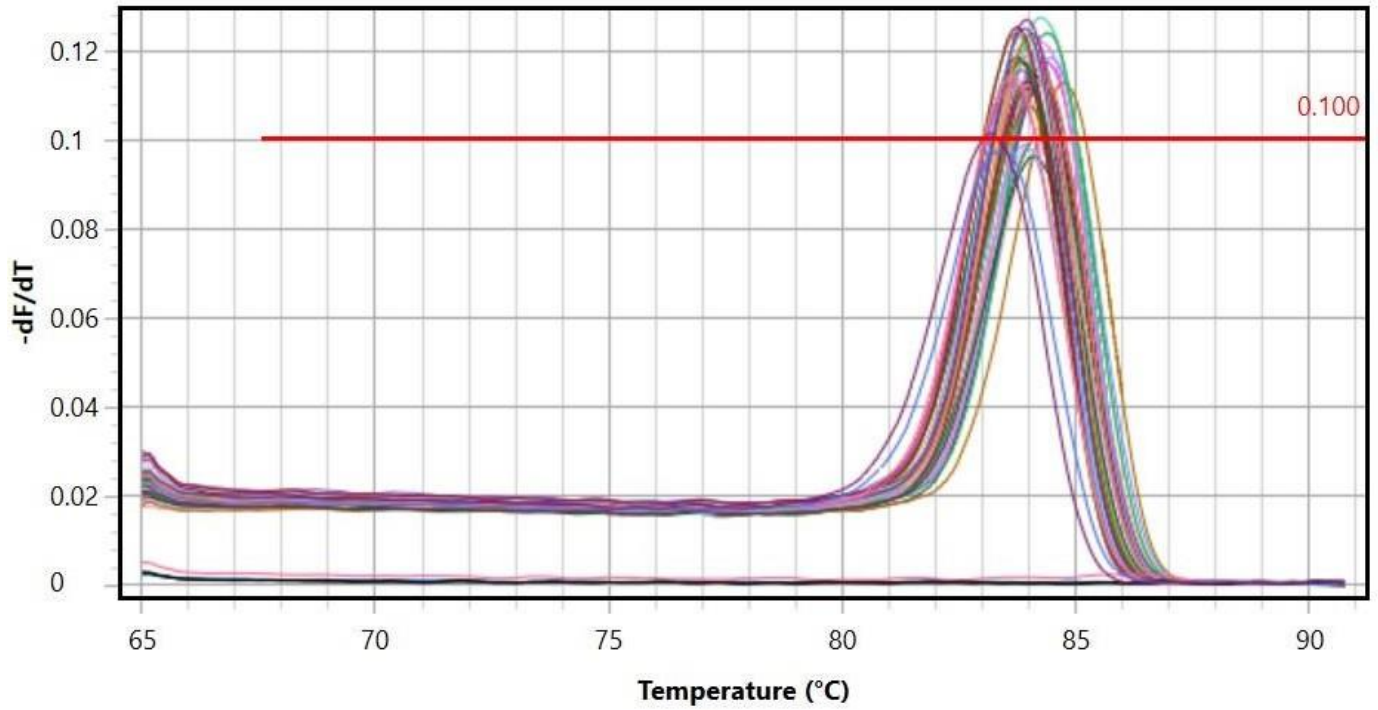


*Figure B4: Melt Curve analysis of final tbp qPCR [Samples 22-42]*

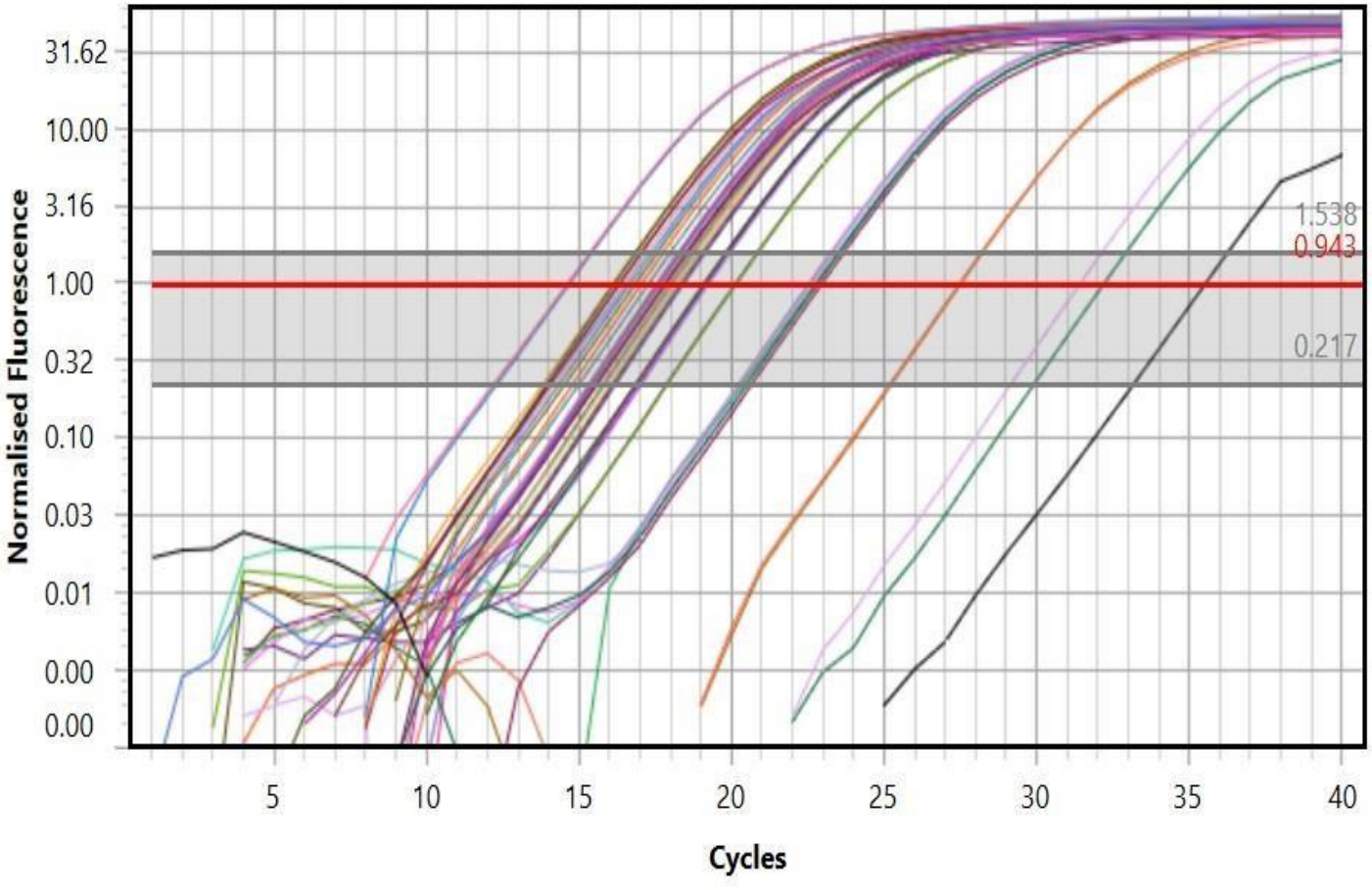


*Figure B5: Normalized Fluorescence of final rpl18 qPCR [Samples 1-21]*

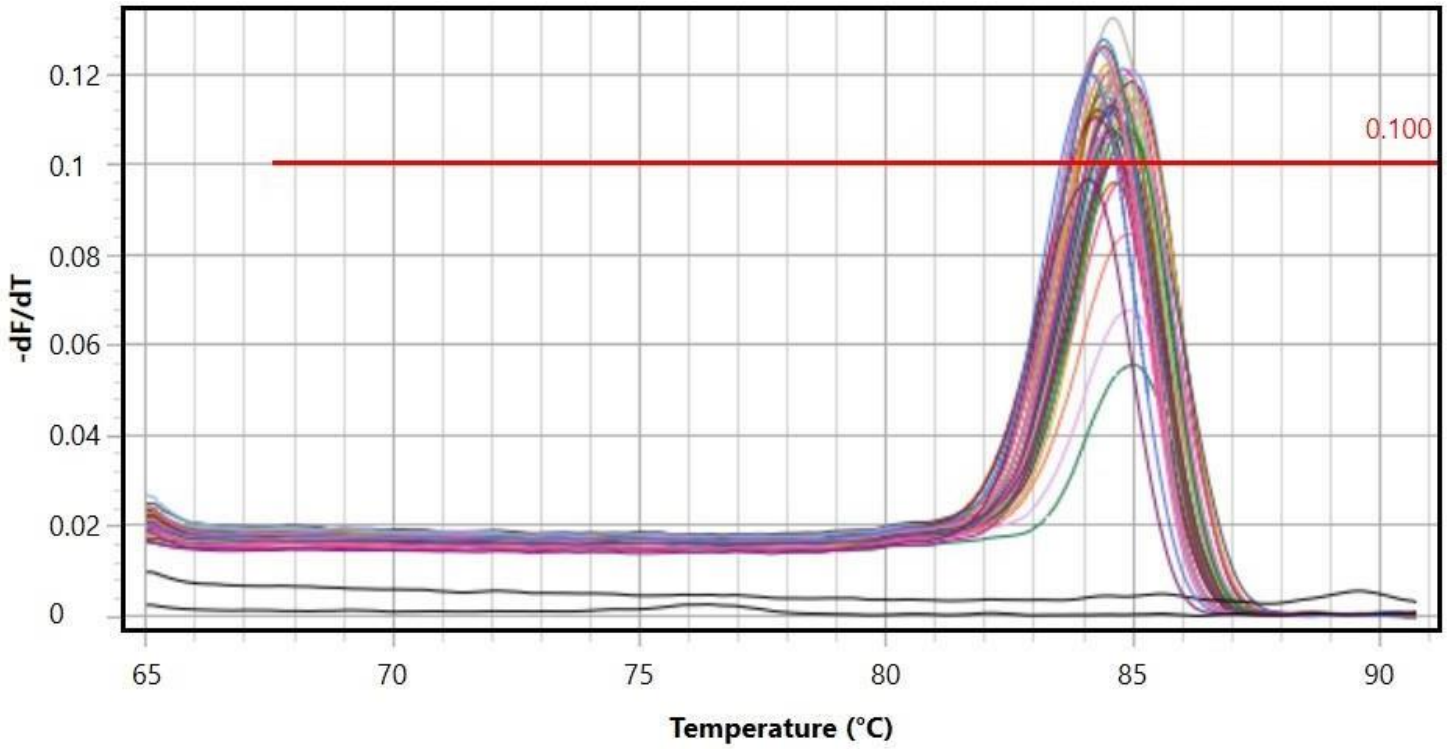


*Figure B6: Melt Curve analysis of final rpl18 qPCR [Samples 1-22]*

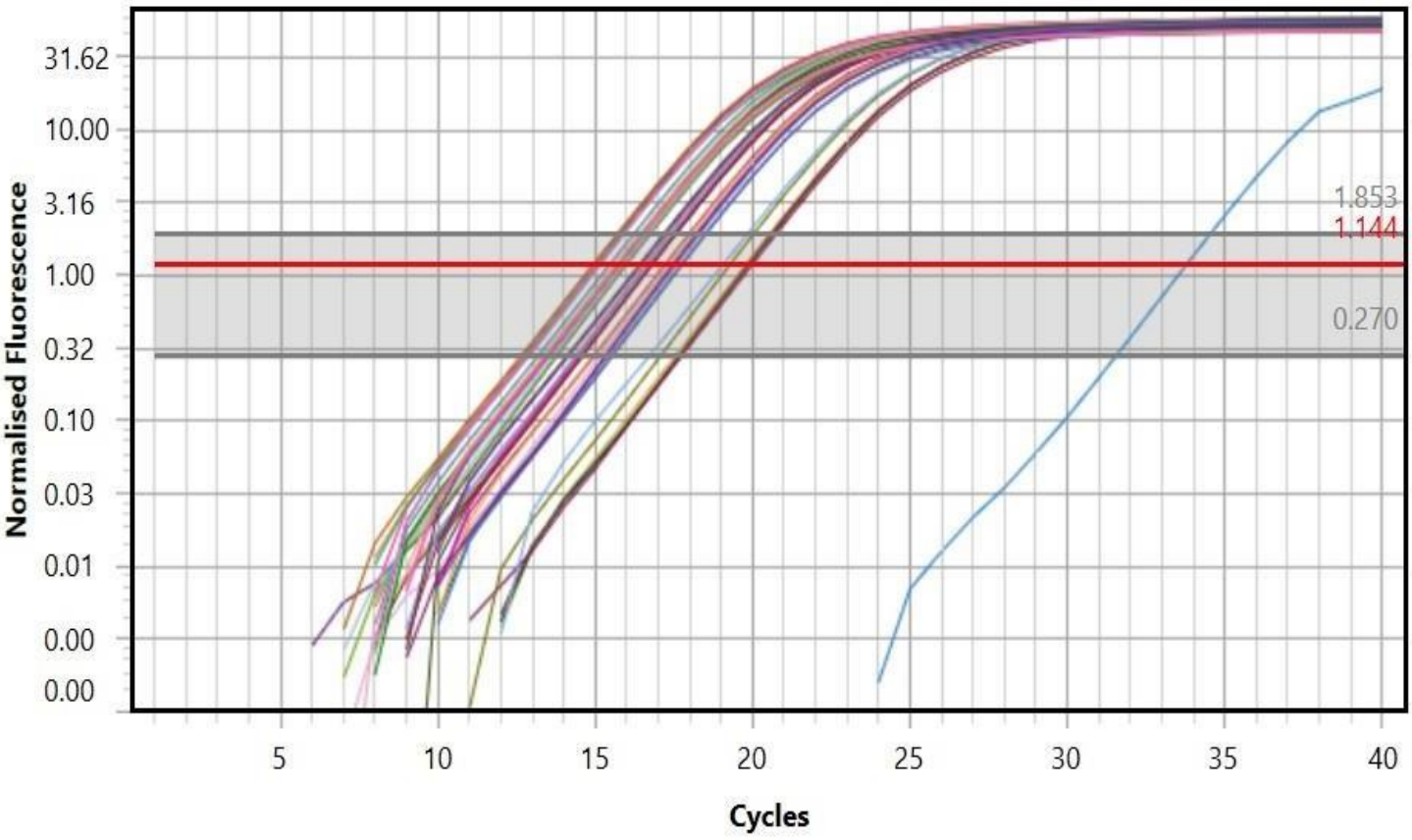


*Figure B7: Normalized Fluorescence of final rpl18 qPCR [Samples 22-42]*

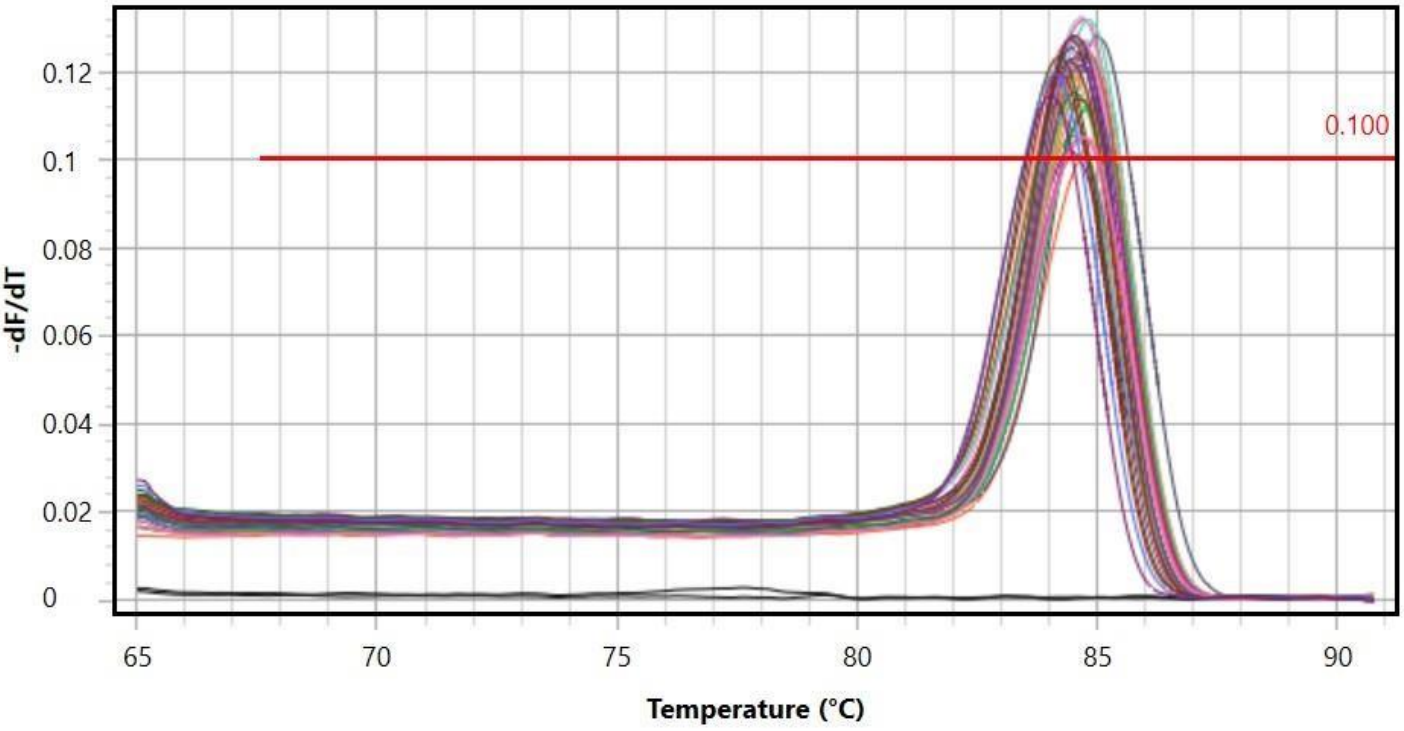


*Figure B8: Melt Curve analysis of final rpl18 qPCR [Samples 22-42]*

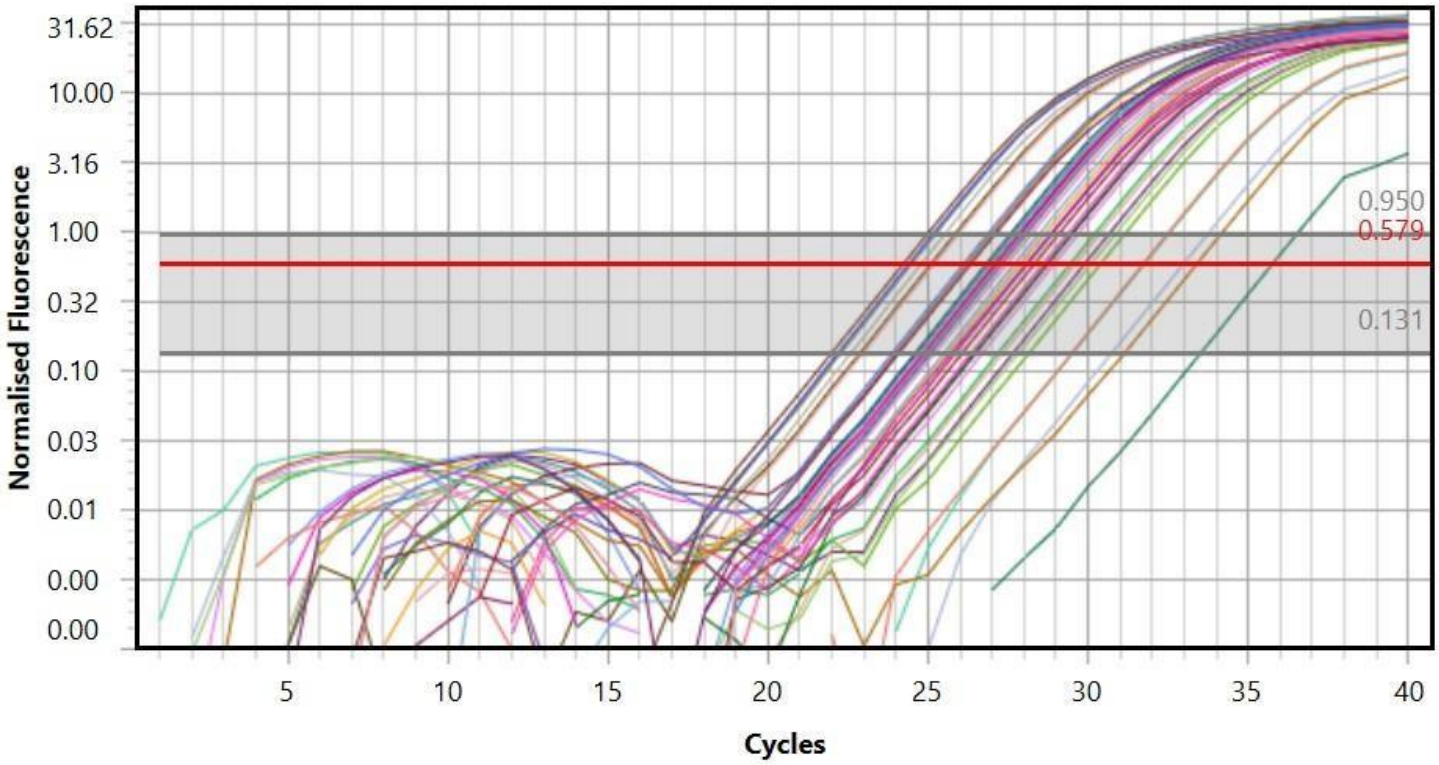


*Figure B9: Normalized Fluorescence of final cyp19a qPCR [Samples 1-21]*

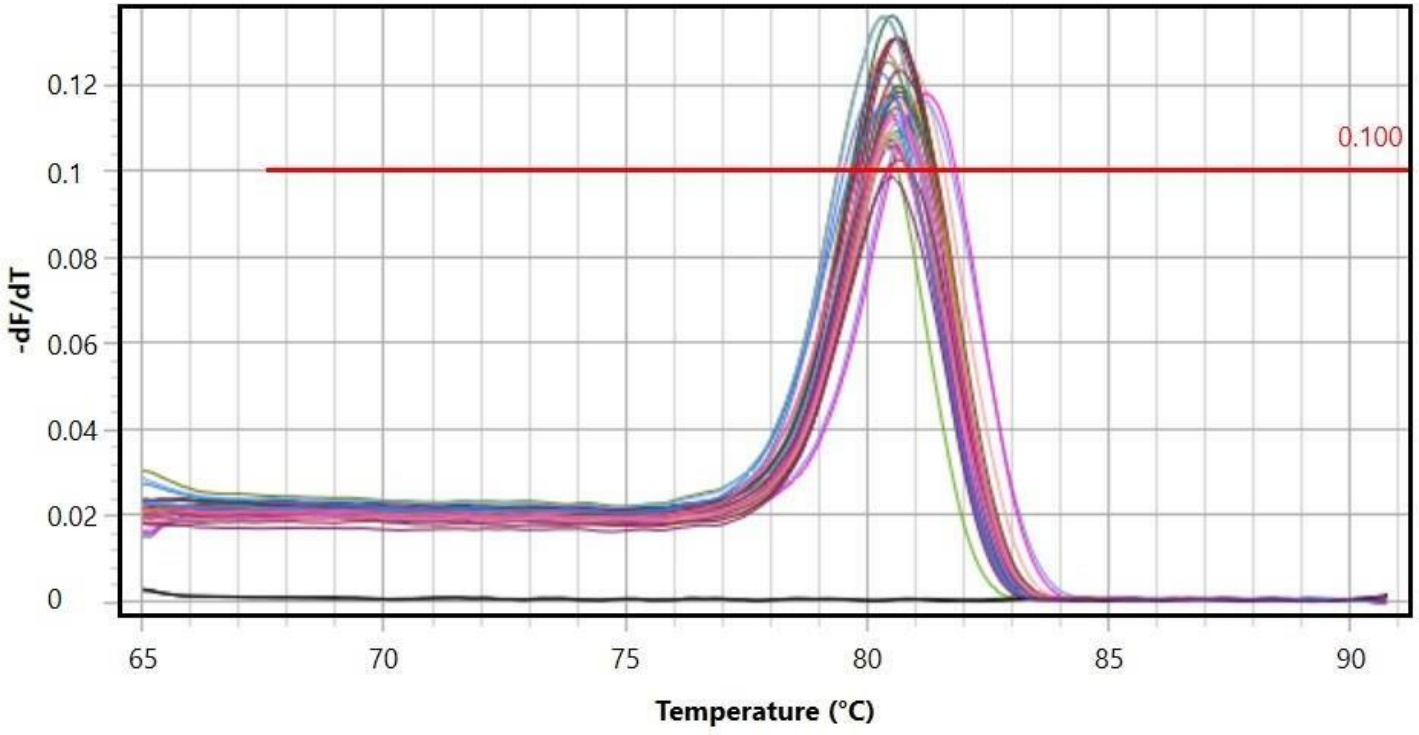


*Figure B10: Melt Curve analysis of final cyp19a qPCR [Samples 1-22]*

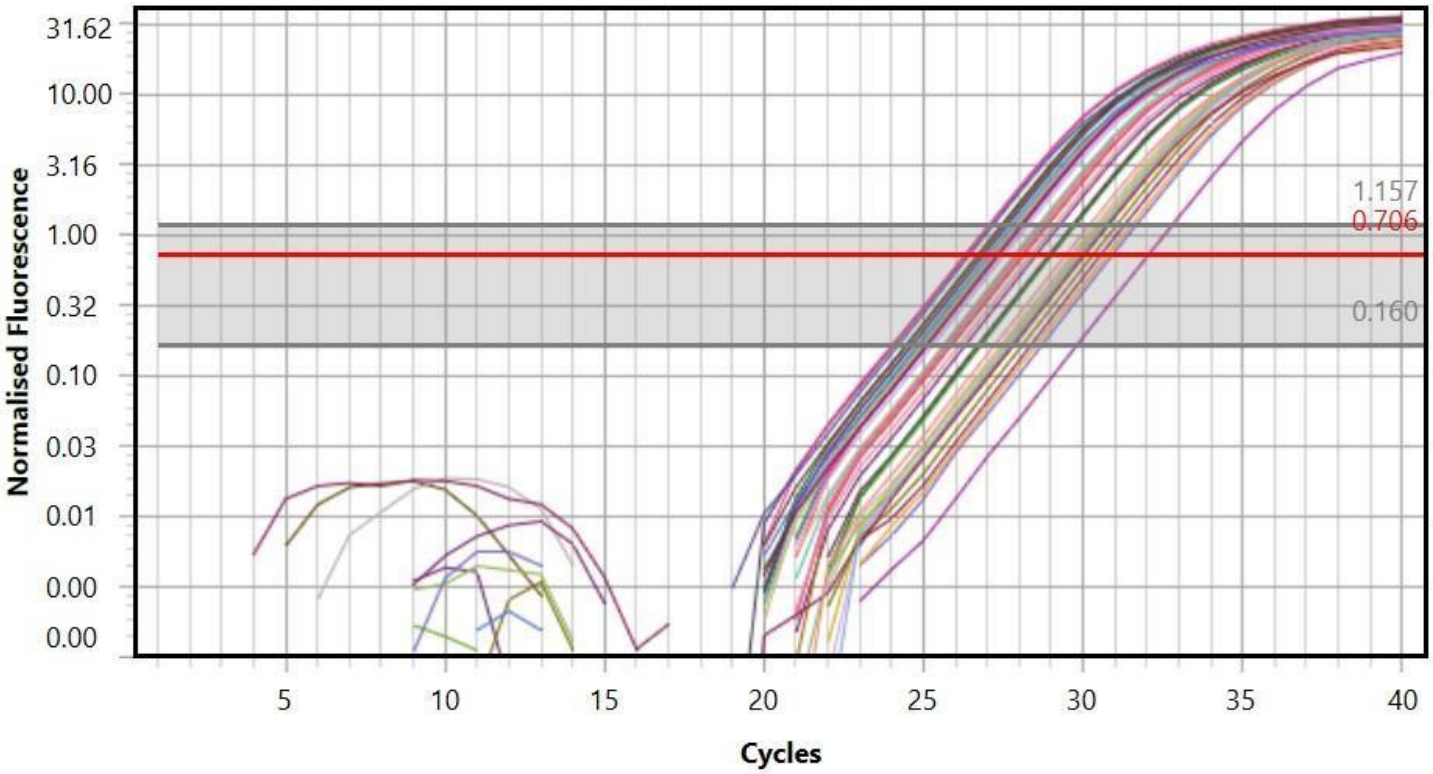


*Figure B11: Normalized Fluorescence of final cyp19a qPCR [Samples 22-42*

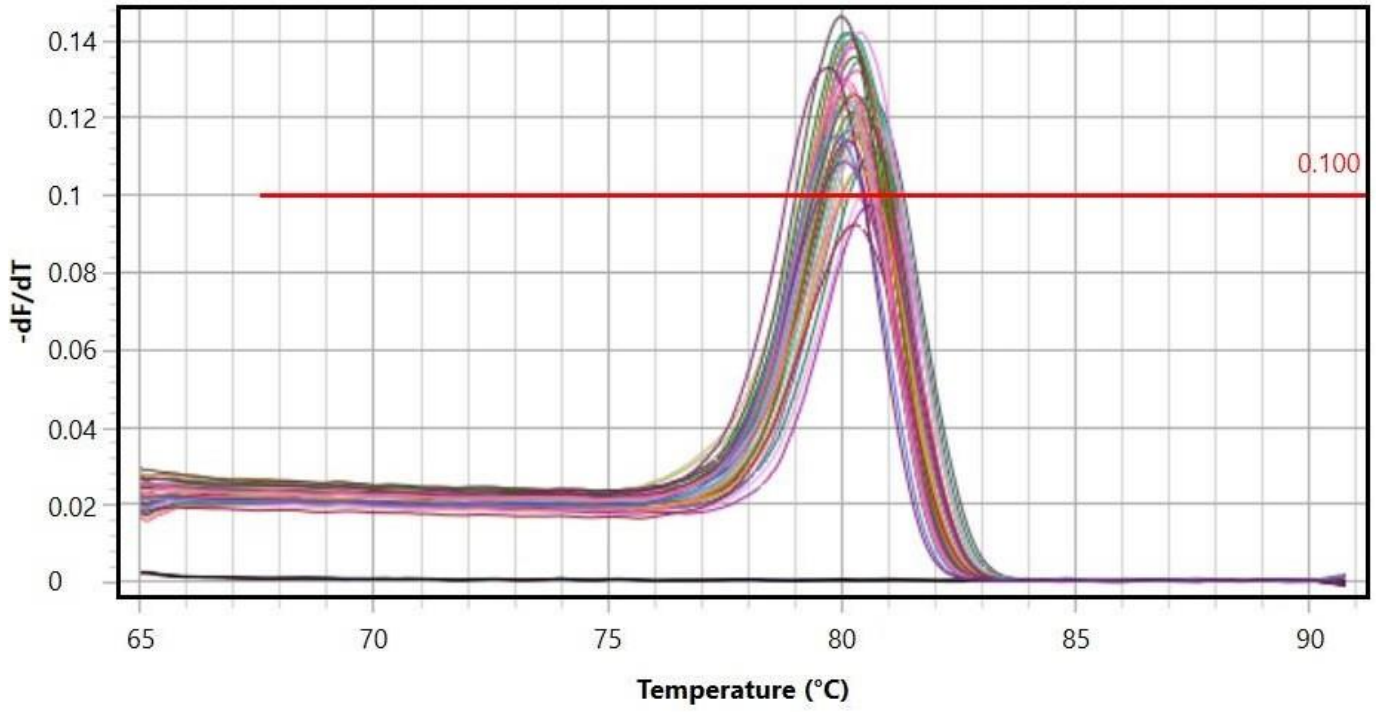


*Figure B12: Melt Curve analysis of final cyp19a qPCR [Samples 22-42]*